FRONTISPIECE

The Jones Camp dike, as viewed from the west from the Jornada del Muerto. The dike, the low ridge in the center of the picture, bisects and tilts the Permian sediments of Chupadera Mesa.

GEOLOGICAL, PALEOMAGNETIC AND GEOPHYSICAL STUDIES AT JONES CAMP DIKE, SOCORRO COUNTY, NEW MEXICO

by

Theodore Paul Jochems, jr.

Submitted in Partial Fulfillment
of the Requirements for the Degree of
Master of Science in Geology

New Mexico Institute of Mining and Technology

Socorro, New Mexico

1987

ACKNOWLEDGMENTS

I wish to thank my advisor, Dr. Clay T. Smith, for the many industrial and academic insights he has given to me during our association. I also appreciate the many efforts on my behalf by Dr. Allan Sanford and Dr. Andrew Campbell, the other members of my committee. I am grateful to several colleagues for their assistance. John Jenkins provided many thoughtful insights, as well as help in the field. Bill McIntosh provided advice and instruction at all stages of the paleomagnetic study. Stan Krukowski processed limestone samples for conodonts. Kelly Vance and Dr. Bill Chavez gave helpful advice in the field. I thank Mr. Ed Bottinelli, president of Zia Steel, Inc., for his generous financial support during my research.

My deepest gratitude goes to my late parents, Ted and Jean Jochems. Without their firm commitment to my early and intermediate education, I would never have attained my present academic level.

ABSTRACT

Magnetite deposits occur as massive replacements at the contact of Permian sedimentary rocks at Jones Camp dike in eastern Socorro County, New Mexico. The dike was emplaced during the late Oligocene and is composed of at least six dioritic intrusions.

Paleomagnetic field directions and intensities were measured on oriented rock cores from eleven sites at Jones Camp. Magnetite ore, actinolite alteration rock and four of the intrusive phases were sampled. Most sites show a wide range of remanent field directions and characteristically have have high alpha-95 values. Only two sites, both intensely altered, have well defined remanent field directions. Magnetic minerals have been completely removed by alteration and the remanent magnetization is carried by secondary hematite introduced during the waning stages of hydrothermal alteration. The wide range of remanence directions is the result of complex chemical remanent magnetizations which were affected by hydrothermal activity. Some evidence suggests that remanence acquisition was further complicated by a reversal of the earth's magnetic field during the emplacement of the dike.

Proton precession magnetometer surveys over the igneous rocks and iron ore show a depressed magnetic signal. Measured susceptibilities of the rocks are lower than would be predicted using empirical formulae. Magnetic data taken over iron ore bodies suffer from a "scatter effect," a wide range of values at a single site. The range of scatter is typically several hundred gammas. Magnetic profiles measured over orebodies are wider and of much lower magnitude than theoretical profiles using predictive formulae from the literature. Proton precession magnetic surveys are extremely useful qualitatively at Jones Camp dike, but quantitative interpretations are unreliable.

Field mapping at several locations along the dike show abundant examples of brecciation and cross-cutting relationships. Three syenodioritic facies have long been recognized: the mottled border facies, the central dike and pyroxene syenodiorite. Three additional facies are described and mapped in the present study: mica syenodiorite, hornblende diorite and albitite. Alteration of igneous rocks and adjacent sediments by later intrusives is quite widespread.

TABLE OF CONTENTS

List of Figures:

List of Tables:

List of Appendices

List of Plates(in back pocket):

INTRODUCTION

PURPOSE AND SCOPE

This investigation of the geological and geophysical characteristics of the Jones Camp dike and iron deposits was undertaken to determine the following: The magnetic behavior of Jones Camp rocks and iron ore on a detailed scale; aspects of the acquisition of remanent magnetization; and details of surficial geology. Information was collected by the following methods: a) field mapping at several scales between 1"=30' and 1"=600'; b) collection of oriented rock cores at eleven paleomagnetic sites and analysis of the direction and intensity of their remanant magnetization; c) measurement of the total field magnetic anomaly at ten foot and 100 foot centers.

LOCATION AND ACCESSIBILITY

The Jones Camp iron district is located on the Jones Camp dike in eastern Socorro County, New Mexico. The dike is located in T5S, eastern R6E, R7E and western R8E. The best access is via the old Socorro-Carrizozo highway, which runs along the northern edge of the dike. The old highway is best entered from highway 380 at Bingham, New Mexico, 36 miles east of San Antonio(figure 1). The old highway is referred to as "Iron Mine Road" on recent United States Geological Survey and Bureau of Land Management maps. Several ranch roads which approach the dike from the south may be entered

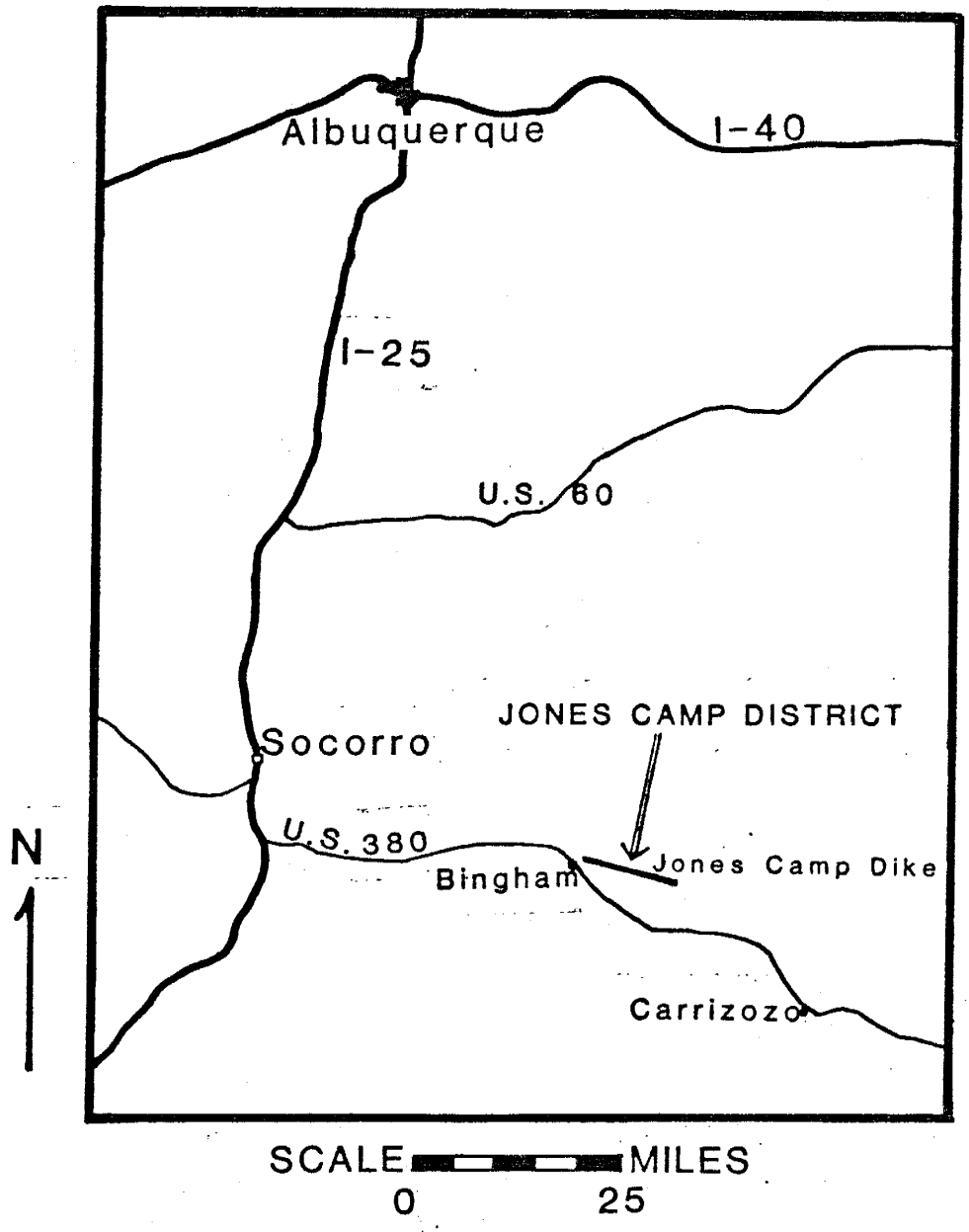

Figure 1. Location map for Jones Camp Dike and Jones Camp District, eastern Socorro County, New Mexico.

from highway 380 a few miles east of Bingham. All roads are difficult to pass in wet weather.

EARLY HISTORY OF THE JONES CAMP DISTRICT

Previous Master of Science theses(Noguiera, 1971; Bickford, 1980; Gibbons, 1981 and Jenkins, 1985) have summarized the history of the Jones Camp District since World War II. They state that no record of claims prior to 1927 is available. Correspondence on file at the New Mexico Bureau of Mines and Mineral Resources documents earlier exploration and development work in the area. Most of this correspondence was between geologists, engineers and supervisors at Colorado Fuel and Iron Co.(CFI) at Pueblo, CO.

The earliest record of exploration in the district is made by Emmons(1906). He states that two shafts, 19 and 48 feet deep, were sunk by gold prospectors in 1880 and 1881. These were located approximately 2000 feet west of Jones Camp in the Jones Camp District(plate 9).

P. C. Bell and Fred Schmidt are credited with the discovery of the deposit in spring, 1902 and F. A. Jones is considered the first to recognize its significance. A plat of claims by Jones(1902) shows a block of 52 claims which extended from the Jones Camp district westward to the escarpment of Chupadera Mesa. A similar map shows two claims four miles south of the district, presumably at the Iron

Horse deposit. Ward(1902), in a report for CFI, stated that Jones owned a half interest in the claims and that the other half was split between Bell and Schmidt. A later, undated plat shows three additional claims to the east of Jones Camp district. Jones(1904) describes development work around the turn of the century at base metal and fluorspar prospects along the western scarp of Chupadera Mesa.

Anderson(1958) refers to early reports by "old-timers" that mining was attempted in 1906 and that some fluxing ore was shipped by oxcart to smelters in Socorro, but there are no records to support these statements. Between 1900 and 1920, there appears to have been considerable effort to promote the deposit, particularly to CFI. Many shafts, trenches and pits were excavated during that period. A memorandum to C. S. Robinson of CFI in January, 1903, states that the district was staked by the New Mexico Railway and Coal Co. of Scranton, PA. However, in that same month Jones, Bell and Schmidt signed an exploration agreement with CFI. A later prospect report(1907) maintains that the claims were sold to "some California and eastern capitalists" for $750,000. In 1911, William Gurnee offered 58 or more claims to CFI for $2,700,000. Gurnee identified himself as an agent for a Mr. Hewett of New York City. In a series of letters in April, 1911, Gurnee's estimates of ore reserves varied between 30 and 150 million tons. He suggests that Reid Kennedy, an engineer from U. S. Steel Corp. in Los Angeles who visited the district at that time, concurred with those

estimates.

CFI again showed interest in the district in 1920. At that time, a Mr. Thomas claimed to be in control of Jones' claims. CFI sent a geological engineer for further inspection in 1926. Although CFI maintained interest in Jones Camp throughout the first quarter of the century, their agents who visited the deposit were pessimistic about its economic viability.

PLACE NAMES USED IN THIS STUDY

Plate 9 is an index map for places mentioned in this study. Locations of the following features are presented: map areas and magnetic grids; place names commonly used by workers in the area(east pit, west pit); places of historical interest(Jones Mine and Jones Camp); names of geologic features coined by the author(offset trend, south side anticline).

ROCK UNIT DESIGNATIONS

For purposes of simplicity and euphony, designations of two to four letters will be used in this study to describe the rock units mapped and discussed in this study:

Tertiary units

Ta - actinolite contact rock
Ti - iron ore
Tj - Jones Camp diorite or syenodiorite, unspecified
Tjh - hornblende diorite
Tja - albitite

Tertiary units(continued)

Tjm - micaceous or medium-grained syenodiorite
Tjp - pyroxene syenodiorite
Tjc - central facies syenodiorite
Tjb - mottled border syenodiorite

Permian units

Psa - San Andres formation
Pg - Glorieta formation
Py - Yeso formation
Pyj - Joyita member
Pyc - Canas member
Pyt - Torres member
Pytl - Torres limestone bed
Pytg - Torres gypsum bed
Pyts - Torres sandstone bed

GEOLOGICAL SETTING

The following section is a discussion of the geology of the Jones Camp dike. It is a summary of previous work, mainly Kelley(1949) and four Master of Science theses written by students at New Mexico Institute of Mining and Technology(Noguiera, 1971; Bickford, 1980; Gibbons, 1981; Jenkins, 1985). These authors provide abundant data with some variety of interpretation. The present author's work is in agreement with some interpretations while disagreeing with others. The present author's interpretations will be discussed in the section on geological observations.

The study area is located on Chupadera Mesa in eastern Socorro County, New Mexico. Chupadera Mesa is a broad(~10 X 40 miles) expanse of flat-lying Permian sedimentary rocks cut by the Jones Camp dike at the southern end of the mesa. The dike is composed of diorite which intruded in several pulses. Throughout this study, the terms "pulse," "facies" and "phase" will be used to denote the igneous pulses. In the present section discussing the geological setting, the igneous intrusions will be subdivided into three groups following the convention of Kelley(1949): an early marginal(border) facies, a later central facies and a pyroxene syenodiorite(field term-"diabase") dikes and sills. Hydrothermal convection cells localized magnetite ore along bedding planes in the sediments close to their contact with the dike. Excellent geologic maps of the entire dike at the

scale 1=12000 are provided by Bickford(1980) and Jenkins(1985). Detailed maps of the Jones Camp District are provided by Noguiera(1971) and Kelley(1949).

PRECAMBRIAN ROCKS

The Precambrian rocks beneath Chupadera Mesa are part of the Central Granite Belt(Muehlberger and Denison, 1964). This northeasterly trending belt is composed of granite, granitic gneiss and granodioritic gneiss. Two thermal metamorphic events have been documented. Granitic and granodioritic gneisses were encountered by three oil tests near Bingham, eleven miles west of the Jones Camp district. Samples from the Sun nr. 1 Bingham State were dated at 1.57 by and 1.35 by. The older date is considered the true age of the rock, as the younger date represents a metamorphic episode. Standard of Texas nr. 1 Heard, drilled twelve miles southeast of the district, encountered a more mafic troctolite(olivine plagioclase rock).

PERMIAN SEDIMENTARY ROCKS

Chupadera Mesa is a relatively undisturbed sequence of Pennsylvanian and Permian sediments resting on the Precambrian basement (Figure 2). Only Permian rocks are considered herein. They comprise the Abo, Yeso, Glorieta and San Andres formations. The upper three formations, as well as the top of the Abo, are included in the Leonardian Series. The lower Abo is assigned to the Wolfcampian

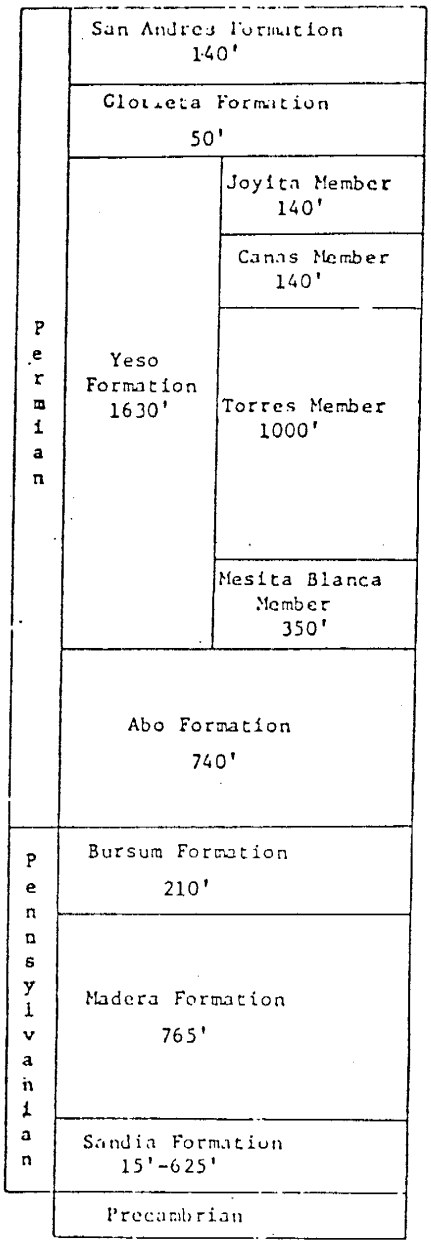

Figure 2. Stratigraphic section of Pennsylvanian and Permian sedimentary rocks underlying the field area of this thesis(after Bickford, 1980).

Series. Lee and Girty (1909) included all four formations in the "Manzano Group." Needham and Bates (1943) continued that convention, but it has not been used in recent literature. Darton (1922) created the "Chupadera Formation" to include all Yeso, Glorieta and San Andres beds but that designation was soon superceded by formational status for these units.

The Permian sequence is conformable or slightly disconformable to Pennsylvanian strata. The Abo Formation consists of terrestial clastic rocks. The Yeso gypsums, sandstones, shales and limestones were deposited in a restricted basin. The Glorieta sandstone and San Andres gypsum, sandstones and limestones were deposited in a deeper marine environment.

Abo formation

The Abo Formation includes dark red sandstone, arkose, shale and conglomerate deposited in a continental setting. It is not exposed within the study area. Its thickness beneath the Chupadera Mesa is approximately 750 feet. It contains about 1% iron. The Abo is of interest in this problem because it has been considered as a potential source rock for iron mineralization in the study area (Bickford, 1980).

Yeso formation

The Yeso Formation is widespread over central New Mexico. Its type locality is 11 miles northeast of Socorro, New Mexico, at Mesa del Yeso. Yeso is the Spanish word for gypsum, which constitutes a large portion of the formation. It is subdivided into the Meseta Blanca, Torres, Canas and Joyita members, in ascending order.

The Yeso is a sequence of sandstone, gypsum, siltstone and limestone beds approximately 1,600 feet thick at Chupadera Mesa. An oil test 12 miles southeast of the central part of the study area drilled 4,255 feet of the Yeso Formation. The additional thickness included over 1,000 feet of halite as well as massive gypsum beds. Lochmann-Balk (1964) considers the area west of Carrizozo to have been a basin filled by evaporite deposition during Yeso time. The formation thickens slightly to the south. It thins drastically, however, at the margins of the intruding Jones Camp dike.

Bickford (1980) notes a cyclic sequence of limestone, gypsum and sandstone, in ascending order, in the Torres and Canas members. This cyclicity reflects alternating changes in sea level and climatic conditions.

Meseta Blanca member

Wilpolt and Wanek (1951) describe the Meseta Blanca member as an uniformly bedded, red-brown and variegated sandstone and sandy shale. Thickness ranges from 190 to 355 feet, increasing southward. It forms topographic depressions along strike between the more resistant Abo formation and the lowermost limestone bed of the Torres member. Noguiera (1971) states that the Meseta Blanca crops out in a gulch one and a half miles west of his field area. Wilpolt and Wanek, however, draw the Meseta Blanca-Torres contact two and a half miles west of the western escarpment of Chupadera Mesa.

The Meseta Blanca member was originally included at the top of the Abo Formation by Needham and Bates (1943). Read and Andrews (1944) recognized it as a distinct member related to the Yeso Formation.

Torres member(Pyt, Pytl, Pytg, Pyts)

The Torres member, which constitutes the bulk of the Yeso Formation, includes alternating beds of sandstone, limestone and gypsum. Only the top of the Torres is exposed along the Jones Camp Dike on Chupadera Mesa. The rest may be seen as one descends the western escarpment of the mesa and proceeds westward toward the plains of Jornada del Muerto.

The Torres sandstones are white, reddish-orange or buff, fine-grained, subangular, friable, moderately sorted subarkose with minor feldspar. They range in thickness from 0.5 to 50 feet. They are discontinuous and often pinch out abruptly. Silt is often present and sometimes dominates the composition of the rock. The Torres gypsum is grey to white and has nodular or laminated texture. It is often interbedded with discontinuous siltstone or sandstone layers. The limestone beds are medium to dark grey, massive to thinly laminated sparite. Originally deposited as lime mud, they have undergone aggrading neomorphism which has increased the grain size to spar. The limestones are locally gypsiferous and are brecciated near faults and zones of bedding-plane slip. A fossiliferous horizon occurs near the base of the uppermost limestone bed. This three-inch horizon contains bivalved organisms which have been recrystallized or replaced by coarse-grained calcite. The broken shell fragments served as nuclei for oncolites. The limestones vary in thickness from three to 50 feet. The uppermost limestone bed is dolomitic, while the next lower bed is calcitic.

Bickford (1980) noted a cyclic nature within the Torres member. Limestone is overlain by gypsum, which is in turn covered by sandstone. He measured three such cycles in the uppermost 140 feet of the Torres. Wilpolt and Wanek (1951) measured a 951 foot section of the Torres 6.5 miles south of the dike. They noted that the Torres thickens towards the

south. They found 14 limestone beds in that section, all medium to dark grey. The widespread basal limestone of the Torres, however, was missing or covered in that section.

Most of the magnetite mineralization exposed on the surface at Jones Camp is hosted by the limestone, sandstone and gypsum beds of the upper Torres member.

Canas member(Pyc)

The Canas member consists of grey to white calcareous and silty gypsum with minor siltstones, sandstones and limestones. The gypsum is either nodular or laminar and is the dominant (~85%) rock type. There are subordinate beds of gypsiferous, discontinuous limestone two to four feet thick and thinly bedded, fine-grained sandstone layers. The lower contact with the top Torres limestone bed is gradational and the upper contact with the Joyita member is sharp and conformable. Bickford (1980) noted rhythmic upward sequences of limestone, gypsum and sandstone similar to the cycles in the Torres member.

Wilpolt and Wanek (1951) give the maximum thickness of the Canas as 198 feet in the central Oscura Mountains. Like the Torres, it thins northward. Weber and Kottlowski (1959) note variable thicknesses between 150 and 190 feet along U.S. 380, six miles south of the dike. Bickford(1980) measured sections with thicknesses of 76, 101 and 140 feet. The thickest section is two miles south of the dike and the

two notably thinner sections are adjacent to the intrusive. These thicknesses agree with Kelley's (1949) measurement of 80 feet. Bickford(1980) speculated that the drastic shortening of section might be the result of faulting. The present author agrees with Jenkins (1985) that the thinning is due to loss of volume by dehydration of gypsum to anhydrite and plastic flow of the evaporitic rocks during emplacement of the igneous intrusives.

Joyita member(Pyj)

The Joyita member is dominated by reddish, fine-grained, poorly sorted, feldspathic sandstone. The member is about 100 feet thick in the study area, less than the 140 feet measured by Bickford (1980) two miles to the south. The Joyita contains two subordinate gypsum beds. The lower is approximately ten feet above the base of the member and the upper at the top of the member. Both upper and lower contacts of the Joyita are sharp and conformable.

Glorieta formation(Pg)

The Glorieta Formation consists of white to grey, medium-grained sandstone with local limonitic staining. In the study area its thickness varies between 50 and 56 feet. Bickford (1980) notes that it thins to the east in exposures along the Jones Camp Dike. Dane and Bachman (1965) show the Glorieta pinching out between the Yeso and San Andres formations to the south in northernmost T6S, R7E. Wilpolt

and Wanek (1951), however, measured 50 feet of Glorieta eight miles south of that location.

Keyes (1915) first described the Glorieta Sandstone, probably at Glorieta Mesa in San Miguel County, New Mexico. Since then, there has been considerable controversy concerning its stratigraphic rank. The lower portion of the Glorieta intertongues with the uppermost part of the Yeso Formation on a regional scale. Hager and Robitaille (1919) conferred formational status on the unit. Read and Andrews (1944) as well as Wilpolt and Wanek (1951) carry it as a subordinate member of the San Andres Formation. Bates et al (1943), Dane and Bachman (1965) and Lochman-Balk (1964) consider it to have sufficient thickness, regional distribution and distinctive character to warrant formational status. It will be treated as such in this paper.

San Andres formation(Psa)

The San Andres formation was originally described by Lee and Girty (1909). Its type locality is in Rhodes Canyon in the northern San Andres Mountains. It is the youngest exposed sedimentary unit in the study area. Only the lowest quarter (~150 feet) remains uneroded on Chupadera Mesa. The San Andres is a thickly bedded, brownish-grey, locally dolomitic limestone. Its texture varies from fine-grained lime mud to wackestone. There are discontinuous horizons of ferruginous chert nodules. Abundant fossils of bivalved

organisms and possibly gastropods have recrystallized to fine-grained spar. A sandstone layer ten to 20 feet thick occurs between 12 and 25 feet above the base. This layer grades laterally to gypsum within the study area and is often the site of emplacement of pyroxene syenodiorite intrusive sills. The resistant San Andres caps cuestas which dip away from the Jones Camp dike.

TERTIARY IGNEOUS ROCKS

In the study area, igneous rocks of dioritic affinity crop out among Permian sediments as a long, thin dike. These intrusives originated in a magma chamber of unknown depth. They probably ascended along a fault in the Precambrian basement and continued upward through the overlying, unfaulted Paleozoic sediments. The distribution of roof pendants along the entire length of the dike indicates that only its very top has been exposed by erosion. Jones Camp dike rocks are generally subdivided into three groups: the Jones Camp syenodiorite, consisting of a border facies and a central facies, and pyroxene syenodiorite. "Syenodiorite" is a term used to describe diorite which has been enriched in sodium and potassium. Field evidence indicates that the border facies diorite was emplaced first, followed by the central facies, possibly while the border facies was still molten. The pyroxene syenodiorite ascended as irregular intrusive bodies via the margins of the dike and outlying fractures and spread

laterally as sills along sedimentary contacts.

The present author subdivides the dike into six distinct intrusive facies based on grain size and mineralogical proportions.

Jones Camp dike(Tj)

The Jones Camp dike forms a thin, linear outcrop approximately 11 miles long with an average width of about 600 feet. The dike strikes N75W and dips ~85 degrees to the south. It is more resistant to erosion than the surrounding sedimentary rocks and forms a prominent ridge throughout its outcrop area. The dike is composed of diorite. Mineralogical variation follows a trend of a more felsic core grading into a more mafic margin.

The dike has been divided into two, three or four facies by various authors. These divisions are based on mineralogical and textural variations. Kelley (1949) describes two facies: a medium-grained hornblende monzonite central facies and a fine-grained monzonite marginal facies. However, according to igneous rock classifications in common use today (Travis (1955), Streckeisen (1967)), the orthoclase content of the Jones Camp Dike is too low for it to qualify as a monzonite. Noguiera (1971) identified four distinct facies:

> "mottled border facies-green, fine-grained diorite.
> outer intermediate hornblende facies-coarse diorite with hornblende as the dominant ferromagnesian mineral.

inner intermediate pyroxene facies-coarse diorite with pyroxene as the dominant ferromagnesian mineral.
central diorite facies-coarse, feldspathic diorite. Noguiera identified a quartz diorite subfacies in this facies."

Gibbons (1981) states that these facies are only vaguely developed on a local scale and that this scheme cannot be used in the field. He divides the dike into a border facies and a central facies.

Bickford (1980) recognizes three facies: mottled border facies, intermediate facies (to include both of Noguiera's intermediate facies) and central facies.

For purposes of summarizing previous work, it is most convenient to subdivide the dike into three rock types: the border facies, the central facies and pyroxene syenodiorite. Field work by the present author shows at least three additional igneous facies as described in the section on geological observations.

Border facies(Tjb)

The border facies is composed of green to pale-green, very fine-grained diorite. It bounds the central facies on both sides. The border facies averages 100 feet in thickness and is often intensely jointed. These joints are probably related to cooling. They served as conduits for hydrothermal solutions and later-emplaced dioritic facies. The border has been intensely altered and contains large amounts of secondary minerals, including tremolite,

actinolite, epidote, calcite, albite, hematite and magnetite. The weathered surface is characterized by 2-3mm bumps which are concentrations of scapolite, tremolite and other secondary minerals which replaced plagioclase. Kelley(1949) gave the facies the field name "mottled border facies."

It has been noted by previous authors that the border, unlike the central facies, lacks abundant primary magnetite but contains veinlets of secondary hematite and magnetite. Primary magnetite content of Tjb is only 1%, lower than central facies rocks. This generalization applies in areas atop Chupadera Mesa, where the dike underwent intensive hydrothermal alteration. Border facies diorite from outcrops on the plains west of the mesa escarpment (Sec 11, 12 and 13, T5S, R6E; see plates 7 and 8) is fresher, though still lightly to moderately altered. No secondary magnetite veinlets are seen in this rock. Very fine-grained ferromagnesian minerals in this rock presumably include primary magnetite. It is fine-grained, moderately altered and shows mottled texture. These observations suggest that the later intrusive pulses were responsible for much of the hydrothermal alteration which leached primary magnetite from the border facies while introducing secondary minerals, including magnetite. Results of the paleomagnetic study suggest that the alteration episodes were quite complex.

There are two plagioclases in the border facies: primary andesine and secondary albite. Ferromagnesian minerals include augite, epidotized pyroxenes and amphiboles.

Central facies(Tjc)

The central facies consists of pink to grey, massive, holocrystalline, medium-grained, intergranular diorite. Miarolitic cavities are common. Its core is generally free of secondary effects, such as hydrothermal alteration. However, these effects often occur on the margins of the central facies.

The major mineralogical variation is in the ratio of pyroxene to hornblende. Pyroxene content(mainly augite, aegerine-augite and hypersthene) decreases outward from the core to the contact with the border facies. Amphibole content (mainly hornblende) shows the opposite trend, increasing outward from the core. Attempts to delineate facies based on relative abundances of ferromagnesian minerals have not been sucessful on a regional scale due to vague, gradational contacts. Orthoclase content increases inward toward the center of the dike.

A quartz dioritic to granodioritic subfacies has been identified by Noguiera (1971) and Bickford (1980). It is cream colored and porphyritic with higher amounts of quartz and orthoclase than other parts of the dike. It forms

small, elliptic patches in the center of the dike. Noguiera maintains that it is the most highly differentiated material in the dike.

Pyroxene syenodiorite(Tjp)

The late intrusive sills and dikes peripheral to the Jones Camp Dike are composed of green to grey, very fine to fine-grained, porphyritic, quartz poor pyroxene syenodiorite. These were originally termed "diabase" by Kelley (1949). However, they do not qualify as diabase either texturally or chemically, and the present author prefers Bickford's (1980) designation as "pyroxene syenodiorite." This rock typically has three to seven percent of feldspar phenocrysts approximately 1mm wide. The groundmass consists of very fine-grained andesine with interstitial clinopyroxene, magnetite or biotite (Jenkins, 1985). It is chemically similar to the Jones Camp diorite, but has much less chemical and mineralogical variation. It shows chill textures at contacts with sediments and other igneous rocks. Jenkins notes that it was emplaced in at least two pulses. The present author treats the later phase as a distint igneous phase(mica syenodiorite).

Some outcrops differ texturally in that they are medium-grained and holocrystalline, with greater amounts of biotite and alkali feldspar. These are often saussuritized and show concentric cooling structures. Bickford's(1981) sample Db-5b is an example of this rock type. The present

author has seen several exposures showing the medium-grained rock intruding the porphyritic rock as stocks or sills. Contacts between the two are very sharp, often with brecciation. These observations indicated two distinct igneous pulses and preclude differentiation in situ. In this study, the medium-grained, micaceous syenodiorite will be treated as an intrusive pulse(Tjm) emplaced after the porphyritic rock.

The late intrusive occurs as proximal dikes or irregular bodies close to the margins of the main dike and as distal necks and sills in sediments. The sills are found along contacts above, below and within every sedimentary unit exposed in the field area. They intrude gypsum beds preferentially, because of softness and increased secondary porosity of those beds. The sills range from one to 75 feet in thickness and intruded the sediments up to one half mile from the dike. They are occasionally discordant, cutting across sedimentary units.

The emplacement of pyroxene syenodiorite is considered a major ore control, as it often occurs near major magnetite pods. Mineralization which occurs at great distances from exposures of the late intrusive is generally of lower tonnage and grade.

GEOCHEMISTRY OF THE JONES CAMP DIKE

Geochemical studies of the Jones Camp dike have been conducted by Noguiera(1971), Gibbons(1981) and Jenkins(1985). Although there is a general trend of the diorite to become more mafic towards the dike's edge, variations of individual major elements do not always display well pronounced trends. Gibbons(1981) sampled across the dike at two locations (sections 18 and 24, T5S R7E). The section 24 suite failed to display trends of variation of major elements across the dike. The variation of these oxides across the section 18 suite, however, agreed with observed modal trends. CaO and MgO increase from the center to the margin of the dike, while SiO2, K2O and Na2O decrease. Total iron, TiO2 and MnO are erratic and unpredictable, though they show mutually similar fluctuations. The failure of the section 24 suite to display predictable trends is likely due to secondary alteration effects. That study area is in close proximity to many pyroxene syenodiorite sills, which maintained the hydrothermal convection cells responsible for much of the secondary alteration. The Section 18 study area is more than a mile from the nearest surface exposure of the late intrusive.

Gibbons(1981) plotted the concentration of each element against the amount of silica in each sample. The resulting graphs showed tight geochemical coherence. That coherence

demonstrated that the rocks can be related to some process of fractionation.

Jenkins(1985) analyzed eleven samples of Jones Camp syenodiorite and later pyroxene syenodiorite for major and trace elements. His data indicate that these rocks are comagmatic. He further suggests that the chemical variability he observed resulted from differentiation in situ.

IRON ORE(Ti)

The iron ore in and near the Jones Camp District (Sec. 14, 23 and 24, T5S, R7E) occurs as discontinuous, lenticular pods which conform to the bedding planes of the intruded Permian sediments. These bodies range in thickness from one to 30 feet (Kelley, 1949) but rarely exceed 12 feet. The average thickness is about six feet. They are usually less than 100 feet long, but some exceed 1000 feet of strike length. The typical down-dip depth cannot be accurately estimated at this time.

The greatest exposed concentration of ore pods is in the Jones Camp District. The ore is emplaced in limestone, sandstone and gypsum and along bedding planes between these rock types. Mineralization in the district occurs mainly within the Torres member of the Yeso Formation. A high density of the later pyroxene syenodiorite intrusives also occurs in this area. Although these late intrusives are not

essential to the emplacement of orebodies, they are often associated with large, high-grade concentrations of ore. Iron deposits are generally best developed on the crests and limbs of anticlines parallel and adjacent to the Jones Camp dike.

Smaller orebodies are also found in a variety of other structural and geological settings:

In anticlines and monoclines adjacent to the main dike without nearby pyroxene syenodiorite bodies.

At the edges of pyroxene syenodiorite sills emplaced along bedding planes of sediments. These orebodies may occur at any level in the Yeso, Glorieta or San Andres formations at distances up to several hundred feet from the main dike.

As replacements of limestone inclusions in pyroxene syenodiorite.

As magnetite veinlets along joints in Tjb, Tjc and Tjp.

In altered Jones Camp diorite within inches of the contact with sediments.

Along contacts between adjacent pulses of the pyroxene syenodiorite.

Although these deposits are of lower tonnage, their occurrence is widespread and represent large amounts of iron.

Kelley (1949) lists ore grades of 19 ore pods within the Jones Camp District. The grades range from 41.96% to 62.04% Fe, with an average grade of 55.82% Fe.

The ore texture varies depending on the lithology of the host rock. Limestone hosted ore is massive, fine-grained and pure. It is generally vuggy with secondary calcite lining the vugs. Contacts between ore and unmineralized limestone are very sharp. Limestone usually is preferentially mineralized and hosts the best ore. Sandstone hosted ore is of variable grade with gradational contacts between ore and unmineralized rock. Bickford (1980) suggests that sandstone with calcareous cement may have been preferentially mineralized. Gypsum hosted ore generally carries disseminated magnetite, though some pods in gypsum are nearly pure ore. The higher-grade ore usually has abundant secondary gypsum, both disseminated and in veins. The largest example of gypsum hosted ore is in the east pit, at the eastern end of Jones Camp District.

Magnetite mineralization is almost always fine-grained. Although occasionally medium-grained crystals can be found in vugs of all host rocks and as replacements of detrital grains in sandstone.

Magnetite is the predominant ore mineral, usually comprising more than 90% of an ore pod. Minor pyrite occurs in gypsum hosted ore near the edge of the mineralization. It sometimes comprises up to 15% of the iron minerals

present. Trace amounts of chalcopyrite occur with the pyrite. Late stage copper oxides and carbonates are found coating fractures in the east and west pits. The ore also contains small amounts of ilmenite as lamellar intergrowths in magnetite.

The principle alteration products are martite, maghemite and hematite. Martite (Fe2O3) is hematite psuedomorphous after magnetite, occurring in black octahedral crystals. Gibbons (1981) states that it is the principal alteration product, comprising 2 to 15% of the iron ore(locally up to 70%). Jenkins (1985) disagrees, maintaining that maghemite is the main alteration product. Maghemite (Fe2.66O4) has magnetite structure with a deficiency of iron in the crystal structure. These alteration products result from the late oxidation of primary magnetite. They may occur as complete replacements or as partial replacement in the rims or along crystallographic planes. The distinction between the two is of interest to the present study because maghemite remains strongly magnetic, whereas martite does not.

Hematite occurs on surface exposures of ore pods. It often is psuedomorphous after pyrite, retaining even the original striations. Noguiera (1971) reported goethite as a surface alteration product. The paragenetic sequence of iron minerals is as follows (Gibbons, 1981): magnetite (earliest) - ilmenite - pyrite - maghemite - hematite.

Gibbons tested 20 ore samples for gold, silver and platinum group elements. No values above background levels were reported and it was concluded that there are no economic concentrations of these metals at Jones Camp.

All recent authors agree that the orebodies were emplaced by hydrothermal convection cells. Textural evidence strongly supports this model (Gibbons, 1981; Jenkins, 1985). The Jones Camp diorite dike was intruded in at least two closely spaced pulses, crumpling and pushing Yeso sediments into parallel anticlinal structures. This deformation caused bedding plane slip at the contacts of the limestone, sandstone and gypsum beds, thus enhancing permeability. The temperature of the country rocks in contact with the dike reached 300 degrees C(Jenkins, 1985), well above the temperature of dehydration of gypsum (57 degrees C). Dehydration increased porosity and permeability. The heat from the dike set up convection cells in formation water in the sediments. These cells dissolved country rocks by hydrolysis reactions which increased pH and lowered the solubility of iron-bearing chloride complexes in the hydrothermal solutions. The resulting precipitation of magnetite liberated hydrogen ions, continuing the process of limestone dissolution and magnetite precipitation. The solutions ascended along the dike contact and joints within the border facies, leaching iron and transporting it to structures favorable for deposition. The Abo formation has been considered as a

source for the iron (Bickford, 1980), but the border facies is generally thought to be the major source.

Larger ore concentrations are associated with later intrusions of Tjp, Tjm and possibly other Jones Camp facies. These sills and dikes had several effects which served to enhance mineralization. They provided additional heat to drive convection cells and acted as a cap rock. They also increased permiability and porosity by fracturing country rock and dehydrating gypsum(Jenkins, 1985). Volumetrically, the pyroxene syenodiorite is only a small fraction of the total amount of igneous rock. One would not expect that its presence would dramatically enhance the size and grade of the orebodies.

Jenkins (1985) ascertained the nature of the hydrothermal solutions through his fluid inclusion studies. The fluids were saline to hypersaline, non-boiling and under a hydrostatic pressure of 154 bars. They were cool, as the mean trapping temperature was 166 degrees C. Magnetite deposition occurred near that temperature, at which magnetite solubility is low.

Bickford (1980) estimated ore reserves based on an average ore pod with a thickness of six feet and a down-dip depth of 75 feet. He calculated probable reserves of 1,117,940 tons and possible reserves of 1,575,630 tons.

ALTERATION

The intrusion of the igneous rocks and the accompanying hydrothermal convection cells caused recrystallization and replacement of primary mineralogy. The alteration ranged from slight to complete replacement of the rock. All igneous and sedimentary rock types were affected to varying degrees. Alteration of sediments was restricted to within inches of the contact between igneous and sedimentary rocks.

Jenkins (1985) notes three stages of alteration in the Jones Camp diorite (figure 3). In the earliest stage, primary hornblende converted to actinolite and secondary calcite filled miarolitic cavities. The intermediate stages introduced scapolite, followed by albite. Both minerals replaced both primary and earlier secondary minerals. The albitization sometimes included clinopyroxene and tremolite. Jenkins describes the mottled texture on weathered surfaces of the border facies diorite as concentric zones of scapolite not replaced by albite. Gibbons (1981), Noguiera (1971) and Kelley (1949) attribute this texture to other minerals, but all agree that it is a replacement texture of primary feldspar. The late stage alteration introduced tremolite, actinolite, chlorite, carbonate (calcite and/or dolomite), magnetite, sphene and apatite. Jenkins' late stage veinlets crosscut earlier alteration. These veinlets contain one or more of the following minerals: calcite, magnetite, sphene, tremolite, actinolite and specular

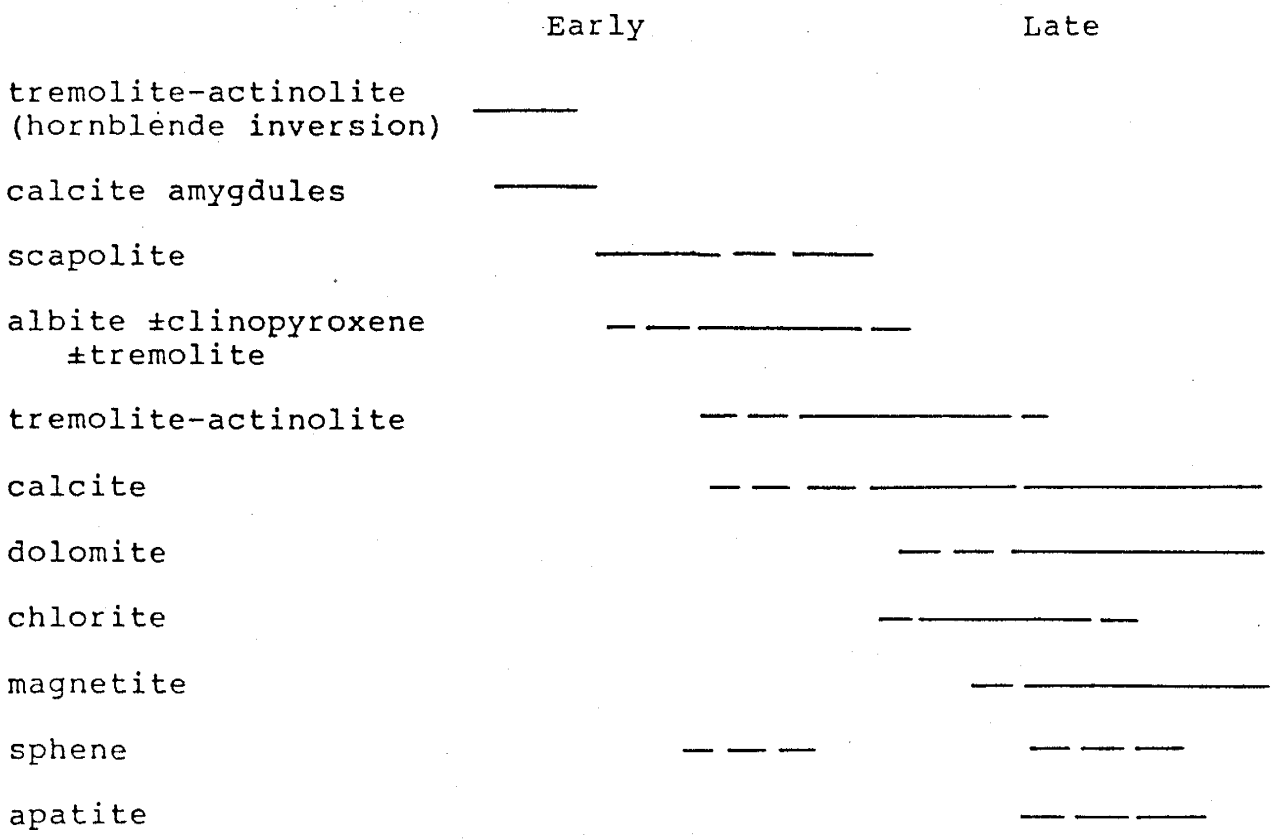

Figure 3. Sequence of alteration in Jones Camp syenodioritic rocks (Jenkins, 1985).

hematite. Iron was removed from ferromagnesian minerals and iron oxides during the intermediate stage and reintroduced as magnetite. Magnetite veinlets were precipitated during the late stage. The magnetite ore pods were emplaced during the late stage. The earliest stage penetrated furthest into the dike and the late stage shows the least penetration. Noguiera (1971) reports epidote coatings on fracture faces and states that it was the last secondary mineral introduced.

Hydrothermal alteration in the pyroxene syenodiorite produced secondary carbonate, chlorite, tremolite, actinolite and magnetite. Veinlets of calcite and magnetite have been observed. Bickford (1980) reports sericite and kaolinite in trace amounts replacing feldspars.

The two uppermost limestone beds of the Torres member are exposed on Chupadera Mesa. Lower limestone beds are exposed west of the mesa scarp. Noguiera (1971) studied locally developed contact metasomatic phases within the sediments. He observed tremolite, actinolite, epidote, andradite garnet, cordierite and aegerine-augite. This mineral assemblage constitutes the albite-epidote-hornfels metamorphic facies, indicating low temperatures (480-510 degrees C) and very low pressures (<1500 bars). The sporadic appearence of cordierite, formed at 510-530 degrees C, places the assemblage within the lower limit of the hornblende-hornfels facies. The contact metasomatic

assemblage is best developed close to the diorite dike at the sedimentary contact between sandstone and dolomitic limestone beds. Only at these "triple contacts" was there sufficient heat, Ca, Mg, and Si to form the metasomatic assemblage. Jenkins (1985) also notes idocrase and spinel. Limestone in contact with earlier diorite was recrystallized locally to white marble. In this study, various degrees of limestone alteration were observed on the section 17 east grid(plate 4) and at the west end of the dike(plate 7).

Hydrothermal activity introduced magnetite and pyrite into gypsum beds. Pyrite is seen only in gypsum as that was the only source of sulfur. Gypsum is often recrystallized to green fibrous or white alabasterine textures. The most important alteration effect was the dehydration of gypsum to anhydrite, which created as much as 37% extra porosity(Jenkins, 1985).

The sandstone beds were metasomatized with development of high temperature secondary silicates and oxides. These include epidote, tremolite, actinolite, clinopyroxene, sphene, apatite and carbonate. Later magnetite replaced detrital quartz and feldspar grains, cement and earlier alteration products. This alteration assemblage is encountered on the Section 19 Prospect Grid(plate 3) and at other locations nearby(plate 5). It is the same rock as that mapped by Kelley(1949) as "actinolite contact rock."

STRUCTURAL SETTING

The Jones Camp Dike intruded the flat-lying Permian strata of the Chupadera Mesa. The mesa is a tableland capped by the San Andres Formation, dipping slightly (~one degree) to the east. In the area of the dike, the maximum elevation is 7,052 feet near the western escarpment. The eastern edge of the mesa is approximately 1,100 feet lower. The mesa extends from the northen edge of the Oscura uplift to the southern margin of the Estancia basin, a distance of about 45 miles. Its eastern boundary is marked by the Chupadera fault, which runs the entire length of the mesa. To the west, the Chupadera anticline separates it from the Jornada del Muerto. The mesa ranges in width from 10 to 15 miles. In the central and southern parts are many local, superficial folds in the incompetent Permian strata. These are due to solution and collapse of underlying beds. Some may overlie buried igneous intrusions (Kelley and Thompson, 1964).

The dike uplifted the strata into a broad east-west anticline dipping away to the north and south. The limbs dip gently except in the immediate proximity of the dike.

The dike is one of several mid-Tertiary igneous intrusions along the Capitan lineament (figure 4), first described by Kelley and Thompson (1964). These include, from west to east, the Jones Camp dike, Lone Mountain, Carrizozo Mountain, Patos Mountain, the Capitan Mountains,

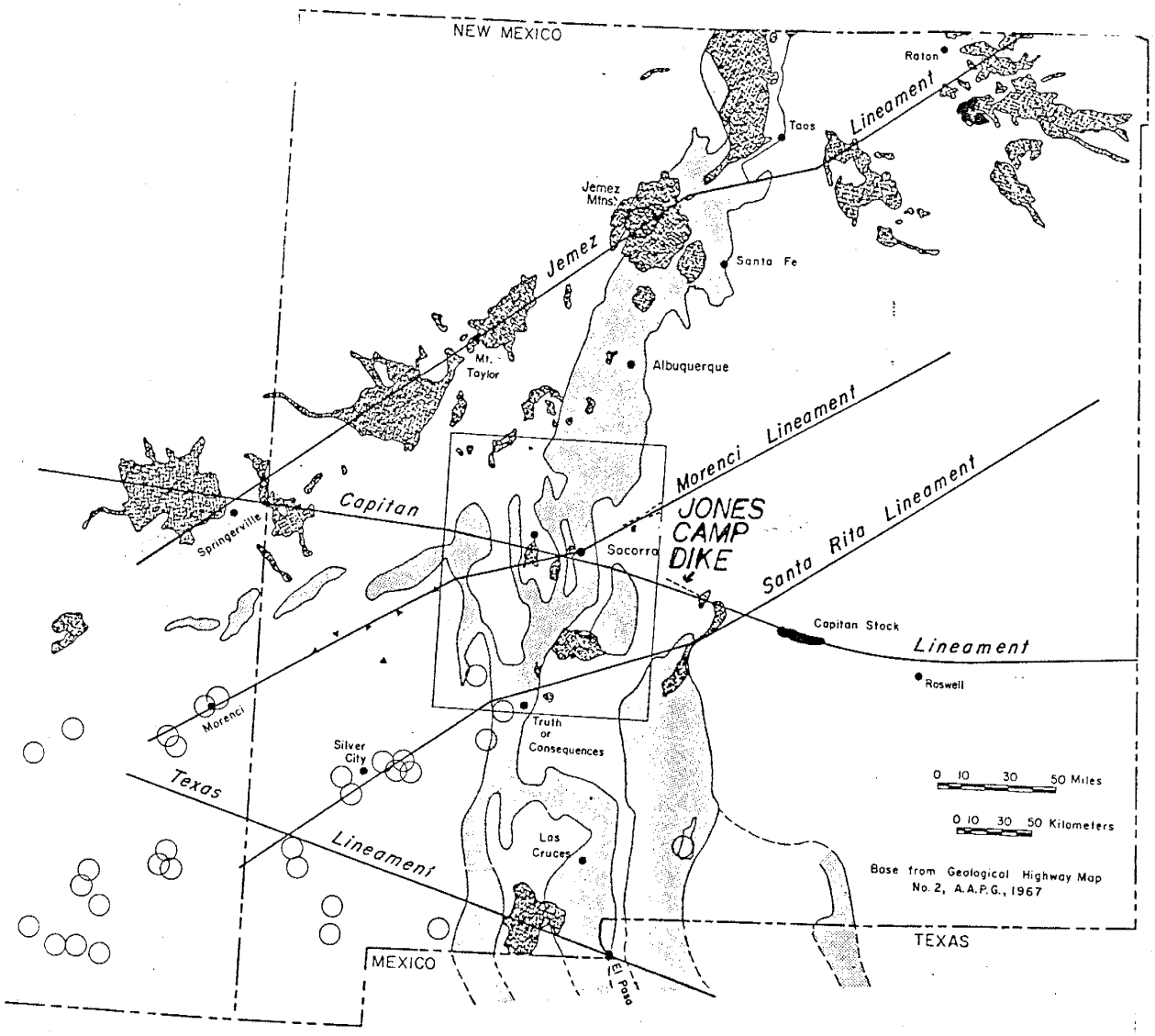

Figure 4. Generalized tectonic map of New Mexico, showing lineaments, volcanic fields and the Rio Grande rift. The Capitan lineament bisects central New Mexico trending west-northwest(Chapin et al, 1978).

the Railroad dikes east of Roswell, New Mexico and the Matador arch in west Texas. To the west, near Bingham Post Office, is an igneous intrusion quite similar to Jones Camp dike. Also on strike of the lineament, a few miles east of Jones Camp, are the vents of the Quaternary Carrizozo basalt fields. Chapin (1978) has tenatively extended the lineament westward into Arizona on the basis of geophysical evidence (personal communication to John Jenkins, 1984). The lineament conspicuously crosscuts the north-south tectonic fabric which has been prevalent in central and eastern New Mexico since Paleozoic time. Along the Chupadera Mesa, there is no evidence that there was any pre-existing fault or fold in the sediments along which the Jones Camp dike could ascend. It appears to have pierced these sediments after coming up a fault in the underlying Precambrian terrane. These considerations suggest that the lineament represents a Precambrian fracture zone.

The Jones Camp dike has been dated by K-Ar methods at 27.9 +/- 1.1 million years (Jenkins, 1985). It crops out in a long, narrow exposure 11 miles long. Topographic ridges and dip reversals in the overlying San Andres limestone indicate that it extends underground at least two miles past its easternmost exposure in section 29, T5S R8E. The dike strikes roughly N75W and dips over 80 degrees to the south. Roof pendants of Yeso sediments are common in the middle of the dike's exposure and at the eastern end. West of the escarpment, sporadic float of limestone and sandstone atop

the dike and the discontinuous outcrop pattern suggest that the top of the intrusion has just been uncovered there. The dike intruded to different levels of the Yeso Formation: to the middle of the Torres member in the west and at least up into the Joyita member in the east.

The structure of the Permian sediments is very complicated in the immediate vicinity of the dike contact. As the dike was emplaced, the beds were crumpled back into long, narrow anticlines parallel and adjacent to the strike of the dike. These anticlines are commonly 100 feet across and high-angle dips are seldom seen more than 200 feet from the dike's edge. Jenkins (1985) noted that these anticlines are often faulted along their axial planes. The dikeward limb is usually situated such that the reconstructed anticline would be asymmetrical. Plastic flowage of gypsum beds appears to have been common. Such flowage removed any confining pressure above and below the limestone beds. The crests of the anticlines probably snapped from brittle failure during deformation and the limbs shifted relative to each other.

The tight marginal anticlines are locally developed against the dike at the west end in sections 11, 12 and 13, T5S R6E(plate 7). That is well to the west of any pyroxene syenodiorite sills or stocks. This suggests that structural ground preparation was accomplished by the emplacement of the main dike.

Small, transverse hinge faults occur in the sediments perpendicular to the dike. They extend about 100 feet from the dike contact.

After the emplacement of the main dike, pyroxene syenodiorite ascended the margin of the dike at many locations. It spread laterally as sills along bedding planes. Some of these sills are a mile along strike and intrude up to one half mile away from the dike. The sills preferentially invaded gypsum beds because of its softness and abundant secondary porosity.

PALEOMAGNETIC STUDY

Outcrops of igneous rocks and iron ore at Jones Camp dike were sampled for paleomagnetic studies. Sample sites were located at eleven places along the dike, as detailed on plate 9. The samples were measured for magnetic intensity, susceptibility and direction of remanent magnetization. One additional site was drilled for susceptibility only. The data suggests several possible models but is not conclusive.

METHODOLOGY

Sample collection

Six to ten rock samples were drilled with a portable drill at each of eleven sites. Each core usually provided two or more specimens for measurement. Bearings and attitudes were measured in the field by sun compass. Brunton compass bearings were not taken due to the high magnetic intensity of the rocks.

Laboratory procedure

The cores had a uniform diameter of 2.35 cm. They were cut to lengths of 2.1 cm, except for ore samples. The ore samples were cut to lengths of 1 cm because of their high magnetite content. The magnetic intensity of each core was measured along three perpendicular axes on a Schoenstadt spinner magnetometer model SSM-1. Measurements were taken after the core was demagnetized along the three axes at

successive levels of 0, 5, 10, 20, 30, 40, and 42 milliTeslas(mT). These are the equivalent of between 100 and 840 times the strength of the earth's field. Demagnetization was performed in a mu-metal shield by alternating field demagnetization. The procedure removes the low coercivity components such as those produced by lightning. Susceptibility was determined for each core by a Sapphire SI-2 susceptibility meter. The magnetometer and susceptibility meter were connected to a North Star microcomputer which stored and processed the data. Fischer(1953) statistical parameters(standard deviation, alpha-95, k, average field direction) were generated. The samples were described by visual examination and reflection microscopy. Appendix III lists the data as well as locations, descriptions and average remanent directions. Appendix IV lists susceptibilities.

PREVIOUS PALEOMAGNETIC WORK

Bickford(1980) measured the intensity and direction of remanent magnetization of an ore sample from section 17, T5S R7E. As no demagnetization was performed on the sample, the measured direction represents natural remanent magnetization(NRM). He measured a declination between north and N10E with an inclination between 55 and 65 degrees below horizontal. This direction is essentially parallel to earth's present magnetic field. The ratio of remanent magnetization to induced magnetization was 2.16:1.

Measurements of NRM(before demagnetization) of 16 cores from ore pods at PM-1 and PM-7 are given in Appendix III. PM-1 had an average declination of 313.2 and inclination of 3.9. It had an extremely wide alpha-95 value of 83.38 degrees. PM-7 had an average declination of 8.8 degrees with an inclination of -17.7 degrees, which is somewhat closer to Bickford's determination. This site also had a high alpha-95; 69.99 degrees.

Because Bickford's sample was not demagnetized, it is likely that Bickford's direction represents viscous remanent magnetization(VRM).

GENERAL REMARKS

A rock's NRM is the summation of remanences acquired by several different mechanisms. The major components of NRM at Jones Camp are VRM, thermal remanent magnetization (TRM) and chemical remanent magnetization(CRM). Isothermal remanent magnetization(IRM), which is acquired during lightning stikes, also affects NRM. Part or all of the remanence may be stripped away by demagnetization, depending on the minerals present and the strength of the alternating field. IRM and VRM are generally removed by low level demagnetization.

During periods of normal polarity, the earth's field is pointed down(positive) and to the north. It points up(negative) and to the south during times of reversed

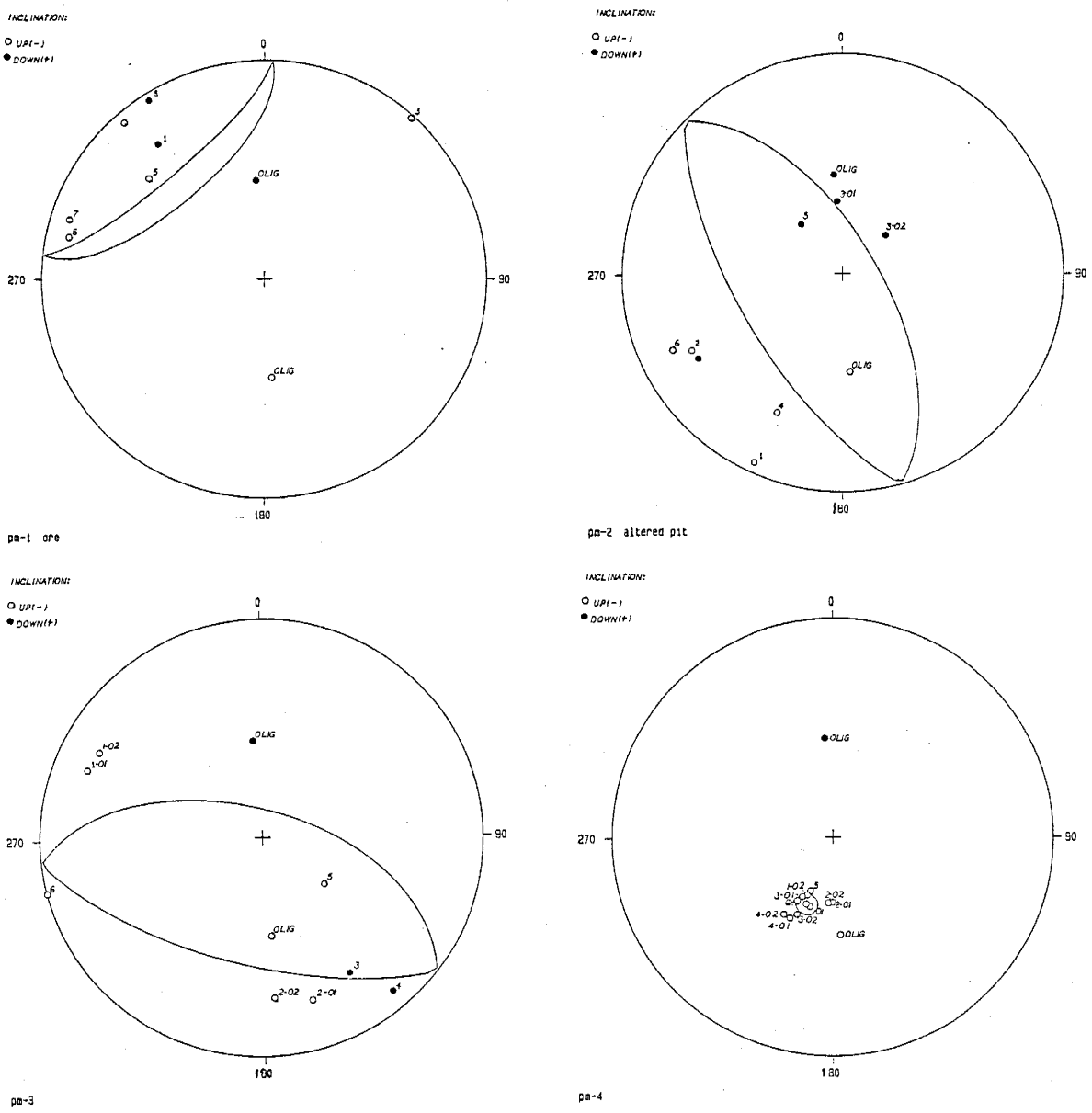

Figure 5. Stereographic projections of paleomagnetic declination and inclination data, Jones Camp dike. All cores have been demagnetized to 42 milliTeslas. The circle across each sphere represents the alpha-95 confidence interval for the average direction(unnumbered) of that site. Average Oligocene directions are shown(OLIG).

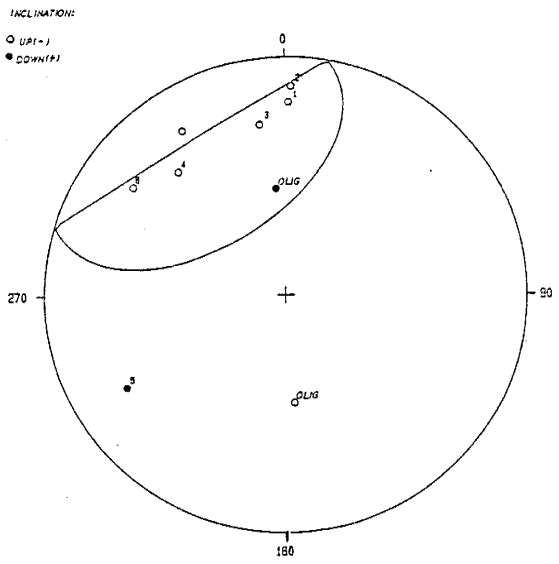

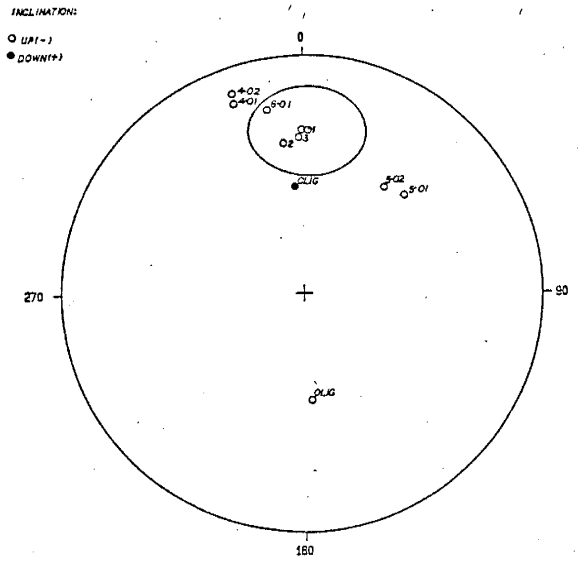

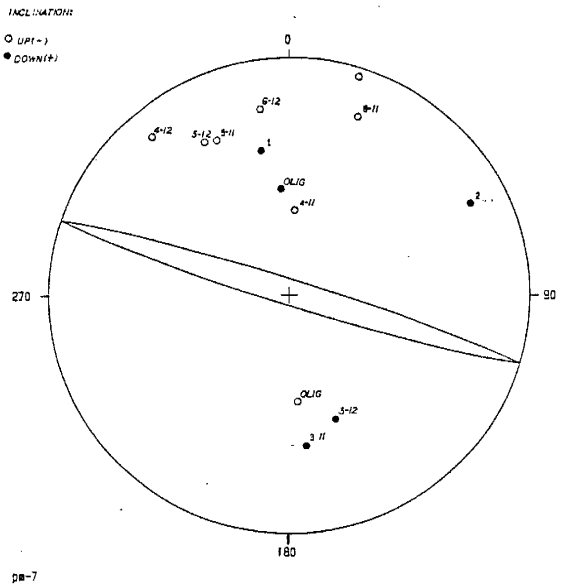

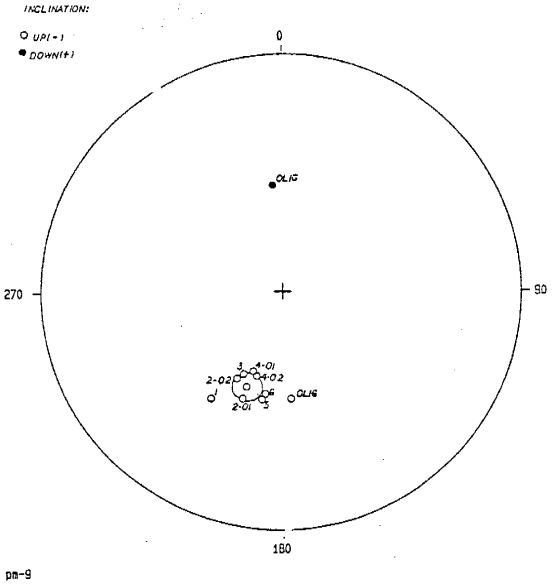

Figure 5. (continued)

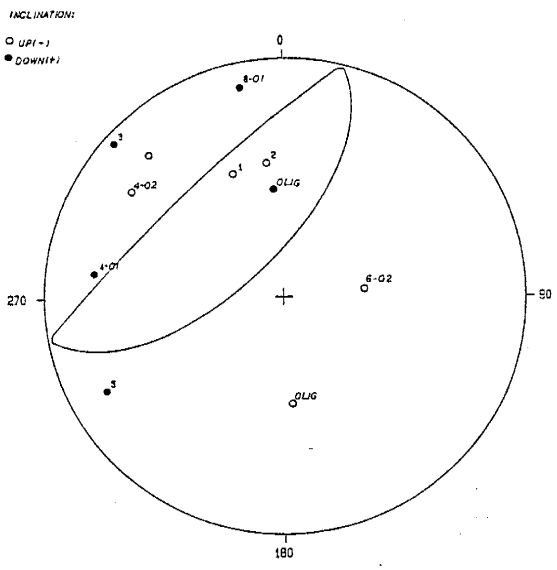

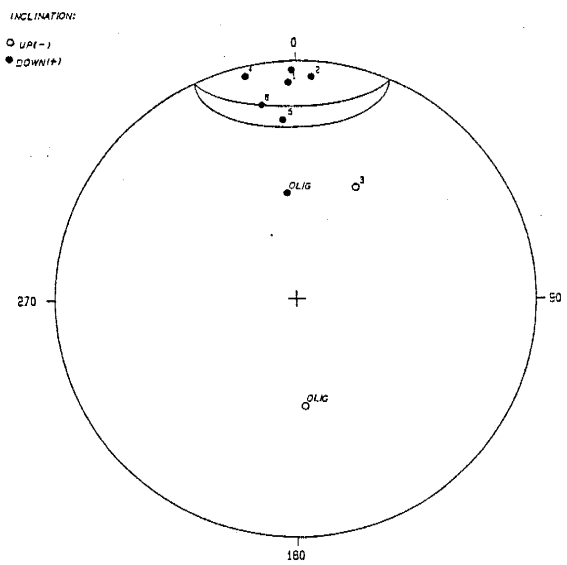

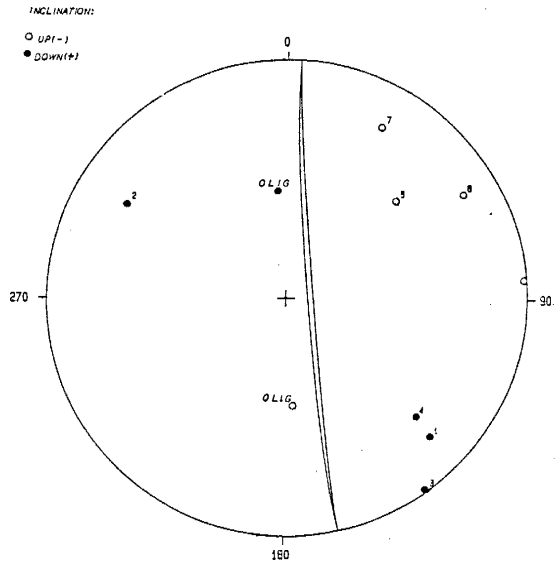

Figure 5. (continued)

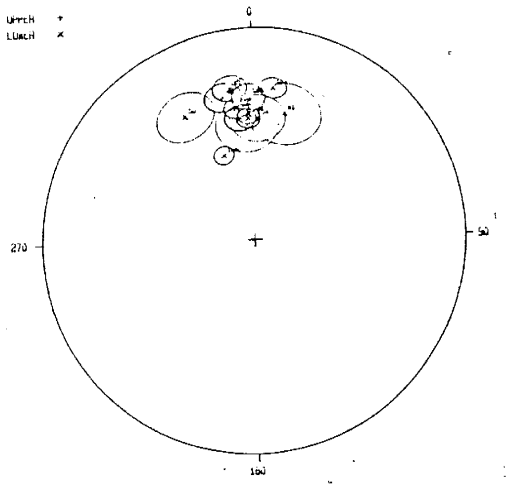

LEMITAR TUFF

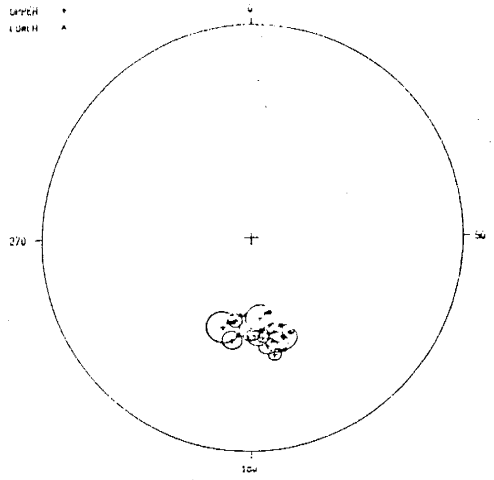

TUFF OF TURKEY SPRINGS

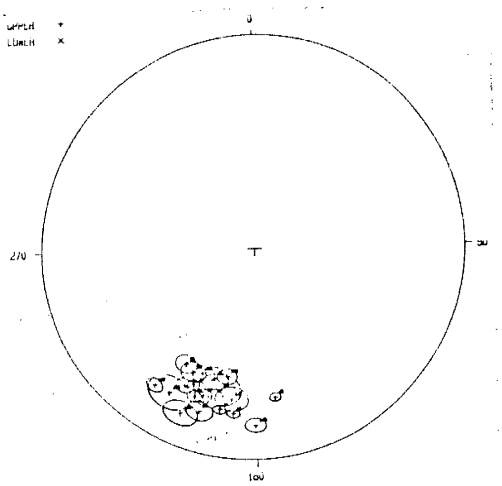

SOUTH CANYON TUFF

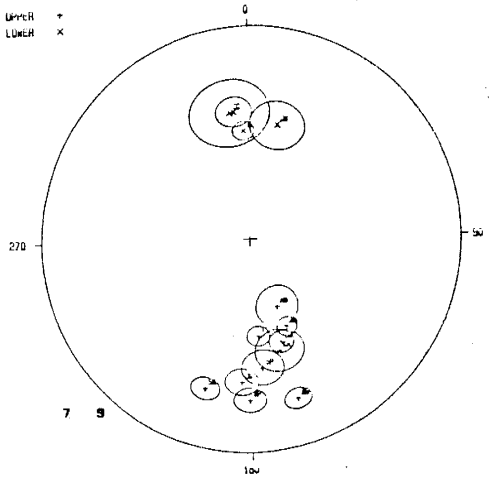

IGNIMBRITE UNIT MEANS

Figure 6. Mean site directions of Oligocene ash-flow tuffs as shown on equal area stereonets. The alpha-95 confidence cones represent the average of cores taken at each site. Sites in the northern hemispheres are positive, or downward-oriented(normal polarity). Those in the southern hemispheres are negative, or upward-oriented(reverse polarity). The Lemitar Tuff has been dated at 27.95 m.y. and the South Canyon Tuff at 27.4 m.y.(Kedzie et al, 1985). The tuff of Turkey Springs is the unnamed ash-flow tuff of McIntosh(1985) which overlies the South Canyon Tuff. The ignimbrite unit means include many older Oligocene ash-flow tuffs.

site		incl	decl	int	k	a95
PM-1	0 mT	3.9	313.2	978.0	1.6	83.38
	42 mT	-5.6	319.2	203.0	3.4	43.18
PM-2	0 mT	50.8	114.3	47.4	3.9	35.06
	42 mT	26.1	239.5	0.452	1.6	76.38
PM-3	0 mT	-39.6	158.8	17.6	1.5	77.38
	42 mT	-29.5	196.1	0.305	1.6	70.85
PM-4	0 mT	-61.4	173.9	0.353	5.7	22.07
	42 mT	-63.0	201.8	0.357	151.4	3.94
PM-5	0 mT	3.8	303.4	2.39	3.1	46.18
	42 mT	-20.2	328.6	0.351	3.1	45.41
PM-6	0 mT	27.1	266.0	2.57	1.7	63.95
	42 mT	-31.4	1.7	0.0966	11.0	17.44
PM-7	0 mT	-17.7	8.8	81.4	1.4	69.99
	42 mT	-4.5	17.7	5.74	1.5	89.07
PM-8	no sample					
PM-9	0 mT	-46.8	210.0	0.314	27.6	10.73
	42 mT	-55.3	201.6	0.217	127.1	4.93
PM-10	0 mT	23.5	325.3	0.00492	2.0	51.24
	42 mT	-19.1	317.2	0.00383	2.0	59.11
PM-11	0 mT	30.1	9.8	2.95	2.8	49.63
	42 mT	4.2	359.2	0.129	8.6	24.35
PM-12	no sample					
PM-13	0 mT	-5.9	89.6	71.7	1.6	74.97
	42 mT	-0.9	85.1	1.57	1.5	82.00

Table 1. Intensities and field directions of remanent magnetization of selected rocks at Jones Camp dike. Data are averages of all sample cores measured from that sample site. Between six and ten cores from each sample site were measured. Data shown for NRM(0 milliTeslas) and for the highest level of demagnetization(42 milliTeslas).

incl - Inclination of average field direction in degrees. Negative(-) inclinations point above horizontal, positive inclinations point below level.

decl - Declination of average field direction in degrees.

int - Remanent field intensity in Oersteds.

k - Precision estimate. k>10 indicates close approximation. Not to be confused with susceptibility, which is also designated as k.

a95 - alpha-95 confidence estimate. a95<10 indicates good confidence.

polarity. Jones Camp stereoplots(figure 5) show the average Oligocene (OLIG) normal and reversed directions(Diehl et al, 1974). For comparison, figure 6 shows paleomagnetic directions of some New Mexican ash-flow tuffs erupted within the error limits of the K-Ar age for the Jones Camp dike(27.9 +/- 1.1m.y.)(W. McIntosh, personal communication, 1985). Figure 6 also shows the mean directions of several Tertiary ignimbrite units.

Fischer(1953) statistical parameters for the remanent directions have been calculated. The precision estimate, k, is an estimate of how closely the observed directions approximate each other. k greater than ten indicates close approximation. This statistical parameter should not be confused with susceptibility, also designated as "k" by convention. The confidence estimate, alpha-95, means that there is a 95 percent chance that the true direction lies in a cone of confidence around the observed mean. The alpha-95 value is the radius of that cone, which is marked as a circle in the stereoplots. Alpha-95 less than ten degrees represents good confidence.

The average remanent directions of rocks at Jones Camp generally have extremely wide alpha-95 cones and low precision estimates(table 1). These represent a wide range of directions measured in cores at each site(figure 5). Measured directions are often oblique or perpendicular to average Oligocene directions. All sites except PM-4 and

PM-9 show flat or shallow(less than 32 degrees) average inclinations.

For 17 of the cores, both the top and bottom were measured. Generally, these cores show good agreement, within five degrees of each other. In the extreme case (PM-10-6, 01 and 02), declinations differed by 96 degrees and inclinations by 73.6 degrees.

Only half the sites(PM-1, 4, 5, 6, 9 and 11) show any tendency to cluster around the mean direction. Alpha-95 values for these sites range from 3.94 to 45.41 degrees. The alpha-95 values for sites 1, 5, 7, 10, 11 and 13 are increased considerably by one or two outlying points which differ radically from the rest of the population.

Demagnetization strips away a certain amount of the remanent intensity, depending on the minerals present and their grain sizes. Loss of original intensity after demagnetization to 42 mT varied widely among the samples, from no change(PM-4) to a couple orders of magnitude (PM-2, 13). The ranges of intensities at each site, both before and after demagnetization, are presented in figure 8. The intensities of some rocks remained virtually unchanged while others were greatly decreased. Ehrlich et al.(1969) reported that Precambrian hematite ore and hematite-bearing andesite at Iron Mountain, Missouri showed stable NRM. However, hematite ore containing more than 2% magnetite required demagnetization at levels of 40 to 80 mT before

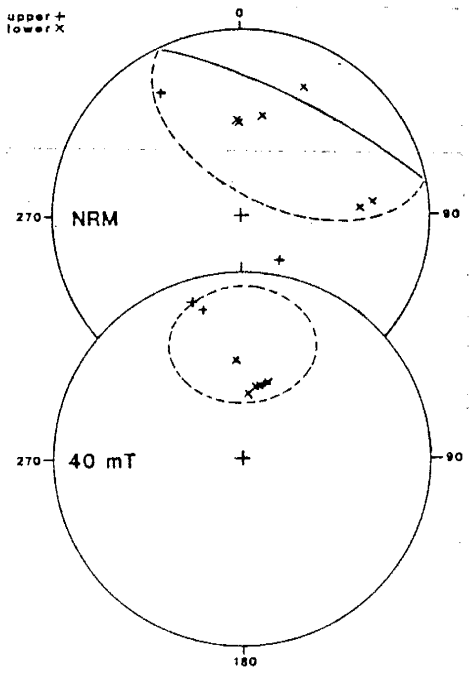

LEMITAR TUFF- Site 30

Figure 7. Demagnetization behavior of hydrothermally reddened Lemitar Tuff(McIntosh, 1983). Although the site shows a wide alpha-95 cone after demagnetization, it has much better precision than the original natural remanence.

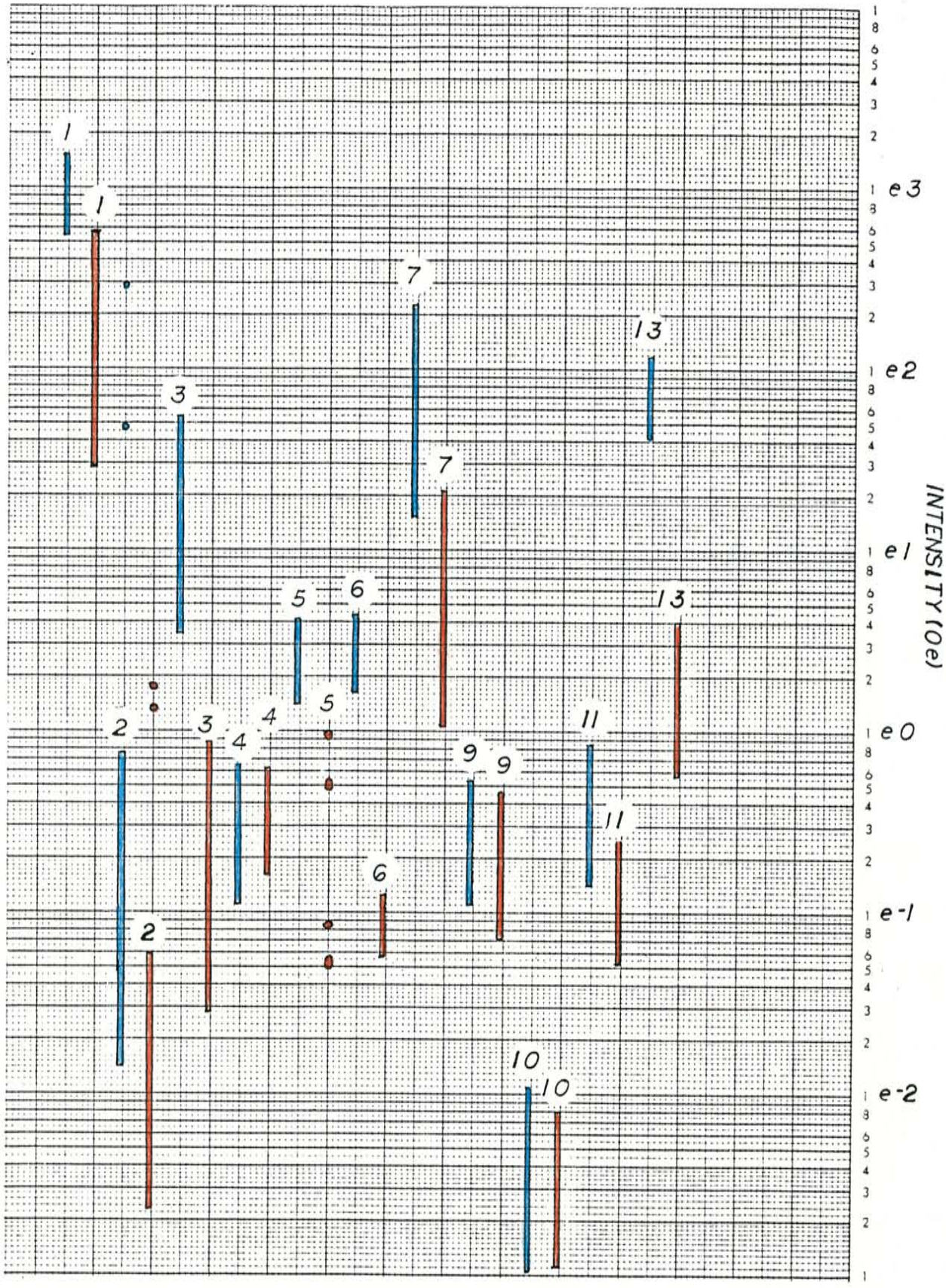

Figure 8. Ranges of magnetic intensities exhibited by paleomagnetic cores collected at the Jones Camp dike. Ranges to the left(blue) represent NRM(no demagnetization). Ranges to the right(red) show remanent intensity after demagnetization to 42 mT.

reliable field directions were obtained. Unfortunately, demagnetization equipment used in this study could not produce fields greater than 50 mT.

INTERPRETATION

The paleomagnetic data collected at Jones Camp indicate a complex history of remanence acquisition. Several strong mechanisms influenced the magnetization of the rocks, imprinting remanent directions which were quite different from the direction of the contemporary field of the earth(figure 6). This process probably occurred over an extended period of time. Earlier authors have amply documented the hydrothermal alteration which is pervasive at Jones Camp. For a contemporary analog, the reader is referred to the stereoplot of a hydrothermally reddened site in the Lemitar tuff(figure 7)(McIntosh, 1983). This site shows a wide distribution of paleomagnetic directions, although the scatter is not as extreme as at Jones Camp sites. The wide range of values seen at most sites in this study indicates that several remanent directions are imprinted on the rocks. These directions cancel one another to some extent, giving an averaged remanent direction. The average can change drastically over short distances within the rock(centimeters to millimeters).

The acquisition of remanent magnetism at the Jones Camp dike is intimately related to the manner of emplacement of the igneous rocks. The diorites were emplaced in at least

six pulses as a long, narrow, tabular body. Hydrothermal activity was prevalent, probably over the entire history of intrusion. The high surface to volume ratio of the dike undoubtedly increased the rate of heat loss. It is not known how quickly each pulse followed its predecessors. If the hiatus was fairly long(several thousand years), the hydrothermal episode caused by each intrusion would conceivably have been short and distinct. However, if the pulses followed one another in rapid succession, they would have all contributed to a single, larger hydrothermal episode. The dike is nearly vertical, so the study area quite likely was affected by heat and hydrothermal solutions ascending from lower portions of the dike and the magma chamber at depth.

Noguiera(1971) studied mineral assemblages in order to define the heat regime at the time of emplacement. He found that the central portion of the dike was emplaced at temperatures of 800 to 900 degrees centigrade. The temperature of the intrusive at the contact with the sediments was 600 degrees centigrade and adjacent alteration was 475 to 550 degrees centigrade. He gave a range of temperatures between 450 and 550 degrees centigrade for magnetite ore pods. Jenkins(1985) studied fluid inclusions in calcite which was cogenetic with magnetite mineralization. He found a trapping temperature of 166 degrees centigrade in a saline to hypersaline, non-boiling solution under 154 bars of hydrostatic pressure. The

present author found conodonts in the top limestone bed of the Torres member at the section 19 prospect grid. One of these was identified as Polygnathus sp.(Stan Krukowski, personal communication, 1985). These conodonts were black, with a color alteration index of six. This color results from temperatures of 450 degrees centigrade(Epstein et al, 1977).

One must consider the heat flow regime of the dike when attempting to interpret its paleomagnetic characteristics. The following text discusses mechanisms and conditions which complicated the acquisition of remanent magnetization.

CRM is acquired as a mineral nucleates and grows in an applied magnetic field. As a crystallite grows past its blocking volume, magnetic domains form and acquire the direction of the prevailing field of the earth. Slow and sporadic growth of a magnetic crystal would create several distinct domains which would counterbalance one another. Tarling(1983) characterizes domains as "very variable, reflecting the presence of impurities, defects, etc. within the crystal lattice..." Extended and possibly intermittent periods of hydrothermal activity controlled the growth of crystals at Jones Camp.

The magnetites in the Jones Camp igneous rocks are rich in titania, with circa 2.5 percent(Gibbons, 1981). Magnetite is in a solid solution series with ulvospinel(Fe_2TiO_4). As the amount of titanium in the

magnetite increases, the Neel temperature decreases(Tarling, 1983; figure 3.2). The high-titanium magnetites have depressed Neel temperatures of ~500 to 520 degrees centigrade, as compared with 590 degrees centigrade for pure magnetite. A similar relationship exists in the hematite-ilmenite solid solution series. The variability of titanium concentration and metasomatism would enable minerals within a single rock to acquire magnetism over a wide range of temperatures. Such a circumstance would allow acquisition of wide range of remanent directions. In a hydrothermal system, minerals with depressed Neel temperatures would also be more susceptible to overprint by secondary TRM. The heat produced by later intrusives and hydrothermal activity at Jones Camp approached the depressed Neel temperatures of the titanium rich iron oxides. Ilmenite exsolution complicated the situation further.

During the concentration of magnetite in the ore pods, grain to grain interactions overwhelmed the earth's field. In other words, the applied fields of large crystals influenced adjacent small grains more strongly than did the earth's field. The larger crystals, which exhibit complex multi-domain behavior, tend to have variable remanence directions and do not create uniform directions in the smaller grains. Bimodal grain size distributions are common in Jones Camp ore.

Due to volume changes caused by dehydration of gypsum and multiple intrusions, some slumping and rotation of rocks at the dike's margin probably occured. It is also possible that late intrusions pushed up earlier emplaced rock, rotating it in the process. Some Jones Camp rocks have reasonable declinations, but their inclinations appear to have rotated away from the average Oligocene value.

Many aspects of the data suggest that the dike was emplaced during a polarity reversal of the earth's field. Two sites(PM-4 and 9) sampled the fine-grained border diorite facies, which was the earliest igneous pulse. PM-5 and 11 sampled porphyritic pyroxene syenodiorite sills, which is the latest igneous pulse included in the paleomagnetic study. The border facies shows a good reversed orientation, whereas the pyroxene syenodiorite shows normal declination with with shallow inclination. The other sites have more scatter in remanent directions. At first examination, the data suggests that the border facies intruded during a period of reversed polarity. The ore, alteration and coarse-grained central facies were emplaced during a reversal and the pyroxene syenodiorite during the subsequent period of normal polarity. The duration of polarity reversals is between 1000 and 10000 years(Tarling, 1983), approximately the lifespan of most hydrothermal systems.

Other considerations cast doubt on this interpretation. It is questionable whether the remanent directions in the border facies are held by primary or secondary mineralogy (see discussion below). Nor can the normal directions of the pyroxene syenodiorite be considered valid without rotation of the rocks. In other studies of rocks magnetized during polarity reversals, the scatter of remanent directions reaches a maximum as the intensity is at a minimum(Dodson et al., 1978). Jones Camp directions were subtracted from average Oligocene directions and the differences plotted against intensity. No coherent trends were observed.

The model of intrusion during a polarity reversal is an appealing explanation for the behavior of magnetized rocks at the Jones Camp dike. At this time, however, it cannot be enthusiastically proposed due to lack of data and the unresolved objections discussed above. There is an additional possiblity that the dike was emplaced during a paleomagnetic field excursion, or failed reversal.

PALEOMAGNETIC SAMPLE SITES

The preceeding discussion listed factors which may have caused the erratic magnetism in the study area. Present evidence favors complex thermal and chemical remanence acquisition as the most likely causes. A specific discussion of the sample sites follows. Refer to plate 9 for locations, table 1 for paleomagnetic data and

statistical parameters and figures 5 and 8.

Iron ore(PM-1, PM-7)

These sites sampled ore outcrops. PM-1 is a vertical, sandstone-hosted ore pod on the Section 19 Prospect Grid (see plate 3). That orebody has a wide range of grain sizes, with magnetite crystals up to 0.5 cm across. Hematite is common, replacing both magnetite and pyrite. The mean direction has a wide alpha-95 which would improve considerably if core 1-3 were excluded. Inclinations would continue to be problematic. CRM and grain to grain interaction are probably the most important influences, with possible minor post-depositional rotation upward and to the north.

PM-7 is located on the section 17 prospect grid(plate 4). It is composed of fine-grained magnetite ore which is a replacement of limestone. It has vuggy texture, with some vugs exceeding one centimeter in length and usually lined with secondary calcite. The sampling site was located on poor outcrop and one or more of the cores may have come from a slump block. The cores show more scatter than those of PM-1, although the alpha-95 is much exaggerated by the top and bottom of core 7-3. Note the large differences between the tops and bottoms of cores 7-4 and 7-6. This indicates a large change in domain directions over the distance of one centimeter. CRM and grain to grain interaction are the dominant influences affecting magnetism here.

Ueno(1967) found vertical inclination in a vertical tabular magnetite body at the Kamaishi iron-copper deposits in northeast Japan. He proposed that the orebody acquired remanance coincident with the direction of elongation of the body. The ore pods sampled at Jones Camp dike do not exhibit this tendency. Similarly, Strangeway(1961) found that declinations of Precambrian diabase dikes on the Canadian shield coincide with the strikes of the dikes. This phenomenom is not observed in the various diorite facies sampled in the present study. However, the Jones Camp rocks which don't have well defined Oligocene remanence directions show shallow(<32 degrees) or flat average inclinations.

Actinolite contact rock(PM-2)

Samples were taken from the walls of a prospect pit on the Section 19 Prospect Grid. The rock was sandstone which was altered to actinolite, tremolite, calcite, hematite and magnetite. Note the moderate loss of intensity. The outlying points with high intensity are the top and bottom of core 2-3, which is predominantly magnetite. Cores 2-3 and 2-5 roughly approximate the average Oligocene normal direction and may represent good remanence acquisition. The other four directions are pointed southwest, perpendicular to the strike of bedding of the original sandstone. One might interpret them as preserved detrital remanent magnetization(DRM) of reversed polarity in the Permian

sandstone. The author rejects this notion. The sandstone dips circa 20 degrees to the northeast, and the rotation should have shifted the inclinations in that direction, not towards a shallow angle pointed southwest. The sandstone has been completely replaced by hydrothermal alteration and all detrital iron oxide in the original rock has been destroyed. Thermal conditions, chemical alteration and grain to grain interactions have set the magnetic directions in this rock.

Central facies(PM-3)

This site is located on an outcrop of the coarse-grained central diorite facies. This facies was probably intruded as a crystal mush. Its magnetites contain circa 2.5 percent titania. Gibbons(1981) found magnetite replacing original mineralogy indiscriminately, particularly ferromagnesian minerals and plagioclase. The titania content of the secondary magnetite is presumably lower and more variable.

PM-3 is near the northeast corner of the section 19 prospect grid and has undergone light to moderate albitization. The intensity of PM-3 was decreased by two orders of magnitude after demagnetization. The titanium content probably affected the acquistion of TRM and chemical alteration certainly affected CRM.

Albitite(PM-10)

Site PM-10 is located approximately 150 feet north of the eastern part of the section 17 east grid. It is fine to medium-grained albitite. It consists of approximately 75% feldspar with minor secondary epidote. There is wide scatter in the remanent directions the tops and bottoms of duplicate cores. A trace of coarse specular hematite as found. Of all samples, PM-10 showed the lowest intensity of any of the facies and showed no drop during demagnitization. The visible hematite and lack of magnetite indicates that it has been heavily altered. It is unknown whether this albitite was a primary intrusive phase or an alteration product.

Mottled border facies(PM-4, PM-9, PM-13)

These sites sampled the fine-grained diorite border facies. Two sites(4 and 9) have been intensely altered, with much of the primary mineralogy replaced by albite, scapolite, actinolite, tremolite and specular hematite. PM-4 and PM-9 were collected on the section 19 and section 17 east grids, respectively. Both show high precision in their remanent directions and no change of intensity after demagnetization. Hematite characteristically retains its intensity at the relatively low demagnetization levels employed in this study. Gibbons(1981) found that hematite in the border facies is secondary, resulting from the breakdown of ferromagnesian minerals. Hematite in the paleomagnetic specimens also appears to be secondary.

The remanent directions were probably imprinted at these sites during the hydrothermal activity which metasomatized the border facies. The high precision suggests that this episode was short-lived. Visual examination of the cores clearly illustrates that it was very intense. The sequence of intrusive events suggests that it occurred relatively early in the history of the dike's emplacement. The high precision of these directions is conspicuous when compared to the wide scatter observed in the less altered, coarse-grained central facies. The alteration of the border facies was probably contemporaneous with the emplacement of the central facies and later igneous pulses and the differences in their remanences are problematic. Early alteration appears to have removed all primary magnetic minerals. The remanence in PM-4 and PM-9 is held by secondary hematite which was introduced during the waning stages of hydrothermal activity. This occurred during a period of reversed polarity.

PM-13 is less altered but has much more erratic remanence. The site is at the zero point of the transverse line(plates 7 and 8) at the west end of the dike. No outcrops of central facies diorite occur nearby. This lends support to the hypothesis that the proximity of the central facies was responsible for the hydrothermal activity which imprinted precise reversed remanence on PM-4 and PM-9. It also suggests that those rocks may originally have had the scattered remanent directions characteristic of other rocks

at Jones Camp dike. The wide alpha-95 of PM-13 would improve considerably if core 13-2 were eliminated. The other cores show two distinct populations: one pointing up and to the northeast, the other pointing down and to the southeast. The cores were collected along an east-west line seven feet in length. Some change has occurred here over a short distance. That change, however, is not apparent on the outcrop. There is not sufficient evidence to allow an interpretation of this site.

Pyroxene syenodiorite(PM-5, PM-6, PM-11)

The cores of PM-11 were collected in a drainage cutting a pyroxene syenodiorite outcrop in NW4 NE4 SW4 section 15 T5S R7E. At the outcrop, stringers of porphyritic pyroxene syenodiorite two to three inches wide intrude an earlier igneous rock. Only the porphyritic rock was sampled. If core 11-3 is excluded, the directions have reasonably good precision. They point down and to the north. These directions are suggestive of normal polarity, though the inclinations are very shallow. The porphyritic pyroxene syenodiorite and its host have intruded the gypsum and sandstone beds between the two uppermost limestone units of the Torres member(Jenkins, 1985, plate 1). They appear to have intruded as a large, northward dipping sill. It is proposed here that the sill slumped downward due to enhanced porosity in the underlying gypsum close to the main dike. This slumpage would have rotated the sill upwards to the

north, thus decreasing the apparent inclination by approximately 40 degrees.

PM-5 and PM-6 were collected from a pit wall on the north side of the main dike at NE4 NE4 NE4 section 23 T5S R7E. PM-5 is porphyritic pyroxene syenodiorite which occurs as one inch stringers intruding a fine-grained, slightly albitized diorite. PM-6 was collected from that fine-grained rock, which is quite similar to PM-13 in appearence and is believed to be Tjb. PM-6 has a reasonably good alpha-95, which is exaggerated by duplicates of outlying values given by 6-4 and 6-5. PM-5 has wide scatter, although the alpha-95 would be much better if core 5-5 were eliminated. The cores for both rocks were collected along a 30 foot exposure of the pit wall. Interpretation will be based primarily on cores 1, 2 and 3 of both rocks, as these were collected within a few feet of each other and show a somewhat good clustering of values. If these cores represent clean remanence, they may have been normal directions which were rotated upwards to the north approximately 80 to 90 degrees. Such extreme rotation probably could not have been caused by slumpage. It is conceivable that a later igneous pulse beneath the sites lifted and rotated them from their original position of emplacement. Although rotation of sites 5 and 6 is highly conjectural, paleomagnetic and field evidence lend support to such an interpretation for PM-11.

DETAIL MAGNETIC WORK

PREVIOUS MAGNETIC WORK

Regional aeromagnetic measurements of the Jones Camp Dike area were made during the Department of Energy's National Uranium Resource Evaluation(NURE) program(Department of Energy, 1977). The data were collected along east- west flight lines three miles apart, which were tied into north-south flight lines spaced 24 miles apart. The flight altitude was 400 feet. The dike fell between latitudinal flight lines. The far western end was intersected by a longitudinal flight line. The dike made no signature on the regional aeromagnetic map(Figure 9). The southern part of the Chupadera Mesa is expressed as a northwesterly dipping negative magnetic gradient related to the Torres anticline to the west. The magnetic map of the immediate area apparently reflects structure on the granitic and gneissic Precambrian basement. The negative readings indicate that the basement carries magnetization of reversed polarity. The NURE data has been incorporated into a statewide aeromagnetic map of New Mexico(Cordell, 1985)

A longitudinal flight line was flown along the boundary between sections 10 and 11, T5S R6E. No anomaly registered on this line. The main dike is buried at its intersection with that section line, but two small(~30 feet wide) parallel dikes crop out approximately 500 feet to the south(offset trend; see plates 7 and 8). One of these

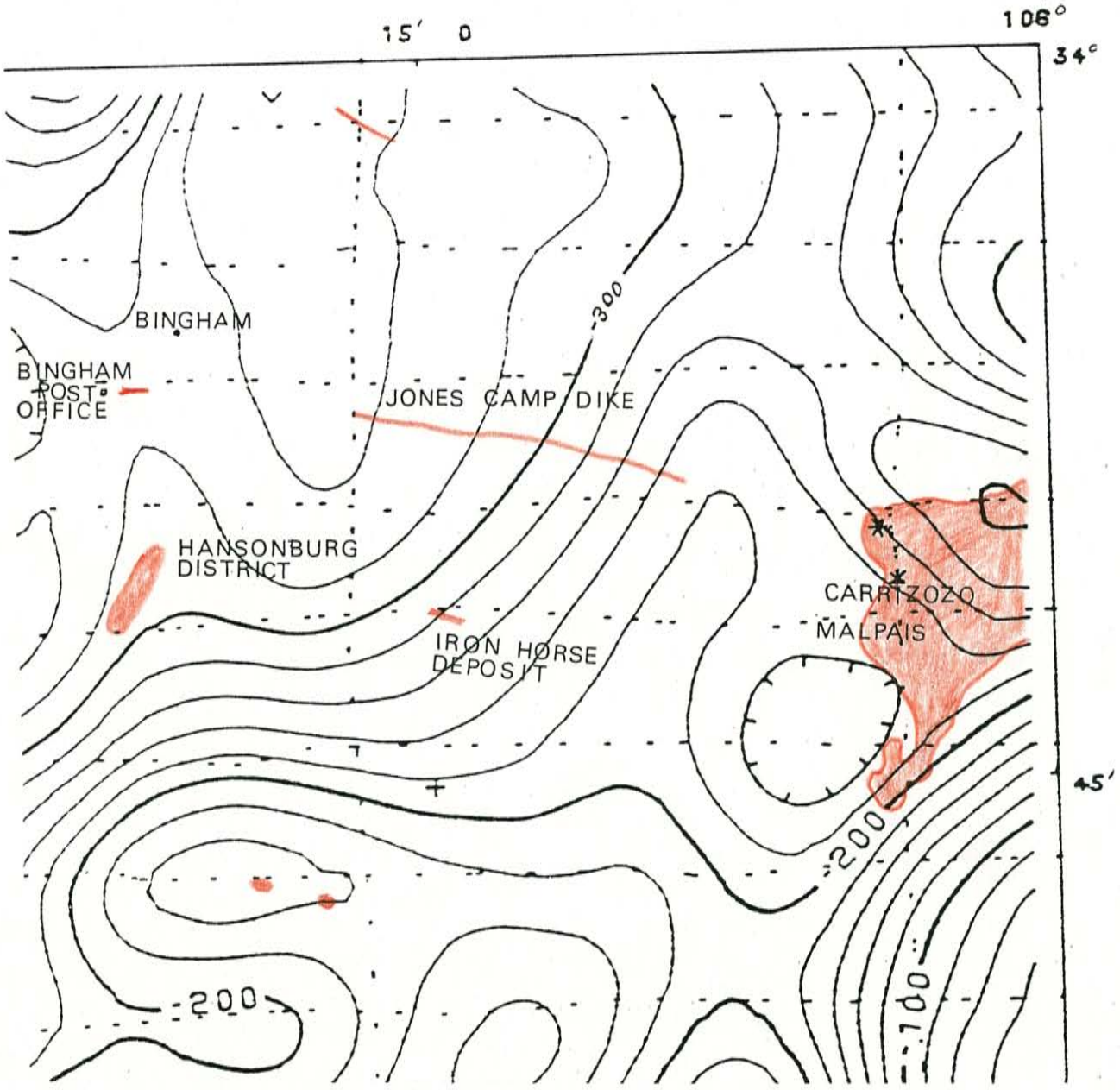

Figure 9. Aeromagnetic data acquired by the National Uranium Resource Evaluation(NURE) program in eastern Socorro County, New Mexico. Solid lines are contours of magnetic field anomaly(contour interval; 20 gammas) and broken lines are flight lines. Igneous features and mining districts are outlined in red. The western end of the Jones Camp dike was intercepted by a north-south flight line. Neither the dike nor the Iron Horse Deposit leave any signature on the magnetic map(after Department of Energy, 1977). 1"=4 miles.

dikes is composed of moderately altered Tjc and produced a positive anomaly of 570 gammas where it intersects the section line. That anomaly was measured by a proton precession magnetometer with an instrument height of eight feet. As magnetic field strength decrease by $1/r^2$, an anomaly measured from eight feet is 2500 times larger than one measured from 400 feet. Hence the 570 gamma anomaly would be undetectable in the aeromagnetic survey. Additionally, aeromagnetic surveys do not make continuous measurements, but rather a series of discreet readings. It is likely that the aircraft conducting the survey did not take a reading directly over the small dike. Iron deposits identical to those at Jones Camp occur at Bingham Post Office and Iron Horse(figure 9). These lie near latitudinal flight lines but produced no anomaly in the NURE study.

Bickford(1980) produced a reconnaissance scale magnetic map of the dike atop Chupadera Mesa. He established a baseline along the crest of the dike and measured magnetic profiles perpendicular to this baseline. His readings were taken 50 feet apart. Profiles were measured every 500 feet, with closer spacing in areas of interest. Bickford located his profiles by pace and compass and collected his data with the same instrument used by the present author.

In the present study, this baseline has been extended two miles farther west to the intersection with the NURE longitudinal flight line(West-end axial line, plate 8).

Magnetic readings were taken at 100 foot spacing. A two mile line perpendicular to the dike was measured(transverse line) and smaller transverse lines were run over areas with high-level anomalies.

METHODOLOGY

In this study, detailed magnetic maps have been generated for two magnetite pods along the southern margin of the dike. These are located in section 17, T5S, R7E and section 19, T5S, R8E. Readings were taken at ten foot intervals over grids approximately three acres in size.

The grids were surveyed with a Brunton compass and 50 foot chain. After an east-west baseline was established, north-south crosslines were located at 50 foot spacing. Data was collected at ten foot intervals along these lines(five foot intervals over anomalies). Areas between the crosslines were sampled at ten foot spacing. This method of "filling-in" the grid allowed several stations on the crosslines to be measured two or three times. The average of these multiple readings has been used on the magnetic anomaly maps(Plates 1 and 2). Magnetic profiles (figures 12, 13, 14, 15, 16 and 18) are generated only from values obtained on the day that particular line was measured. Stations are marked at 50 foot intervals by stakes or cairns.

Magnetic base stations were established near the grids. Care was taken to place these stations in sediments well away from igneous or magnetic rocks. It was necessary to locate them within short walking distance of the grids so that they could be measured several times daily. For this reason, the base stations fall within the range of marginal magnetic effects of the dike. The measurements, however, were stable and reproducible and the base stations are considered trustworthy. Since diurnal variations were insignificant compared to the anomalies observed, no corrections were applied. Base station readings are included with the magnetic data in Appendix II. Descriptions and locations of the base stations are given in Appendix I.

The use of a surveying chain allowed highly accurate location of the stations on the grid. As magnetic readings were taken, the geology at each station was noted. Later detailed mapping improved the geologic maps of the grids(plates 3 and 4).

The magnetic surveys were conducted with a Geometrics G-816 proton precession magnetometer, which measures the total magnetic field. At least three measurements were taken at each station. The average of these readings is the value for that station. Readings are reproducible within one or two gammas under normal circumstances. However, the magnetometer displays a curious effect in the proximity of

magnetite pods. In such areas of extremely high magnetic gradient, the signal degrades as evidenced by successive non-repeating measurements at the same location. This "scatter effect" produces a wide range of values, often several hundred gammas. In extreme cases, the difference between high and low readings exceeds two thousand gammas. The effect is most pronounced over exposed magnetite and less severe or non-existent over buried orebodies. The scatter effect is observed over large positive and negative anomalies and the transitional zone between them. For example, station 10S 420W on the section 19 prospect grid, in a transition zone, has a value of 51345 gammas, only five below the background level. Yet the readings ranged between 51101 and 52368 gammas. The scatter effect generally indicates ore, even though the values may not necessarily be high.

The scatter effect is commonly associated with proton precession magnetometers. It has been described by Breiner(1973), who attributes it to high magnetic gradients. The gradients are caused by high concentrations of magnetite in the ore pods. Breiner suggests that the magnetic sensor be raised as high as 15 feet or that multiple readings be taken and averaged. A longer sensor pole would have been cumbersome due to wind and trees in the field area, so the latter solution has been employed. Under normal conditions, with less than ten gammas of difference, three readings were taken. When the scatter ranged between ten and 100 gammas,

five readings were taken. Nine readings were taken when more than 100 gammas range was observed in the initial measurements. As might be expected, the average values are not always reproducible. As was mentioned earlier, many stations on crosslines were measured two or more times on different days. The range between averaged values is generally two or three hundred gammas. In the extreme case, the difference was 3309 gammas(Section 19; 70S 450W). Away from areas of high magnetic gradient, however, readings are reproducible within one or two gammas.

Magnetic anomaly maps have been prepared from the data(Plates 1 and 2). The values plotted on these maps are net anomalies, derived by subtracting the "zero" (background) value from the absolute value. The maps are contoured at intervals of 1000 gammas. Positive anomalies start at +1000 gammas. Throughout this study, "low-level" (1000-2000 gammas), "medium-level"(2000-3000 gammas) and "high-level"(>3000 gammas) will be used to describe the magnitude of positive anomalies. These terms coincide with the colors of the positive anomaly ranges. Negative anomalies begin at -500 gammas. The zero value was determined from measurements taken over sediments away from the dike on the transverse line at the west end of the dike. The zero value is set at 51350 gammas and all corrections and anomalies have been adjusted to that value. It is at variance with Bickford's(1980) zero value of 51764 gammas. This value represents the average of his base station

readings. Fabiano et al.(1976) give a background value of approximately 52170 gammas for the year 1975. Application of the annual change factor cited in that reference(-45 gammas per year) gives a total intensity of 51720 gammas for the Jones Camp Dike latitude(T5S) for the year 1984. The western end of the dike is approximately 350 gammas lower than this predicted intensity. That negative anomaly is consistent with the NURE data (Figure 9). Bickford's unspecified base station was probably located within a positive magnetic anomaly.

The highest positive anomaly recorded during the surveys was 7,157 gammas(absolute value: 58,507) at station 80S 390W in the section 19 prospect grid. The lowest negative anomaly was -2,028 gammas (absolute value: 49,322) at station 10N 650W of the section 17 east grid.

SUSCEPTIBILITY

Magnetic susceptibility determines the degree to which a rock may be magnetized by an applied field. Magnetite has the highest susceptibility of any known substance, between 0.1 and 1.6(Telford, 1976). During the course of the paleomagnetic study, various Jones Camp rock types were measured for susceptibility. The results are presented in figure 10 and Appendix IV. The range of values covers four orders of magnitude. Magnetite ore(PM-1 and 7) has the highest values, roughly two orders of magnitude greater than the other rocks. The intensity of one sample at site

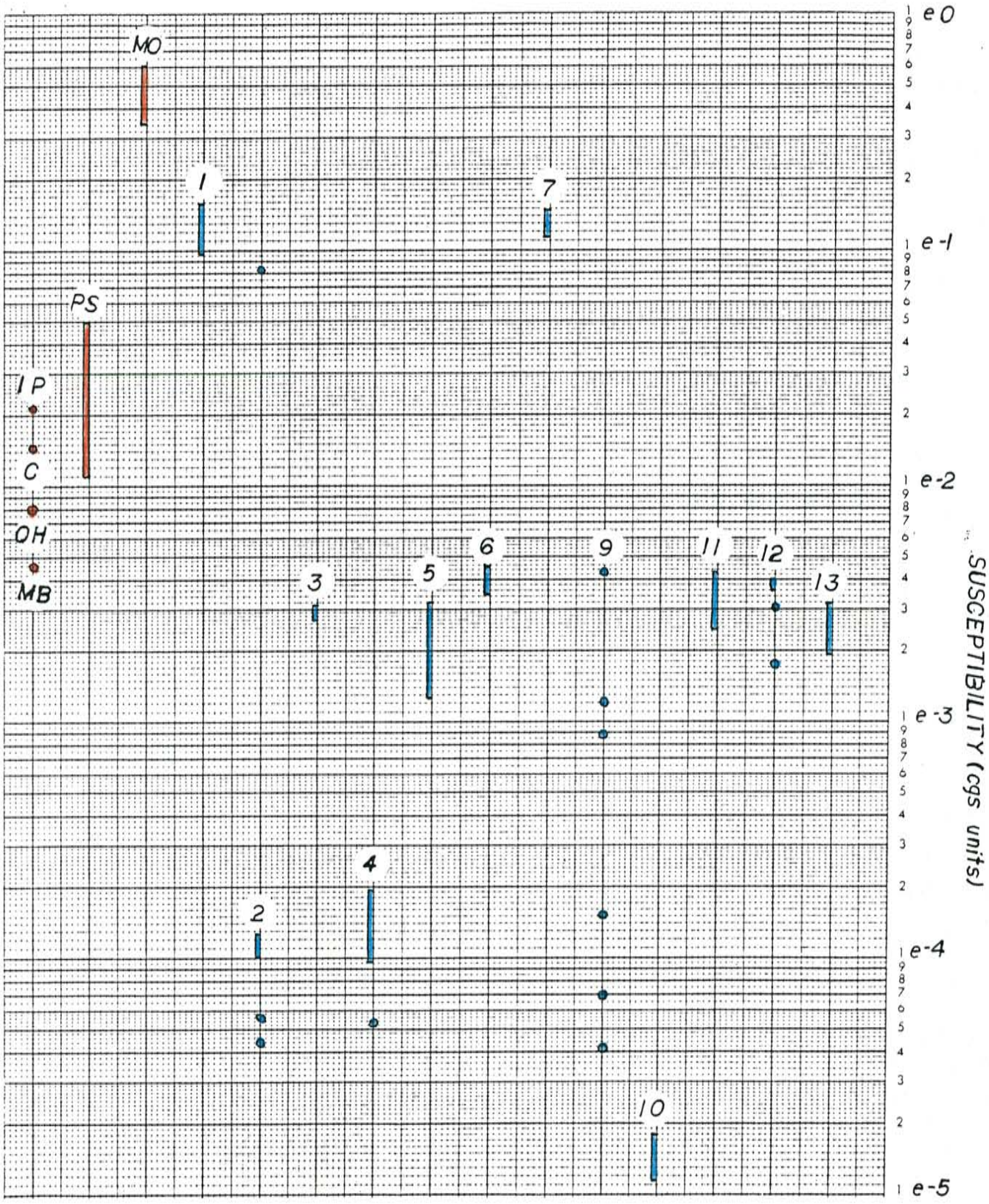

Figure 10. Susceptibilities of rocks at Jones Camp dike as measured by the Sapphire susceptibility meter are shown in blue. Bickford's(1980) calculated susceptibilities are shown in red. MB-mottled border facies OH-outer hornblende facies C-central facies IP-inner pyroxene facies PS-pyroxene syenodiorite("diabase") MO-magnetite ore

2(altered Pyts) is as strong as the ore. It is composed predominantly of secondary magnetite. The lowest values are seen in the other altered sandstone cores, the Tjb(PM-4 and 9) and a heavily altered outcrop of the Tja(PM-10). Rocks which have not been heavily leached and metasomatized have susceptibilities ten to 100 times greater than their altered correlatives, as shown by a comparison of four samples of Tjb showing varying degrees of alteration(PM-4, 6, 9 13). PM 9 shows a wide range in values. No explanation for this range is readily apparent in the cores or on the outcrop. The values of the dioritic rocks of the main dike(PM-3, 4, 6, 9, 10 and 13) fall within the same range as those of Tjp(PM-5 and 11). This confirms Bickford's(1980) prediction that these rock types would be indistinguishable in a magnetic survey.

Included on figure 10 are estimated susceptibility ranges for Jones Camp rocks as calculated by Bickford(1980, figure 10). He calculated these values from petrographic data using the following empirical formulae;

$k=.0026V^{1.33}$ for $0.1<V<10$ (Balsley et al, 1958)

$k=.00116V^{1.39}$ for $V>10$ (Bath, 1962)

where V is the volume percent of magnetite in the rock and k is the calculated susceptibility(not to be confused with the statistical precision parameter, k, in the paleomagnetic

study). The calculated susceptibilities of the ore are two to four times greater than those measured, while igneous rocks are roughly an order of magnitude greater. The above formulae are based on the assumption that the field directions of induced magnetization are uniform.

Point counts performed on polished paleomagnetic cores collected at PM-1 on the section 19 grid show that the ore pod there contains 78% magnetite(Appendix VI). The susceptibility of these cores was measured on a sapphire susceptibility meter(Appendix IV). By Bath's formula, the measured k of these cores would represent only 30% magnetite.

In any case, Parasnis(1975), showed that the formula of Balsley et al.(1958) is inconsistent with another by Jahren(1963). These formulae are empirical and differ according to the findings of each investigator. Parasnis(1975) warns that there is no universally valid relationship between susceptibility and magnetite content and that only direct measurement of susceptibility should be considered completely reliable.

The depressed values of both induced and remanent magnetizations explains the failure of observed magnetic anomalies to match those predicted by theoretical curves for orebodies of given geometries. Several formulae are described in the literature by which one may calculate a theoretical magnetic profile for a dipping sheet of given

size(Cook, 1950; Koulumzine, 1970; Telford et al., 1976). Attempts to model the ore pods using these formulae failed. Predicted peaks were of the same magnitude as those observed in the field when using measured susceptibilities. However, the predicted peaks were only as wide as the modeled ore pod(four feet in the case of the section 19 grid). The observed anomalies, however, show their peak values over a space of 20 or 30 feet. The predicted anomalies are much narrower than those observed in the field. The position of the peak relative to the ore body was also different than the observed profile. It was concluded that the theoretical profiles don't approximate observed profiles closely enough to be useful in predicting ore tonnage at Jones Camp.

The anomalies at Jones Camp are of similar magnitude to those seen elsewhere in central New Mexico. Spahr(1983) conducted magnetic surveys over magnetite pods at Lone Mountain in Lincoln County, New Mexico. The orebodies are of similar size and grade as those at Jones Camp and her measured anomalies were of the same magnitude. The present author ran three profiles across the Iron Horse deposit, five miles south of Jones Camp(Appendix II). That deposit is identical to the orebodies at Jones Camp with respect to igneous rocks, sedimentary rocks and iron ore. The anomalies were of magnitude similar to those at Jones Camp dike. However, they were three to four times smaller than those observed by Johnson (1953). The disparity is probably due to the difference in instrument heights(A. Sanford,

personal communication, 1985). Johnson used a Schmidt vertical balance and an Arvela torsion-head magnetometer, which have heights of three and a half feet. The proton precession sensor is at a height of eight feet.

INTERPRETATION CONCEPTS

Due to objections outlined in the preceding section, quantitative analysis of the magnetic data will not be attempted in this study. Qualitative analysis based on the size and shape of the anomaly will depend largely on the amount of supportitive geological information. Figure 11(Parasnis, 1972) shows calculated anomalies for bodies with various directions of total magnetization. This guide will be compared with observed profiles. These profiles will be used only in a general sense and with caution. Assuming that the direction of induced magnetization coincides with the direction of the earth's field(circa 62 degrees), the middle row of profiles in figure 11 should approximate profiles observed in central New Mexico. South-dipping beds, such as those on the section 19 prospect grid, are shown on the left side of the figure. North-dipping beds, such as those on the section 17 east grid, are shown to the right. The peak of the total field anomaly is offset slightly to the south of the top of the southerly dipping beds. The peak lies directly over the top of the northerly dipping beds. The ore pods on the grids(plates 3 and 4) follow this rule. The profiles also

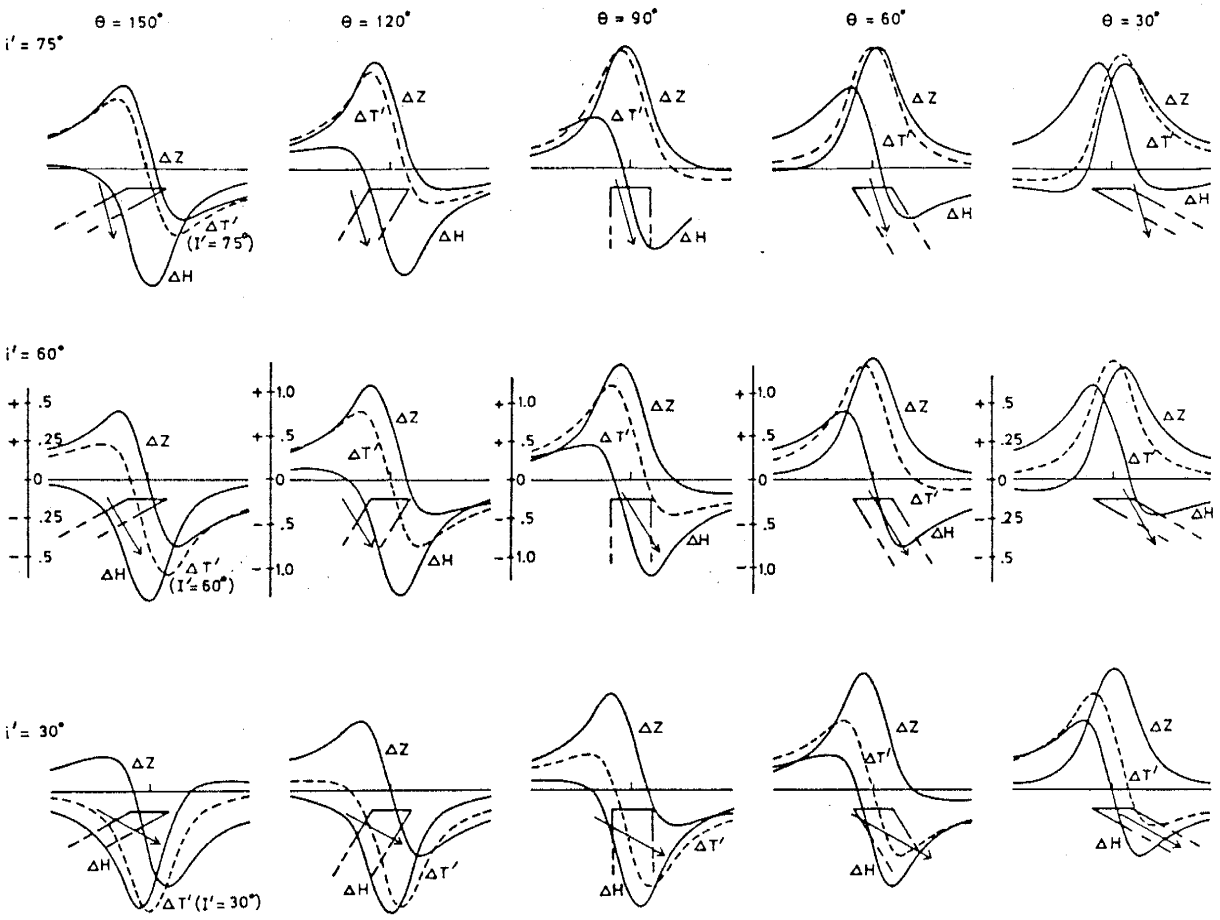

Figure 11. Theoretical magnetic profiles across a thick sheet(Parasnis, 1972). The width of the body is two times greater than the depth to its top. i' is the net direction of the induced and remanent magnetizations. The examples illustrated show the effects of positive(downward oriented) directions of magnetization. See Parasnis(1972) for similar examples showing anomalies due to negative magnetization. I' is the inclination of the earth's field. ΔZ is the anomaly of the vertical component of magnetization, ΔH is the anomaly of the horizontal component and ΔT' is the total field anomaly. Θ is the dip, as measured clockwise from horizontal.

show pronounced negative anomalies associated with the south-dipping beds and no negative anomalies associated with north-dipping beds. At Jones Camp, however, negative anomalies are better developed(larger area and greater magnitudes) over the north-dipping beds on section 17.

Bickford(1980) lists five factors which affect the magnitude and shape of magnetic anomalies:

1) The lateral magnetic susceptibility contrast between a body and its surroundings
2) The direction and intensity of remanent magnetism in the body
3) The direction and intensity of the earth's field relative to the body
4) The size and shape of the body
5) The depth of burial of the body

The lateral susceptibility contrast between the dioritic rocks and the surrounding sediments is large, and the contrast between magnetite pods and sediments is extreme. Susceptibility ranges of the different igneous rocks overlap(figure 10). However, peculiar mineralogical characteristics and differing degrees of hydrothermal alteration may make them magnetically distinct. Detailed field data and geological mapping would both be necessary for any rules or generalizations one might make.

The rocks at Jones Camp generally have a wide range of remanence directions which depresses the intensity and makes the rocks magnetically unpredictable.

The dike and ore pods generally strike N75W, almost perpendicular to the declination of the earth's field. The ore stringer on section 19 prospect grid strikes ~N65W with dips between 58 degrees south and vertical. Dips on the section 17 prospect grid range between 40 degrees north and 85 degrees north.

The ore pods are long, thin and tabular. Thicknesses of exposed outcrops are three feet in the detail study areas. Dip lengths(depths) are unknown, but are probably between 25 and 75 feet.

Several anomalies were encountered on a magnetic line along strike of the dike-sediments contact in sections 16 and 17, T5S R7E(plate 4). These anomalies sometimes had scant ore float on the surface, but no visible outcrop. They are interpreted as buried orebodies. These anomalies are of the same magnitude as those of exposed orebodies.

SECTION 19 PROSPECT GRID

A survey grid was established over ore pods in SE4 SE4 SW4 section 19 T5S R8E. The grid is approximately three acres in area and is located on the south side of a ridge formed by the Jones Camp dike. The hillside slopes ~15 degrees southward, except for a flat region in the central part of the grid over the crest of an anticline. The valley to the south is floored by the Canas and Joyita members of the Yeso Formation. Figures 12, 13 and 14 show north-south

cross sections across the grid, detailing topography, geology and the magnetic anomaly. Figure 15 is a measured section of sedimentary beds at the top of the Torres member on the grid. Figure 16 shows magnetic profiles across the contact between Pyc and Pyj. Plate 1 is a map of the magnetic readings and Plate 3 overlays the anomalies on a geologic map. Plate 5 shows the geology of the surrounding area.

Geology of the section 19 grid

The author interprets the geological structure as an anticline of upper Torres sediments tilted and arched by two successive intrusions of the Jones Camp diorite. The anticline is truncated at the eastern end of the grid but extends west of the grid ~300 feet. The northern limb of the anticline is formed by altered Pyts beds which dip gently into the Tjb of the main dike. The southern limb consists of Torres limestone, sandstone and gypsum beds which dip steeply to the south. In the central portion of the grid the limestone is vertical and locally overturned. Dips decrease away from the dike to ~35 degrees in the Glorieta sandstone 500 feet south of the crest of the anticline. Dips vary somewhat on the southern limb due to pinching and swelling of the gypsum and intrusions of diorite. The crest of the anticline is in the lower of the two Torres gypsum beds exposed on the grid. It has been pierced by intrusions of the border facies and central

facies diorites. These intrusions are moderately to intensely altered near the orebodies. Alteration products include albite, scapolite, actinolite, tremolite, calcite, specular hematite and sphene. The altered diorite shows no attraction to hand magnets.

The grid area was mined on a small scale prior to World War II(C. T. Smith, personal communication). The northwest and southeast corners of the grid were cleared by bulldozer. There are several prospect pits and trenches on the prospect, as well as ore piles containing up to a ton of ore. A 77 foot vertical shaft was sunk in the central part of the grid. It is collared to a depth of 16 feet by local pinon and juniper trunks.

Interpretation of magnetic anomalies

The anticlinal structure is not well expressed by the magnetic anomaly(plate 3). The northern limb is weakly magnetized and shows only discontinuous, low-level anomalies. The sandstone beds are locally altered, showing varying degrees of metasomatism to an assemblage of actinolite, tremolite, magnetite, hematite and calcite. In the area of 450W 125N the sandstone is replaced by magnetite, yet has a magnetic anomaly of limited areal extent. The prospect pit at 410W 130N samples pervasively altered sandstone which locally has magnetite concentrations similar to the iron ore(for example, paleomagnetic sample PM-2-3). However, outcrops and floatcrops of actinolite

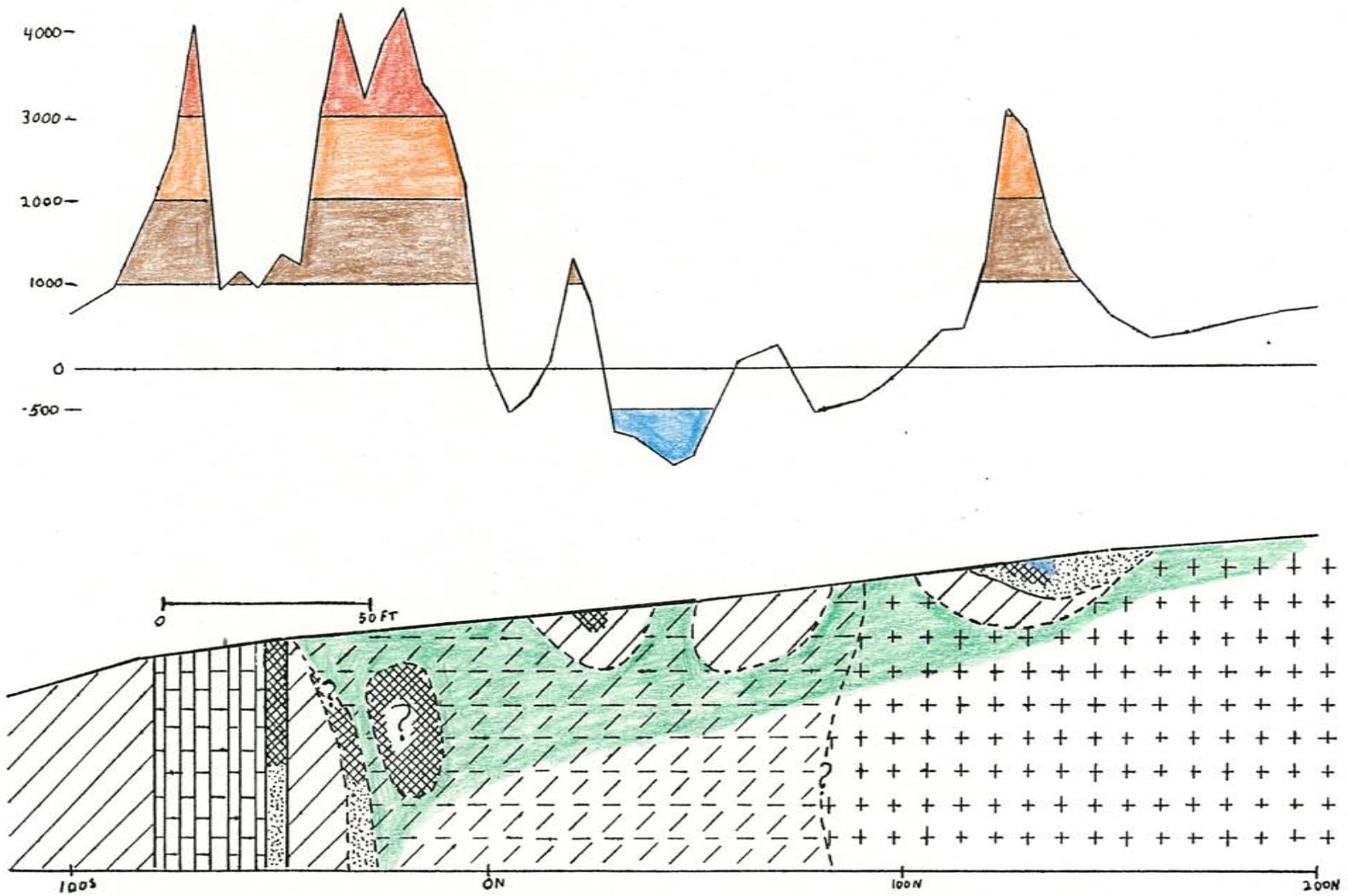

Figure 12. Line 450W, Section 19 Prospect Grid. The double peaks between 100S and 0N are interpreted as representing two ore layers, only one of which is exposed on the surface. That outcrop is correlated to the southern peak. Two possible subsurface bodies are suggested for the northern peak. As the northern peak is wider, The buried orebody is probably thicker than the four foot pod in the upper Torres sandstone bed. The low-grade mineralization at 25N has a low-level anomaly. The high-grade but spatially limited mineralization at 125N produces a medium-level anomaly. Symbols and color scheme are explained on plate 3.

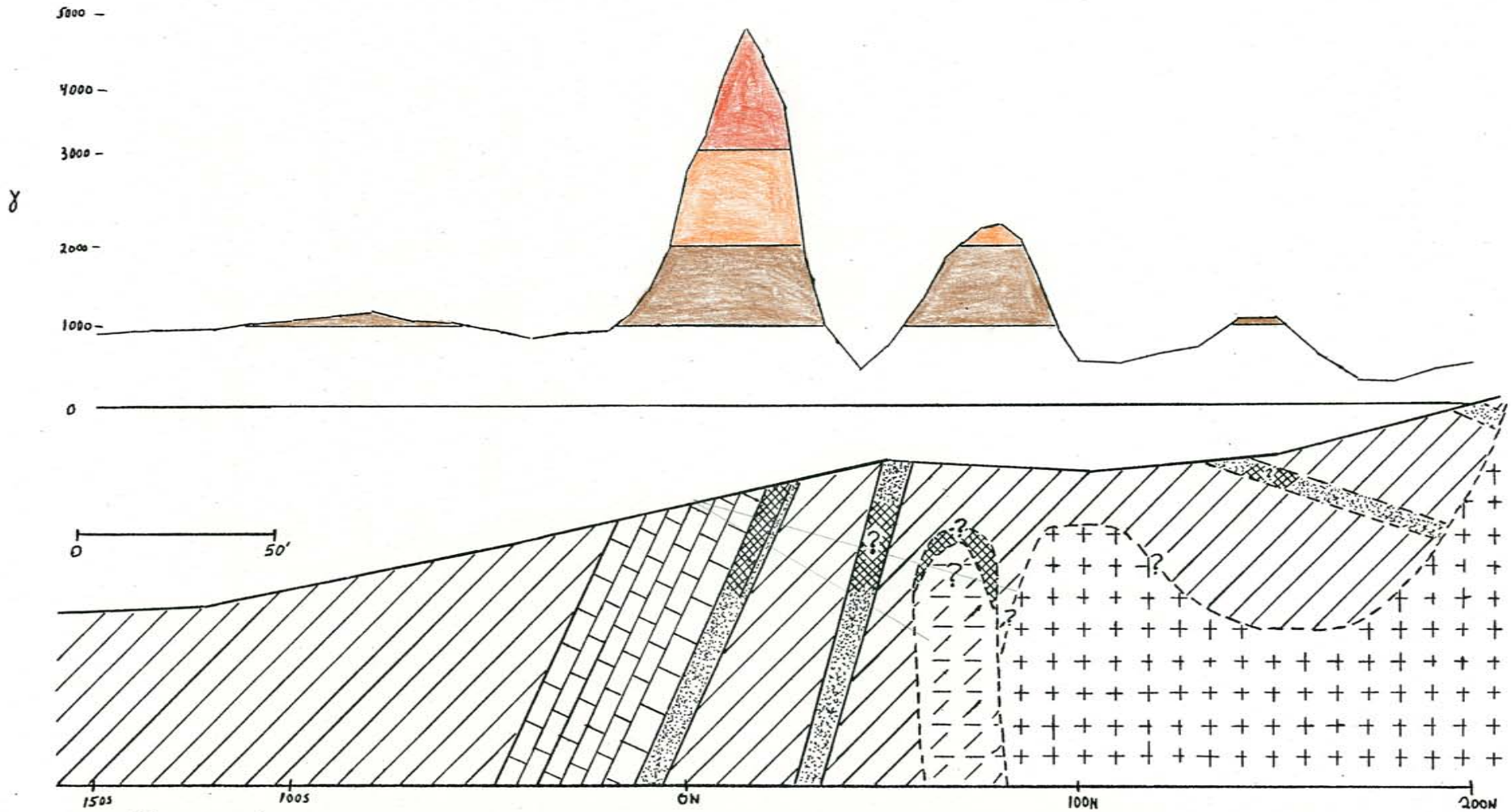

Figure 13. Line 600W, Section 19 Prospect Grid. The high-level anomaly is produced by the outcroping ore pod in the upper Torres sandstone bed. The medium-level anomaly at 60-90N is caused either by low-grade mineralization down dip in the lower sandstone bed or by a subsurface intrusion of central facies diorite with attendant low-grade mineralization. The low-level anomaly at 60-110S is interpreted as low-grade mineralization or an intrusive sill in the Canas gypsum member. The lower sandstone bed dips nine degrees steeper than the limestone, suggesting that it was shifted by a later intrusion. Symbols and color scheme are explained on plate 3.

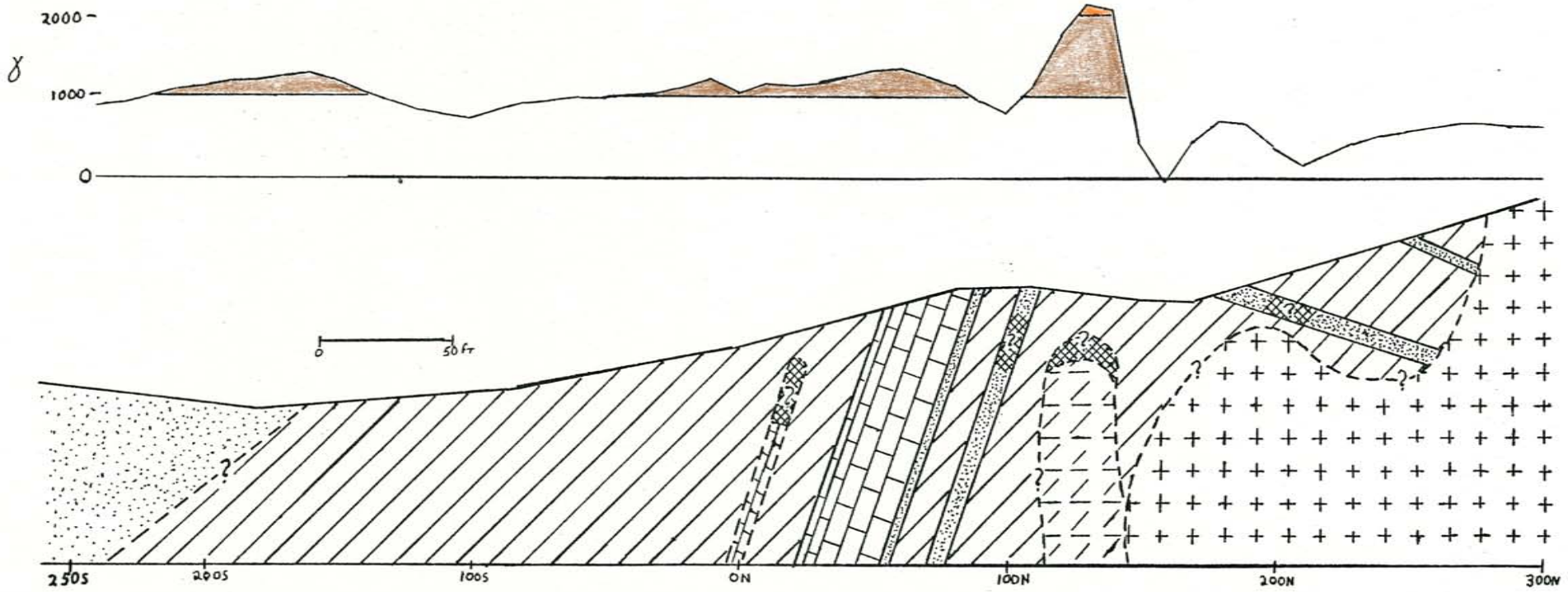

Figure 14. Line 700W, Section 19 Prospect Grid. The medium-level anomaly is produced by a subsurface magnetic body. The level of the anomaly suggests that it is low-grade iron ore on the margin of an intrusive dike of central facies diorite. The broad low-level anomaly between 50S and 80N buried low-grade ore or intrusive sills in the top Torres limestone bed or the Canas member. The low-level anomaly from 140S to 230S is interpreted as iron mineralization or an intrusive sill along the Canas-Joyita contact. Symbols and color scheme are explained on plate 3.

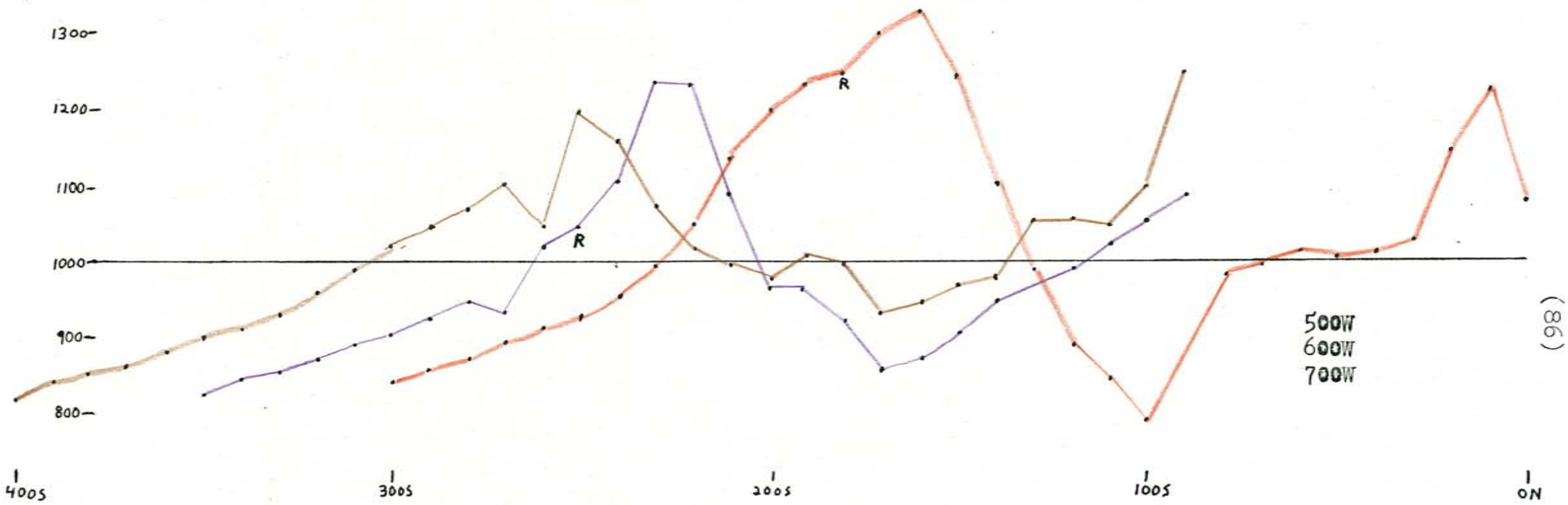

Figure 15. Southern extensions of magnetic profiles 500W, 600W and 700W. The low points in the curve at approximately 800 gammas probably represent the marginal effects of the magnetic field of the main dike. R shows the location of the road, which approximates the contact between the Canas and Joyita members. The contact is tenatively placed under the peaks on the anomalies. The dip of the contact is ca. 35 degrees, consistent with attitudes seen on sandstone outcrops on the ridge to the south. The contact produces an anomaly which is ca. 500 gammas greater than that produced by the dike. That enhanced anomaly is believed to represent an igneous body or iron ore pod along the contact in the subsurface. The widths and heights of the peaks indicate that the proposed magnetic body thickens to the west.

rock do not correlate with even low-level anomalies, and this alteration assemblage is not considered to be the sole source of any anomaly. Outcrops of the upper Torres sandstone bed along the northern edge of the grid suggest some sort of imbricate strike-slip or hinge faulting.

Exposures of the lower gypsum bed at the crest of the anticline are pierced by necks of the border facies and central facies diorite in the central part of the grid. Discontinuous positive and negative anomalies in this area are correlated to these intrusions and their subsurface extensions. The medium-level anomalies suggest that the intrusions have iron oxide mineralization on their margins. One such anomaly of ~2800 gammas overlies the inferred contact between outcrops of the two intrusives at 500W 80N. There is abundant iron ore float in the area immediately to the north. The low-level anomaly at 650-700W 170N indicates mineralization in the lower Torres sandstone. A small, moderately altered outcrop of sandstone borders the anomaly at 700W. This anomaly is on strike with other positive and negative anomalies and an outcrop of Tjb. The distribution of anomalies indicates that the Tjb occurs as a WNW-trending dike in the subsurface. The low to medium level of the anomalies (1000-2000 gammas) is greater than the magnitude of anomaly generally created by the igneous rocks(~500 gammas). The two dikes of diorite which intruded the crest of the anticline are thoroughly altered and their magnetite has been removed. The anomalies associated with them are

presumed to have been caused by attendant concentrations of iron oxides. These are considered to be of low grade and small size, as their anomalies are not as large as those seen with other subsurface orebodies. An exposed example of such a concentration is the low-grade mineralization at 450W 25N. It covers about 25 square feet of area, is of variable grade and is hosted by gypsum. However, if these bodies are shallow and have considerable amounts of hematite or limonite, they may be economically exploitable.

The southern limb of the anticline shows the most abundant magnetization and exposure of iron ore. It dips more steeply than the northern limb, particularly on the eastern side of the map where an intrusion of central facies diorite pushed the limb to a vertical attitude. In several places, the limestone, iron ore and sandstone beds have been displaced by strike-slip or hinge faults perpendicular to the strike of the limb. Brecciation along bedding planes has been noted in the limestone and sandstone beds. Slickensides on an ore exposure at 600W 30N indicate movement of the beds after mineralization. The upper sandstone bed has been mineralized for approximately 310 feet of strike length. Magnetic anomalies indicate 55 additional feet of mineralization along strike. The base of the Pytl is only locally mineralized within a few inches of the contact with the sandstone bed, a zone where brecciation has been noted. The preferential replacement of sandstone indicates that porosity was the most important control on

mineralization. The ore exposures are generally four feet wide and carry approximately 78% magnetic iron oxides(magnetite and maghemite). Locally, the ore has been oxidized to hematite or hydrated to limonite. Figure 27 shows two iron ore outcrops on the section 19 prospect grid.

The south limb is reflected by two parallel magnetic anomalies which coalesce at the ends. Curiously, outcrops of the orebodies fall between these anomalies. Due to lack of ore outcrops downslope to the south(up-section in the limestone bed), the southern anomaly is correlated with the exposed orebody. The northern anomaly is believed to represent subsurface mineralization. It is on strike with the lower Torres sandstone bed to the northwest and with a large outcrop of altered Tjc to the southeast. The northern anomaly is interpreted to represent mineralized slabs of lower sandstone contacting or enveloped by Tjc. It is wide where associated with the diorite. It narrows near the shaft and the Tjc is assumed to be absent in the subsurface penetrated by the shaft, as it is not seen on the dump. The anomaly broadens to the west of 550W and the Tjc is inferred in the subsurface there.

There is a pronounced gap in the anomaly between 625W and 650W. This gap occurs over mineralized(50 to 70% magnetite) surface exposures of sandstone and limestone. This mineralization is approximately three feet deep, as a trench at the southeast end of the outcrop is floored by

gypsum and sandstone(figure 27). The ore is too thin to register on the magnetometer. This outcrop also shows localized hydration to limonite, including psuedomorphs after pyrite.

The shaft was sunk along an ore-gypsum contact. On the dump is gangue of altered sandstone with late, coarse-grained intergrowths of pyrite, specular hematite, selenite and tremolite. There is minor hydration to limonite and lepidocrosite. This intergrowth of oxidized and reduced iron is evidence of two mineralizing fluids of differing chemistries. The diminished magnetic anomaly suggests that the shaft is not in an area of intensive magnetite replacement.

A third notable gap in the anomaly occurs at 420-440W 80S. As with the other gaps, it coincides with an outcrop of ore. These gaps represent gaps in the orebody at depth and surface exposures are considered to be very shallow. The correlation of geology and magnetic anomalies on the grid suggests two stages of mineralization. The first, driven by heat from the intrusion of the Tjb, produced the actinolite alteration assemblage. This assemblage is not seen on the southern limb, possibly because it was shielded from the early intrusive by a thicker section of gypsum. The second stage is associated with the intrusion of the Tjc and resulted in massive replacement by magnetite.

Bickford(1980, plate 4 and figure 6) shows that the high-level anomaly extends ~30 feet west of the grid to a gulley which has no ore outcrops. Ore exposures are found both to the east and west of the grid. There are approximately 850 feet of ore outcrop or magnetic anomaly along strike of the southern limb of the anticline.

To the south of the high-level anomalies is a WNW-trending low-level anomaly. It occurs over the lower part of the Pyc and possibly represents mineralization of a limestone or sandstone bed within that member. A small outcrop of mineralized upper Canas limestone occurs on the north side of the dike ~550 feet northeast of the shaft(see plate 5).

Magnetic profiles of 500W, 600W and 700W were extended across the valley to the south(figure 16). These show an anomaly of 1200 to 1300 gammas, which is ~650 gammas greater than that produced by the dike. The anomaly is greater than would be expected from the Pyj, which has only traces of detrital iron oxides. It may result from low grade mineralization or a Tjp sill along the Canas-Joyita contact. Such an intrusion may be an extension of that seen 1000 feet to the east-southeast(plate 5). It is impossible to precisely locate the contact in the valley due to soil cover. The road down the drainage, which follows its low points, roughly approximates the contact. This generalization is supported by the differences in soil color

N: White, fossiliferous lime mudstone. 3% vugs(≤2mm). Moderately abundant fractures up to 1 cm long. Vugs and fractures are often filled by tannish-brown, translucent, secondary calcite. There are scant fossils of bivalved organisms(1-5 mm). Massive at base, grading to 10 cm beds at top.

M: Dark grey, fine to medium-grained lime mudstone. Contains 5% vugs which are up to 2 mm in diameter.

L: Buff-white, massive, fine to medium-grained lime mudstone. 3% vugs(<1 mm) and local iron oxide stain. White secondary calcite(locally coarse-grained) fills some vugs. Slightly fossiliferous(bivalved organisms).

K: Dark grey to black, fine-grained, massive, recrystallized lime mudstone. 3% vugs(<2 mm). Abundant fine-grained, white, secondary calcite. Fine to medium-grained oolites. Scarce fossil fragments.

J: Dark grey, bedded, very fine-grained, recrystallized lime mudstone. Beds are 5 to 10 cm thick.

I: Light grey, massive, fine-grained, recrystallized lime mudstone. 1% vugs(≤5 mm) are sometimes lined with secondary calcite or iron oxide stains.

H: Black, massive, fossiliferous, very fine-grained, recrystallized lime mudstone. Abundant fossils(bivalved organisms, gastropods, oncolites and conodonts) are replaced by white calcite with occasional iron oxide.

G: Grey, massive, recrystallized, fine-grained lime mudstone. 3% vugs(<1 mm). Midway up the bed is an 8 cm fine-grained, light grey, recrystallized, possibly oolitic horizon.

F: Buff to light grey, brecciated, massive, fine-grained, recrystallized lime mudstone.

E: White-buff, brecciated, fine to medium-grained, recrystallized lime mudstone. 4% vugs(≤5 mm). Laminated with iron oxide stain. The basal oolitic horizon has been recrystalized and brecciated by bedding-plane slippage.

D: White, fine-grained, well-sorted, clean quartz arenite with subrounded, frosted grains. Sparse secondary specular hematite. Good porosity. Moderately cemented by calcite. 2 to 4 feet thick. Very light iron oxide stain. Commonly altered to actinolite, tremolite, calcite, magnetite and hematite or massively replaced by magnetite.

C: White, powdery, microcrystalline gypsum. locally laminated.

B: Buff-brown, fine-grained, moderately well-sorted quartz arenite with frosted, subrounded to subangular grains. Approximately 10% ferromagnesian minerals and mica. Good porosity and moderately well cemented. Believed to be mineralized in the subsurface.

A: White, powdery, microcrystalline gypsum, locally laminated. Intruded by the fine-grained border diorite facies and the later coarse-grained central diorite facies.

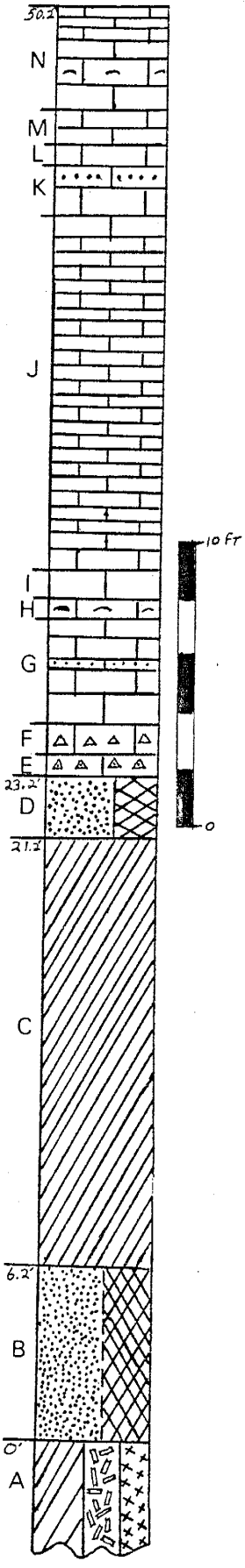

Figure 16. Measured section of the top of the Torres member at the Section 19 Prospect Grid. The limestone beds, uppermost in the Torres member, are calcitic, fetid and recrystallized. It was described in the gulley approximately 30 feet west of the 700W line. The lower beds were described at various outcrops on the grid. Scale: 1" = 6'

on either side of the road. On plate 3, however, the contact has been tenatively placed along the peak of the anomaly, somewhat to the north of the road. There is no evidence that the anomaly is caused by placer deposits of eroded magnetite.

MAGNETIC ANOMALIES IN SECTIONS 16 and 17

A magnetometer survey was run along the contact between the Torres member and the Jones Camp dike in western section 16 and eastern section 17, T5S R7E(plate 2C). The survey covered 3000 strike-length feet along the contact. The eastern part of the survey(east magnetic line) has a total of 515 feet of strike-length anomaly, including 100 feet of high-level anomaly. This is in agreement with an unpublished survey conducted by Thomas Gibbons in 1980. The central part of the survey is detailed in the section 17 east grid(plates 2A and 4), showing several high-level anomalies. The western part of the survey(west magnetic line) shows 565 strike-length feet of anomaly, including 165 feet of high-level anomaly. These anomalies were first identified by Bickford(1980, overlay 6, profiles 92-94). Although his profile 91 crossed the hillside covered by the section 17 east grid, (Bickford's plate 1 and overlay 2), it shows only the anomaly produced by the dike(~600 gammas). At the western end of the survey is a well developed high-level anomaly on the section 17 west grid(plate 2B).

Geology of the section 17 east grid

The section 17 east grid is 2.5 acres in area and located on the southern slope of a ridge. There is a valley directly to the south which is floored by the second highest Torres member gypsum unit. This valley is the crest of the south side anticline, which is 250 feet wide here. It continues east and west for over 3000 feet of total length(plate 6). The grid covers 550 strike-length feet of the north limb of that anticline. The top of the Torres member, including the top two limestone beds, dip to the north in this area. A small piece of an overlying sandstone bed is present. This bed is assumed to be part of the Joyita member. A long, narrow apophysis of Tjb intrudes along the contact between the upper sandstone and gypsum units of the Torres member for most of the length of the grid. It is traced westward for an additional 600 feet. Slight variations in grain size are observed in this apophysis. Poor outcrop control precludes confident interpretation of these variations. Plausible possibilities include differentiation in-situ, intrusion of another magmatic pulse and variable hydrothermal alteration. Two smaller(100 feet long) apophyses intrude along bedding in the sediments. The northern limb shows various directions of strike and dip in bedding. These changes in attitude are attributed to the apophyses(figures 17 and 18). Transverse faulting may have contributed to these attitude changes. No such faults were mapped due to poor outcrop exposure on the grid. Similarly, contacts were often approximated by

distribution of float rock.

The upper Torres limestone bed shows two distinct alteration types(figure 19). In its upper part, where it contacts the border facies diorite, it has been replaced by epidote with lesser amounts of calcite, sphene, specular hematite, magnetite, tremolite and feldspar. A small floatcrop of Joyita(?) member sandstone is found at 0N 500W. This sandstone has been silicified with lesser replacement by epidote and actinolite and intruded by concentric veins of albite and actinolite. It contains clasts of the epidotized limestone, which was brecciated by bedding-plane slippage during folding. This sandstone bed is regarded as the source of the silica in the epidote alteration assemblage.

The middle and lower levels of the upper limestone bed have been dolomitized with traces of pyrite. This dark grey rock(I, figure 19) may be siderite or ankerite rather than dolomite, due to its somewhat heavier density and the general abundance of Fe relative to Mg at Jones Camp. On the west end of the grid, this alteration intensifies with the introduction of green bands of calcite containing pyrite and magnetite(~3% combined). Its occurrence between and adjacent to magnetic anomalies suggests that it is an incipient stage of magnetite replacement of limestone.

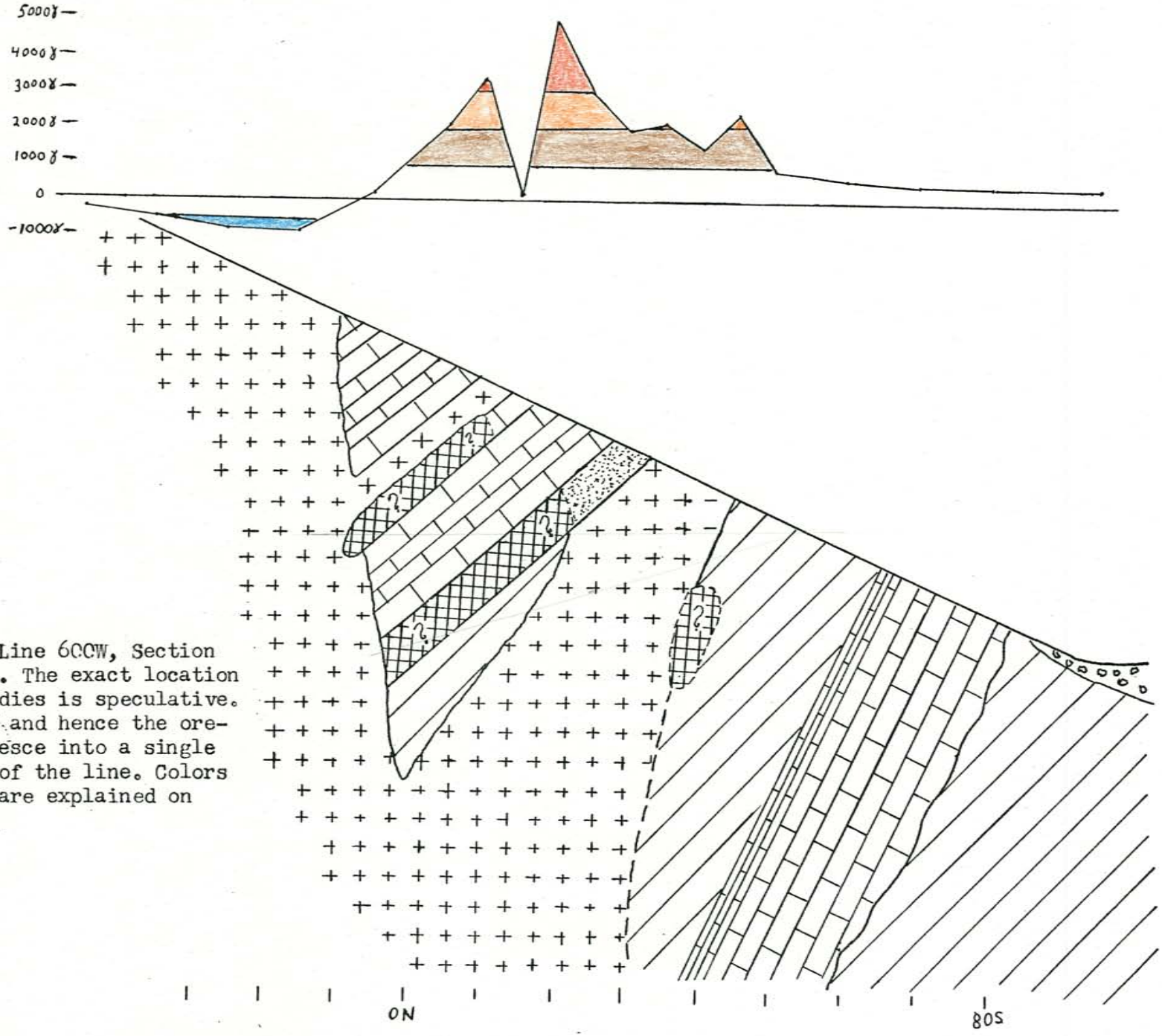

Figure 17. Line 60CW, Section 17 East Grid. The exact location of the orebodies is speculative. The anomaly, and hence the orebodies, coalesce into a single entity east of the line. Colors and symbols are explained on plate 4.

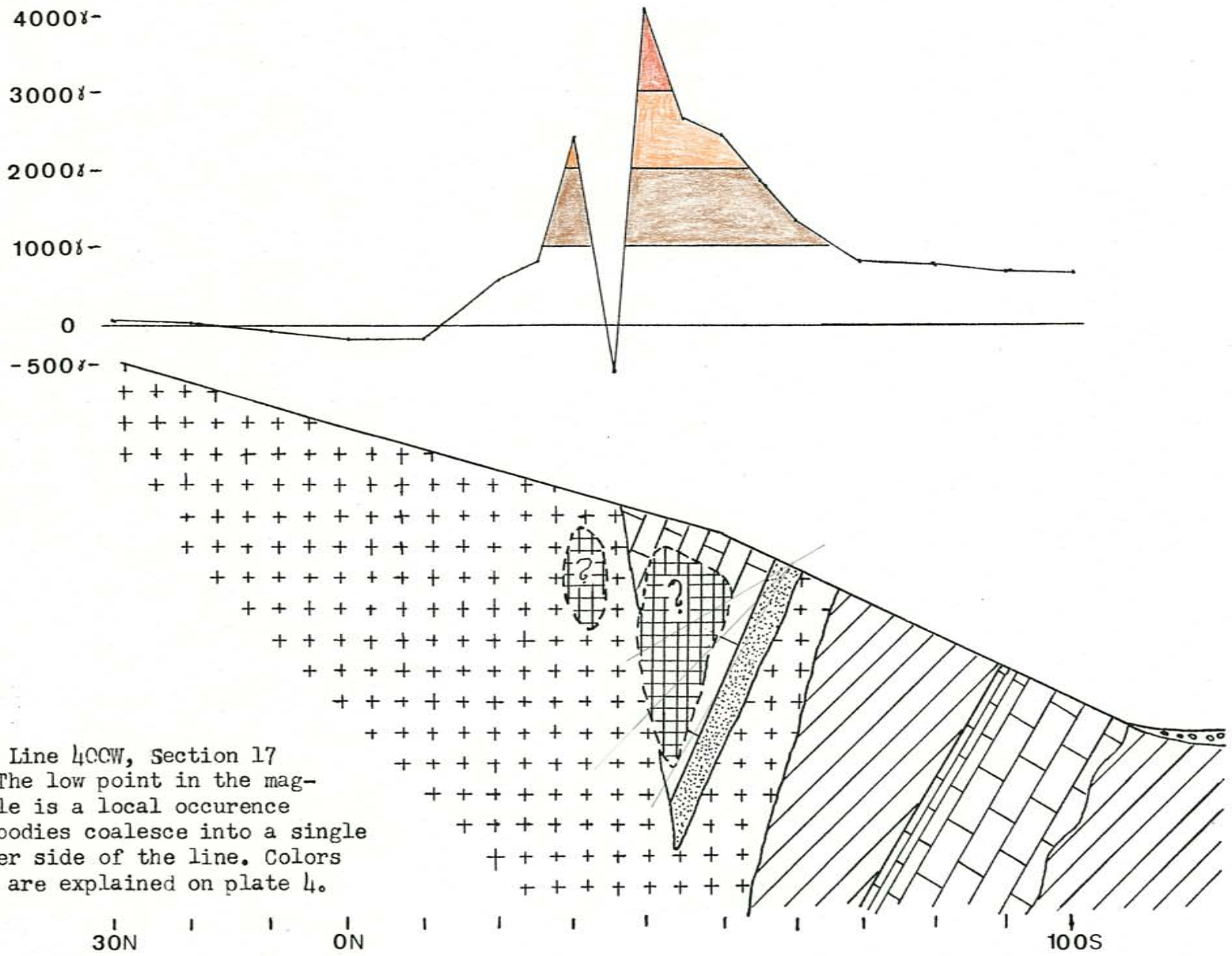

Figure 18. Line 4OOW, Section 17 East Grid. The low point in the magnetic profile is a local occurence and the orebodies coalesce into a single pod to either side of the line. Colors and symbols are explained on plate 4.

Canas member (?Joyita member?)

L: Very fine to fine-grained, silicified quartz arenite with alteration assemblage of epidote and actinolite in elliptical patches 1 to 3 mm thick. Sandstone is intruded by thin(1 to 5 mm) veins of albite and actinolite.

Torres member

Upper limestone unit is approximately 25 feet thick.

K: White, fine-grained sparite with very little porosity and 1% hematite blebs(C.1 mm). This horizon shows varying degrees(often complete) of alteration to an assemblage(E) of epidote, calcite, sphene, specular hematite, magnetite, tremolite and feldspar. Brecciation due to bedding-plane slip at top.

J: A small, altered diorite dike has intruded along strike at this level at the western end of the grid.

I: Dark grey to black, dense, cryptocrystalline dolomite with no porosity. Trace of very fine-grained pyrite. Becomes slightly more calcitic(C) to the west and develops 1-2 cm bands of cryptocrystalline green calcite with very fine-grained pyrite and fine to coarse-grained magnetite(3% combined). The high density of hand samples suggests the presence of siderite or other heavy minerals.

H: Numerous magnetic anomalies and ore floatcrops indicate magnetite mineralization in the lower portion of the upper limestone unit.

G: White, fine to medium-grained, sucrosic sparite with little porosity. It is partially dolomitized on the extreme western end of the grid, showing enhanced porosity and a trace of very fine-grained specular hematite. At the east end, the more calcitic limestone is coarser with up to 10% coarse-grained magnetite.

F: A small, altered diorite dike has intruded along contact on the eastern end of the grid.

E: Buff to white, clean, fine-grained quartz arenite with abundant porosity and calcitic cement. Secondary tremolite lines vugs and scant iron oxide stain occurs throughout rock. Circa five feet thick.

D: Greenish-white, altered, fine to medium-grained diorite. Alteration assemblage includes albite, calcite, tremolite, actinolite, magnetite and specular hematite. Dike intrudes along contact across most of grid, but cuts disconformably across underlying gypsum at east end. Circa five feet thick.

C: White, powdery gypsum. Locally occurs as alabaster and recrystallized selenite. Near exposed ore pod on west end, it is altered to a recrystallized mass of gypsum fibers and crystals with melanterite, very fine-grained magnetite and abundant porosity. Thickness varies between 10 and 40 feet.

B: Buff-white, very fine-grained sparite with a trace of hematite blebs(C.1 mm) and moderate porosity. Replaced by magnetite at west end of grid.

A: Dark grey to black, dense, fossiliferous, dolomitic, microcrystalline lime mudstone. Contains fossils of bivalved organisms and traces of very fine-grained specular hematite. Becomes more calcitic, less dense and lighter grey away from igneous rocks.

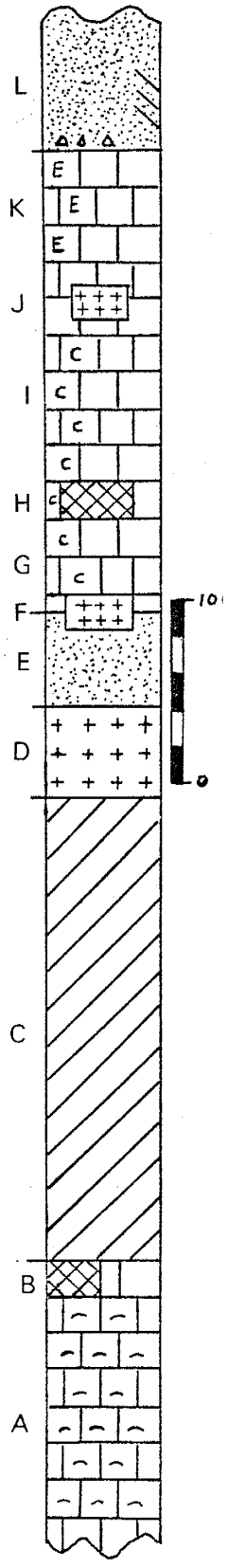

Figure 19. Lithologic section of rocks at the Section 17 Prospect Grid.

The fossiliferous horizons of the upper Torres limestone bed observed on the section 19 prospect grid are conspicuous by their absence on the section 17 east grid. They are, however, quite evident on the southern limb of the anticline. Hydrothermal alteration has obliterated fossil morphology close to the igneous contact. Fossils in the lower Torres limestone are preserved on the eastern end of the grid and along the East Magnetic Line.

Due to poor outcrop exposure on the hillside, no measured sections are presented. Unit thicknesses given in figure 19 are approximate. They are inferred from dip angles and floatcrop patterns. The top Torres limestone bed is 25 to 30 feet thick. The subjacent sandstone bed is approximately six feet thick. The lower sandstone bed seen on the section 19 prospect grid is absent in section 17. Comparison of these thicknesses with those measured nearby by Bickford(1980, plate 2, MS-2 and MS-3) indicates that the top limestone bed thins locally in the center of Section 17 but that the sandstone bed thins progressively to the east.

Exposure of the top Torres bed thins in the eastern part of the grid. The white, fine-grained sparite bed is absent there, as is its epidotized lateral equivalent. Outcrop patterns of the border facies diorite suggest that this bed was truncated by intrusion and folding at this location.

Interpretation of magnetic anomalies

There are numerous discontinuous high-level anomalies in the lower part of the upper Torres limestone bed. These are considered to represent mineralization in the limestone, or possibly in the underlying sandstone bed. None of these anomalies overlies an outcrop of magnetite, but ore float is commonly associated with them.

There is only one poorly exposed outcrop of magnetite ore, on the southwest corner of the grid. It is approximately 55 feet long and shows one to two feet of exposed thickness. Paleomagnetism site 7 sampled this outcrop. Parts of this outcrop may have slumped or rotated out of their original position. A well developed magnetic anomaly, the largest on the grid, is centered on the magnetite outcrop. This is the only anomaly on the grid associated with the lower Torres limestone bed. However, anomalies on the east and west magnetic lines represent mineralization in this unit(plate 2C). The lower Torres limestone shows effects of alteration close to the dike. It has less porosity and is less calcitic than its lateral equivalent on the southern limb of the anticline 250 feet south of the grid. As dolomitization is usually accompanied by an increase in porosity, this provides further evidence that the limestone beds have been variably replaced by siderite or ankerite.

Figures 17 and 18 show magnetic profiles, topography and surface geology of lines 400W and 600W. The size and disposition of subsurface orebodies has been inferred by surface geology and magnetic anomalies. Their true dimensions and depths will be defined only by drilling. Based on the attitude of a joint plane at 0N 200W, the dip of the dike is inferred to be 80 degrees to the south. Assuming consistent dip with depth in the sedimentary beds, an approximate estimate of the amount of limestone and sandstone is displayed. As the sediments are preferably mineralized, the tonnage of ore is limited by the amount of sediments present. The tops of the orebodies have been placed directly beneath the peaks in the magnetic profiles. Proposed orebodies beneath the middle-level anomalies are assumed to be of limited extent or low grade.

The greatest concentration of anomalies lies on the west side of the grid. Ore pods are inferred in the lower part of the upper Torres limestone bed and in the dioritic apophysis. As discussed above, ore crops out along the contact between the upper Torres gypsum and lower Torres limestone beds.

The anomaly over the base of the upper Torres limestone bed on the section 17 east grid is discontinuous. Iron mineralization is therefore considered to be discontinuous along strike. Dips of the sedimentary beds suggest that they may extend to depths as great as 70 or 80 feet(figure

17). It is conceivable that mineralization may be continuous at such depths and would be undetectable at the surface by the magnetometer. At several points along strike, magnetic readings fall sharply within a medium or high-level anomaly. These are interpreted as local gaps in the mineralization or pockets of oxidation to less magnetic iron oxides.

Actinolite alteration of the upper Torres sandstone unit is of limited areal extent on the section 17 east grid. As in section 19, it does not create large magnetic anomalies.

Although anomalies are discontinuous along the extent of the section 17 east grid, the general area on the south side of the dike shows geophysical evidence of abundant iron mineralization. Several hundred strike-length feet of magnetic anomalies are delineated on the west and east magnetic Lines (plates 2B and 2C). On the section 17 west grid, an anomaly 160 feet long by 45 feet wide is outlined. This anomaly is open-ended to the west and occurs over colluvial cover. Geologic mapping(plate 6) suggests that an extension of the north limb of the south side anticline is buried here. The width of the anomaly suggests that a very thick orebody has replaced the upper Torres limestone bed. The north limb of the anticline dips into steep hillsides along the valley. This circumstance would greatly accomodate pit design and it is likely that most or all of

the ore would be easily won if mined.

As mentioned earlier, the magnetometer may be used only for qualitative interpretation at Jones Camp and ore tonnage estimates based on magnetic data are not possible. Magnetic surveys would be extremely useful, however, in identifying targets for developmental drilling, which would allow such estimates. Preliminary surveys should be run along the dike-sediment contact, with later transverse crosslines run in order to delimit anomalies.

WEST END RECONNAISSANCE MAGNETIC SURVEY

The western end of the dike was studied during the course of the field work for this thesis. Reconnaissance scale geologic mapping and magnetic surveying were conducted. The area studied is a three mile strip of igneous and sedimentary rocks in sections 10, 11, 12, 13, 14 and 15, T5S R6E and section 18, T5S R7E. Igneous rocks include at least five distinct diorite and syenodiorite phases. The intruded sediments are limestone, sandstone and gypsum beds in the middle of the Torres member of the Yeso formation. Alteration and mineralization occur along the length of the dike outcrop. Two surveys were run with the G-816 proton precession magnetometer. The first is the transverse line, a profile run perpendicular to the dike. The second is the axial line, run along the crest of the dike with short transverse lines at points of interest. The results of the magnetic surveys are shown in plate 8, figures 20, 21, 22, 23, 24 and 25 and appendix II. Plate 7 is a geologic map of the west end. All stations were located with Brunton compass and topofil hip-chain.

TRANSVERSE LINE

Methodology

The transverse line was measured on a north-south line roughly perpendicular to the dike. It extends one mile from the dike in either direction for a total length of two miles. The profile is centered on the dike(the "zero

station"). Readings were taken on ten foot centers up to 300 feet from the zero station, 20 foot centers between 300 and 500 feet, 50 foot centers between 500 and 1000 feet and 250 foot centers farther than 1000 feet from the zero station. The maximum positive anomaly ws 374 gammas at 110S, roughly the southern edge of the dike outcrop. The maximum negative anomaly of 306 gammas was at 130N, about 50 feet beyond the northern edge of the dike outcrop. Care was taken to locate the line away from exposures of iron ore.

The scatter effect seen on the detailed grids was much less of a problem on this line. If the station showed more than five gammas of scatter on the first three readings, nine readings were taken. Five readings were taken at stations which showed greater than three gammas difference. The maximum scatter observed was only 27 gammas.

The zero station was measured twice during the course of this survey. There was a difference of 53 gammas between the two readings. A somewhat larger difference was observed the following winter when the axial line was measured. Because of the small maximum anomaly, drift corrections were applied to the transverse line. The corrections were based on readings taken at the base station, located ~1000 feet NNW of the zero station.

The zero value(background value) for magnetic work at Jones Camp dike was ascertained from the transverse line. The magnetic effects of the dike influence the magnetometer

for approximately 2500 feet to either side of the crest of the dike(figure 20). Measurements taken further than one half mile from the dike reflect background levels of the earth's magnetic field. The south end of the transverse line had values near 51345 gammas and the north end had values near 51365. Extrapolation of the slope between them through the anomaly produced by the dike would give a background value of 51355. Since most of the dike lies one quarter to one half mile south of the zero station longitudinally, the zero value for this thesis was rounded down to 51350 gammas.

Interpretation

The zero station was the sample site for paleomagnetic site PM-13(chapter III). It is located on an outcrop of heavily jointed, moderately altered Tjb. Its remanent magnetism shows much scatter(figure 5), though it is generally the sum of two dominant remanent directions. Demagnetization stripped away approximately 95% of its remanent intensity. This suggests that it has retained much of its primary magnetite and has undergone less alteration than other border facies rocks at Jones Camp. Its magnetic susceptibility is similar to that of other Jones Camp igneous rocks(figure 10) and is approximately one half the level predicted empirically by Bickford(1980).

An attempt was made to model the dike using a theoretical formula to predict the curve of an infinite(bottomless) inclined dike(Dobrin, 1976: p. 505). The resulting curve was narrower and of much greater magnitude than that observed. Theoretical curves are deemed inappropriate for modeling the Jones Camp dike and its magnetite pods.

Figure 20 is a magnetic profile of the transverse line. Due to the small scale, areas of high sample density have been generalized. Figure 21 is a detailed profile between stations 1000S and 1000N. The geologic cross section in that figure is based on surface geology. The later igneous intrusions shown at depth are hypothetical.

The maximum anomaly produced by the dike here is +374 gammas, less than generally seen in the Jones Camp igneous rocks. The border facies diorite which composes the dike at the transverse line is lightly to moderately altered and exerts light attraction to a hand magnet.

Although the magnetic behavior of Jones Camp rocks is not considered predictable, it is interesting to compare figure 21 with theoretical curves generated by Parasnis(figure 11). The reader is reminded that the geographical(north to south) orientation of figure 21 is opposite that of figure 11. As the inclination of the earth's magnetic field at Jones Camp is approximately 60 degrees, the middle set of curves in figure 11 is

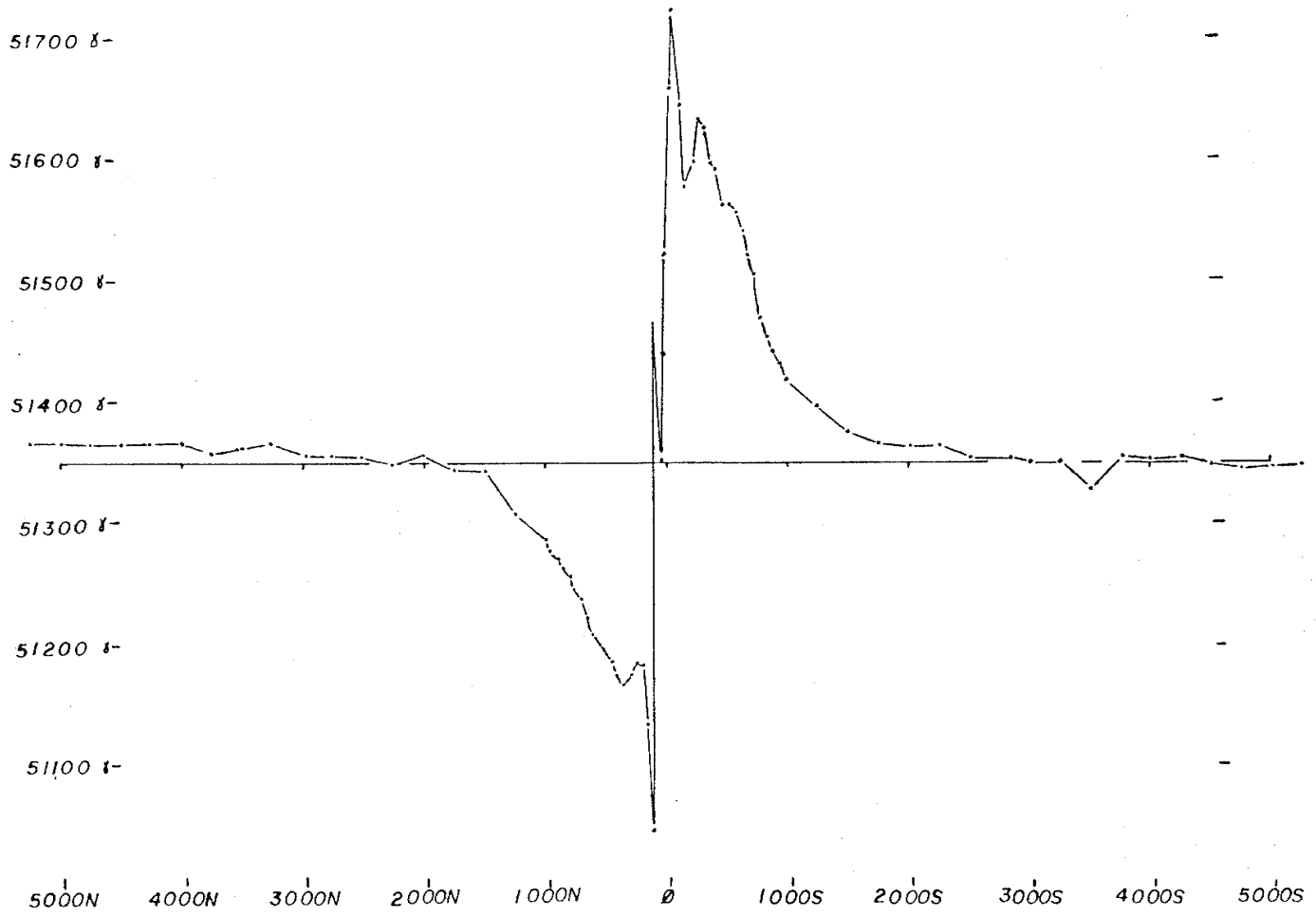

Figure 20. Profile of the total field magnetic anomaly as measured along the two mile transverse line at the west end of Jones Camp dike.

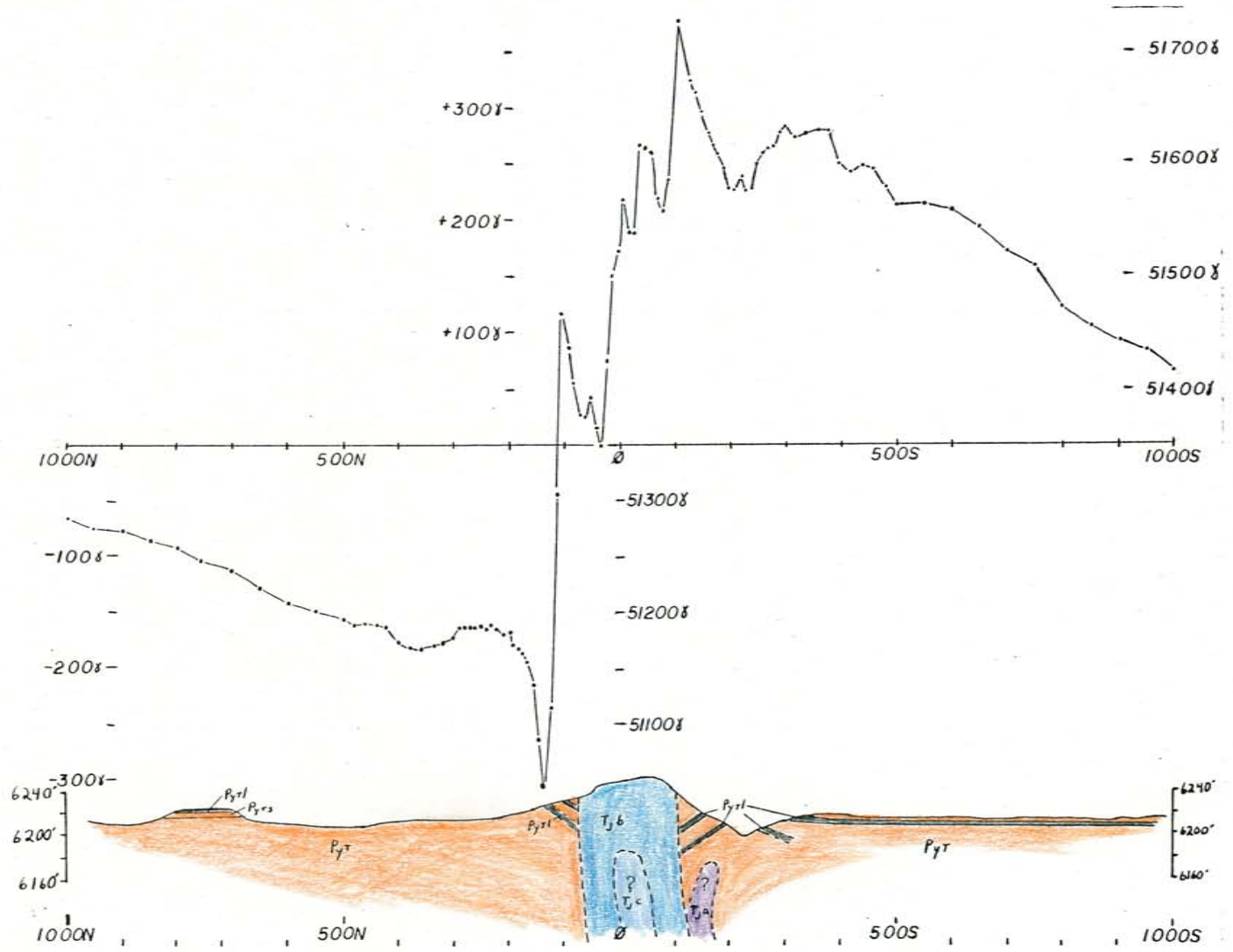

Figure 21. Profile of geology and total field magnetic anomaly between 1000N and 1000S of the transverse line at the west end of the Jones Camp dike. Color schemes and abbreviations are explained on plates 7 and 8. Vertical exaggeration: 2X.

appropriate for comparison. Of interest here is the total field anomaly(delta T') and the relative magnitude scale to the left of each curve. The positive and negative anomalies over a body dipping 60 degrees to the south are of equal magnitude. The positive anomaly over a vertical body is twice the magnitude of the negative anomaly. The positive anomaly on the transverse line is 1.2 times greater than the negative anomaly. By comparing anomaly magnitudes with the examples on figure 11, one would estimate the dip of the dike to be 65 or 70 degrees to the south. The dip of the dike has not been conclusively determined, but previous workers consider it to be vertical or dipping only slightly to the south. There is no geologic evidence to support a 65-70 degree dip. The reader is again cautioned that theoretical curves are not considered trustworthy at Jones Camp. Further, the positive anomaly may be slightly depressed(see following paragraph). On the basis of field evidence, the author believes that there is a southerly dip of at least 85 degrees.

The magnetic profile in figure 21 is quite irregular, with several peaks and depressions superimposed on the main curve. Extrapolation of the slopes leading into the positive anomaly(1000S to 400S) and into the negative anomaly(100N to 150N) would intersect at a point just north of the dike crest and 50 to 75 gammas higher than the observed peak. Some factor appears to be depressing the positive anomaly at several places(200S-250S, 80S, 20S-30S

and 30N). Such depressions indicate a decrease in the magnetic field at that station. Two causes for these depressions are proposed; irregularities of magnetic field orientation within the rock or later, less magnetic igneous intrusions cutting the border facies diorite in the subsurface.

Paleomagnetic remanence directions at the zero station (figure 5; Pm-13) are grouped into two populations which would partially cancel each other. However, the data collected with the proton precession magnetometer show only very small scatter effects. The factors which cause irregularities in the magnetic field at other locations at Jones Camp dike are presumably operative at the west end.

Plate 7 shows that two or more dioritic intrusions are internestled at most locations along the west end of the dike. It is plausible to suspect that later intrusions ascended within or alongside the Tjb at the transverse line. Two possible examples are illustrated in figure 21.

AXIAL LINE

Methodology

A two mile axial line along the dike was sampled at 100 foot centers with the proton precession magnetometer. This line runs 8800 feet west and 2000 feet east of the zero station on the transverse line. The line was terminated to the east at the boundary between ranges 6E and 7E, the

approximate western terminus of Bickford's(1980) magnetic baseline. Four transverse lines of several hundred feet were measured roughly perpendicular to the axial line(plate 8; figures 22, 23, 24 and 25).

The axial line runs along the crest of the dike or over sediments on strike with the dike. The dike becomes discontinuous to the west of the zero station, with Torres member sediments lying in situ between igneous outcrops. Anomaly patterns continued over the sediments, indicating that the dike is continuous at a shallow depth.

In southwestern section 11 the main dike is buried. A trend of igneous rocks striking the same direction as the main dike is offset approximately 500 feet to the south. These outcrops will be referred to in this study as the "offset trend." The offset trend was sampled with the magnetometer.

The scatter effect is defined by the same criteria as on the detail grids; nine readings at stations with >100 gammas of scatter, five readings where the scatter lies between ten and 100 gammas. The scatter effect was not often encountered on the axial line, and usually was associated with medium and high-level anomalies. The base station for this survey was located on a hill approximately 1000 feet NNW of the zero station.

Interpretation

Plate 8 details the location and total field anomaly of the axial line. The dike is characterized by a wide range of values(-895 to +1623 gammas). Approximately 75% of the dike produces low to medium level negative anomalies. The western end of the line shows a broad negative anomaly. Measurement of the offset trend and the transverse lines shows complimentary positive anomalies lying to the south. These anomalies are believed to represent buried igneous intrusions or iron ore bodies. A weakly developed positive anomaly lies to the east of the zero station over Tjb and altered Tjc.

The data allows no generalization about the magnetic characteristics of the dioritic rocks encountered at the west end of the dike. Tjb produces a slight positive anomaly between stations 200W and 1100E, yet has a slight to low-level negative anomaly between 600W and 2000W. Tjc was measured between 1200E and 2000E and on the offset trend. At both locations, wide ranges of values were encountered, usually with high gradients over short distances. The anomaly on the east end may be associated with iron ore occurrences, as mineralized limestone is found nearby and ore float was found along the line. A wide range of values(1500 gammas) and high gradients were observed along the offset trend. It is assumed that these represent mineralogical variations not readily apparent on the outcrop of altered Tjc. Tja was measured over three outcrops between 2600W and 6900W. At 2600W(figure 23) the albitite

is an alteration of Tjb and has a low-level positive anomaly(1623 gammas). At other locations which showed low to medium-level negative anomalies, the albitite appears to be a primary intrusive phase which carries very little magnetic mineralogy. Measured susceptibilities and intensities of Tja at paleomagnetic site PM-10(figures 8 and 10) are the lowest of any rocks tested at Jones Camp. This would suggest that albitite produces a very weak field. However, there is not sufficient data to discern whether primary and secondary albite rich rocks produce characteristic magnetic signatures. Overall, the wide range of values encountered over each rock type precludes confident assignment of typical magnetic signatures to any particular dioritic facies.

Low and very low-level negative anomalies occur along the road between 7500W and 8800W. This segment of the line lies over Torres member sediments along strike of the main dike 500 feet north of the offset trend. The magnitude of these anomalies is comparable to that of the negative anomaly an equivalent distance north of the zero station on the transverse line. They may correspond to the positive anomaly associated with the offset trend rather than buried igneous rocks. However, float of igneous rocks and iron ore and tilted limestone beds occur in section 10 along strike of the main dike. These support the notion that the main dike extends underground to the west of its last outcrop at 7000W.

North-south transverse lines were run at stations 2400W and 2600W(figures 22 and 23) to examine the high gradient between these stations. The gradient lies over the contact between Torres sediments and altered Tjb. Sandstone and gypsum crop out at 2400W(figure 22). Rubble of Torres member limestone is scattered along the line, but no coherent outcrop is seen. A positive anomaly of 865 gammas occurs at 70S with a corresponding negative anomaly of the same magnitude at 10N. This anomaly indicates an igneous intrusion below the surface which is on strike with altered Tjb outcrops to the east and west. The buried intrusive is believed to be of that same facies. 2600W profiles a dike of heavily altered(mainly albitization) Tjb which has pierced Torres gypsum and sandstone. The sandstone bed forms a ledge along the south side of the dike. A medium level positive anomaly(2257 gammas) lies at 10N. The scatter effect was observed here. This anomaly may represent iron ore, as speculated in figure 23. At 40N-50N and 40S-110S are very low-level positive anomalies(<200 gammas). It is not known whether these represent background magnetic values for the albitized Tjb or distorton of the curve by the more magnetic body causing the medium-level anomaly. The data and observable geology indicate that the area between 2400W and 2600W underwent hydrothermal alteration. That episode of alteration may have introduced magnetite mineralization.

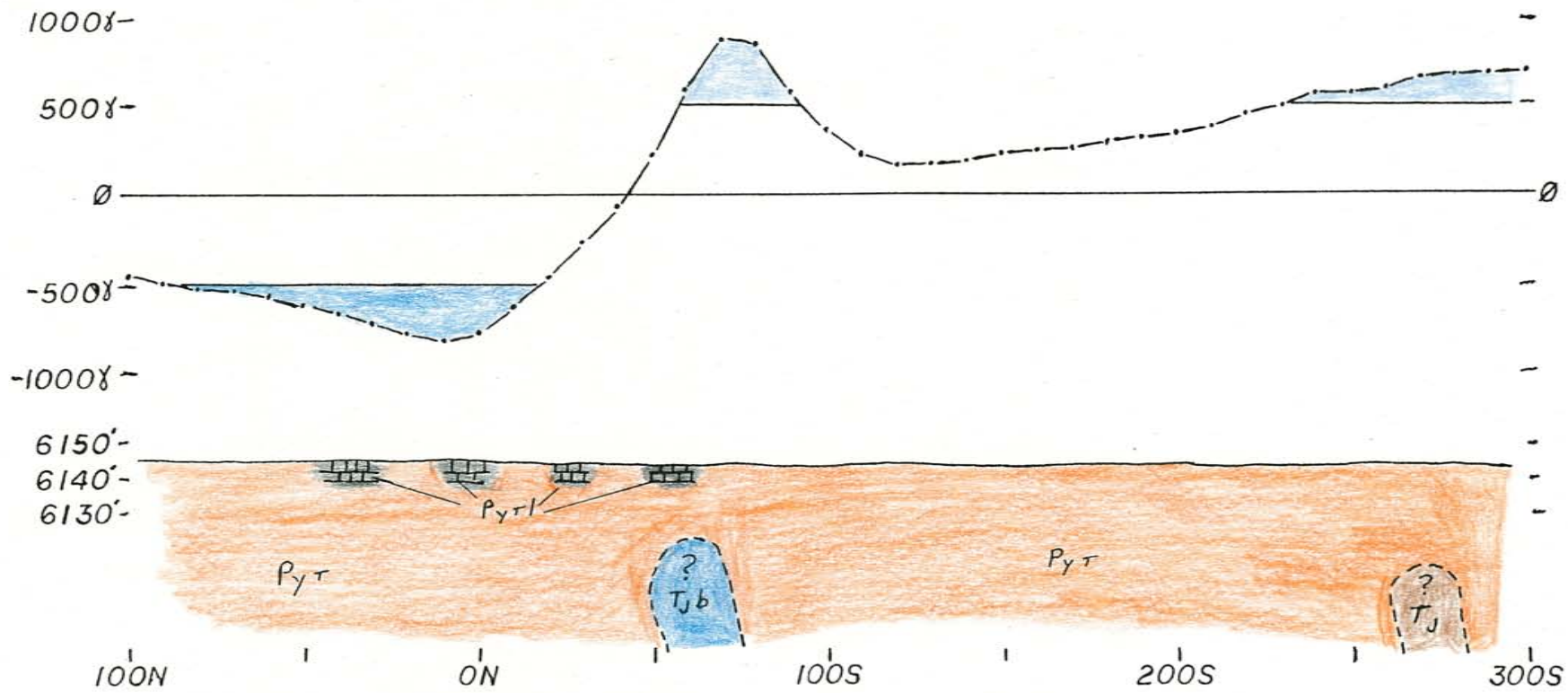

Figure 22. Profile of geology and total field magnetic anomaly at station 2400W on the axial line. Torres member sediments are exposed at the surface. However, the well-developed magnetic anomaly between 100S and 100N indicates a buried igneous body. Border facies syenodiorite is proposed, as the anomaly lies between altered outcrops of that rock. The very low-level positive anomaly at the southern end is interpreted as a buried igneous intrusive. Color schemes and abbreviations are explained on plates 7 and 8.

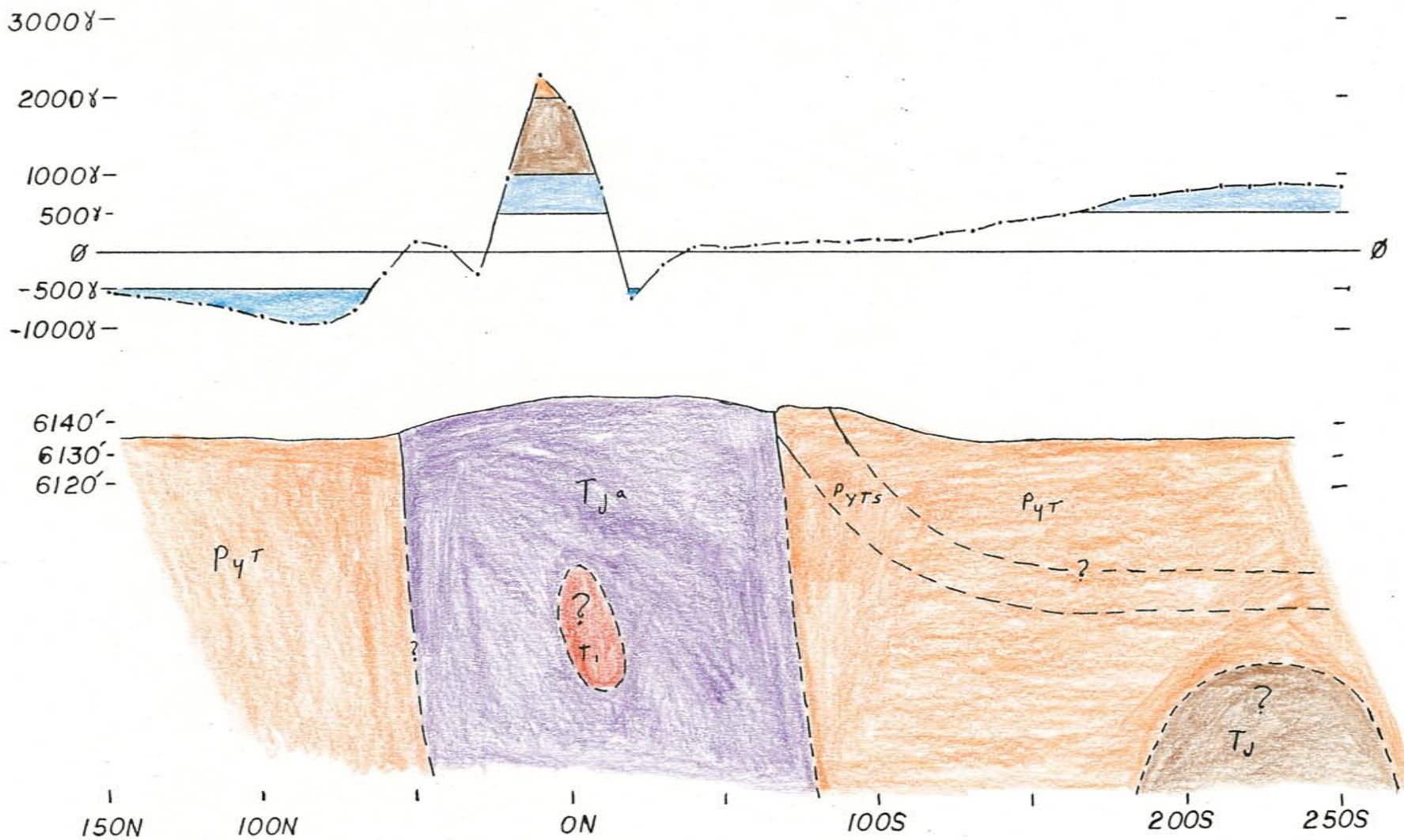

Figure 23. Profile of geology and total field magnetic anomaly at station 2600W on the axial line. The medium-level positive anomaly over the dike may represent magnetite ore at depth. The very low-level positive anomaly at the southern end indicates a buried igneous intrusion. The albitite outcropping here is an alteration of border facies syenodiorite. Color schemes and abbreviations are explained on plates 7 and 8.

Both transverse lines show a very low-level(500 to 1000 gammas) positive anomaly at their southern ends. This anomaly is interpreted as a buried igneous intrusion. It is off strike of the main dike, though oriented in the same direction. In this respect it is similar to the intrusives of the offset trend to the west. Both lines also have well developed negative anomalies to the north of the main dike, which are considered to be part of the magnetic curve produced by the main dike.

Between 5000W and 6300W is a dike of Tjh which ascended along the south face of prevously emplaced albitite and border facies syenodiorite. The coarse-grained Tjh shows very little alteration and forms a prominent ledge along its outcrop. This facies was not sampled in the paleomagnetic study or other magnetic work in this thesis and its magnetic characterstics are unknown. It exerts moderate attraction to a hand magnet. North-south transverse lines were run across the ledge at 6000W and 5490W(figures 24 and 25). Both profles show medium and high-level anomalies across the Tjh. The scatter effect was seen at stations under these anomalies.

Station 6000W(figure 24) has two associated high-level anomalies; one over Tjh(60S-200S), the other over Pyts. The northern anomaly lies between prospect pits dug into the sandstone. The pits are located 60 feet east and 15 feet west of the transverse line. They are two to three feet

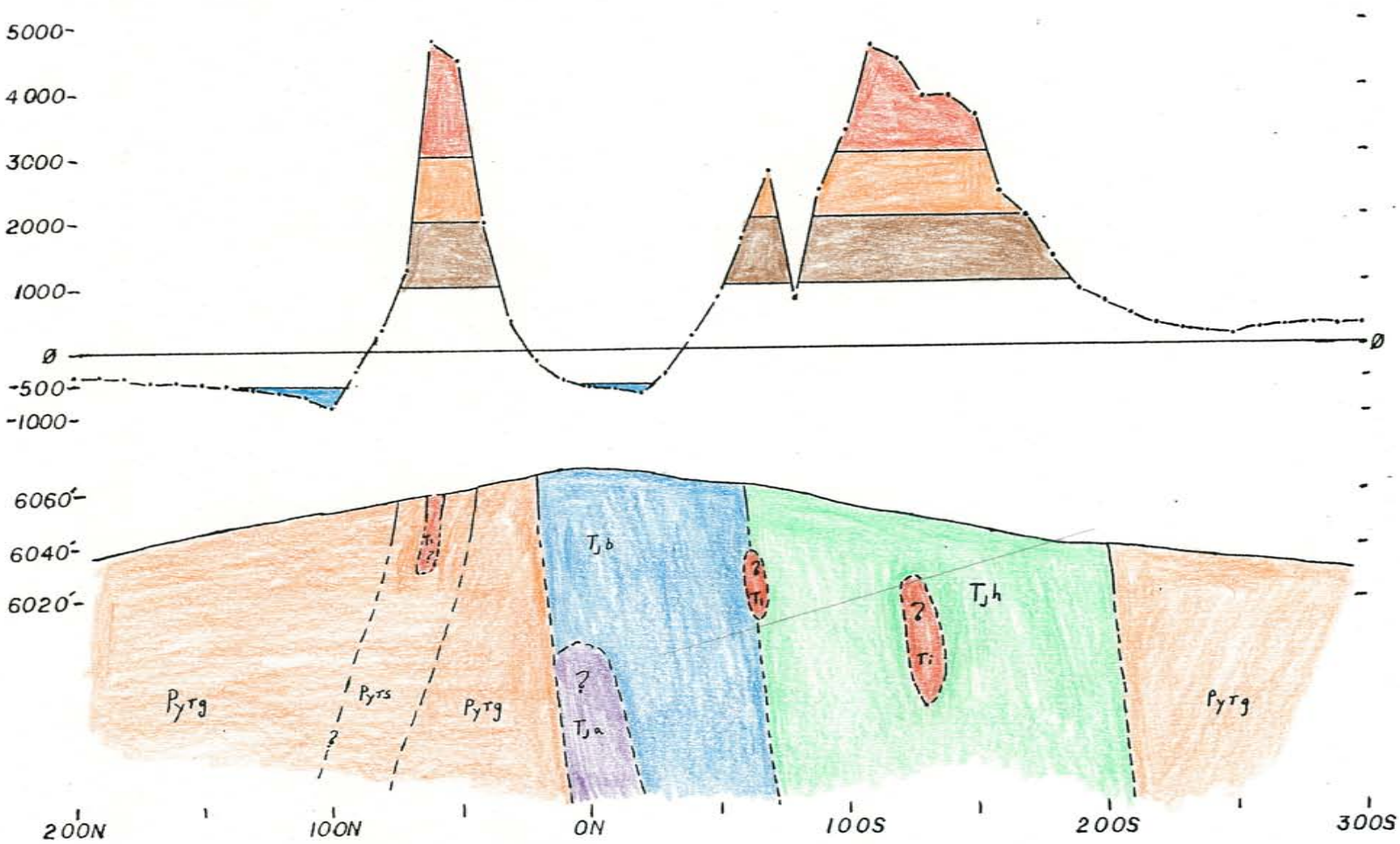

Figure 24. Profile of geology and total field magnetic anomaly at station 6000W on the axial line. The northern high-level anomaly(50N-60N) represents a magnetite pod hosted by a sandstone bed of the Torres member. The southern high-level anomaly(100S-150S) is interpreted as buried magnetite mineralization in the hornblende diorite. The medium-level anomaly at 70S may overlie low-grade mineralization at the contact between hornblende diorite and albitized border facies syenodiorite. Color schemes and abbreviations are explained on plates 7 and 8.

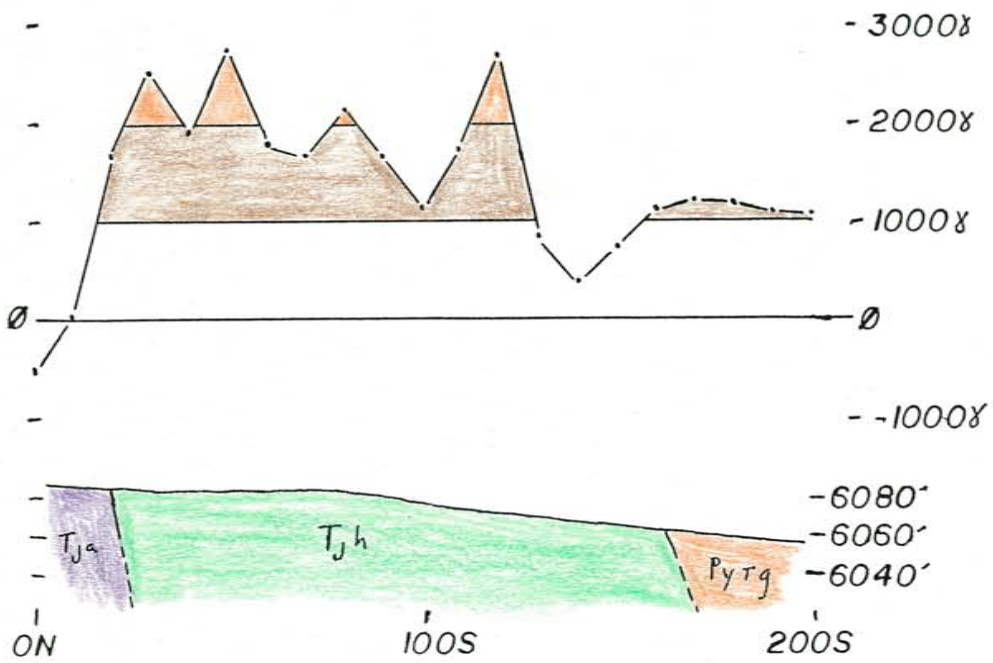

Figure 25. Profile of geology and total field magnetic anomaly at 5490W on the axial line. The low to medium-level anomaly over the coarse-grained hornblende diorite gives way to a negative anomaly over the adjacent albitite. The magnitude of the medium-level positive anomalies suggests that they are associated with concentrations of iron oxides. Color schemes and abbreviations are explained on plates 7 and 8.

deep and have scant pieces of sandstone-hosted ore scattered about. Heavy mineralization is not seen in the pits. The maximum positive anomaly(4613 gammas), is comparable to anomalies over iron ore outcrops at other locations at Jones Camp dike. It is considered to represent magnetite ore at depth in the sandstone bed. Similarly, the high-level anomaly over the Tjh(100S-150S) is interpreted as buried ore even though none is evident on the surface. It is possible, however, that the magnetic field of Tjh is much more uniform than other igneous rocks at Jones Camp, and that the high-level anomaly represents the background value for that facies. The medium-level anomaly at 70S may indicate a buried ore pod or later intrusive along the contact between the Tjh and the albitized Tjb. The albitized border facies produces a negative anomaly here.

The transverse line at 5490W(figure 25) was run over the Tjh. It shows a jagged profile of low and medium-level positive anomalies. There is no evidence to show whether these are the result of low grade iron mineralization or whether the diorite has a uniform magnetic field powerful enough to create an anomaly of 2000 to 3000 gammas. The magnetic work conducted over the Tjh establishes it as a good exploration target for magnetite mineralization.

GEOLOGICAL OBSERVATIONS

During the course of field work for this study, the author visited most areas along Jones Camp dike and several other locales in eastern Socorro County. Geologic maps were prepared for the areas surrounding the magnetic study areas (sections 19/30, sections 16/17 and west end). These maps are presented in plates 5, 6 and 7. Each map will be discussed in this chapter, as well as observations on the geology of Jones Camp dike.

CROSS-CUTTING RELATIONSHIPS

The present author takes exception to Nogueira's(1970, pages 40 and 46) contention that the Jones Camp dike is a single differentiated dike rather than a composite of distinct intrusive pulses. He states that cross-cutting relationships, xenoliths and chilled margins are absent, that contacts are gradational and that there is symmetrical repetition of facies on opposite sides of the center of the dike. During the field mapping exercise of the present study, the author noted numerous apophysitic dikes and necks intruding and brecciating previously emplaced igneous facies. Cross-cutting affected the following facies; Tjb(intruded by Tjc, Tja, Tjp and Tjm), Tjc(intruded by Tja and Tjp), Tja and Tjp(intruded by Tjm). Xenoliths of earlier-emplaced facies are common in the igneous rocks. Nogueira maintains that these are "pseudo-xenoliths" which

are segregation pockets of the same rock rich in volatiles and which crystallized more slowly. In fact, the xenoliths have sharp contacts with their hosts and are often too small(<1cm) to have an appreciable amount of volatiles. Chilled margins, though uncommon, have been observed and are one or two millimeters wide. Contacts between igneous phases are sharp and distinct, though generally obscure due to poor outcrop. The only symmetry seen by the author is that of Tjb flanking Tjc. This is the result of the bisection of Tjb by Tjc and even that symmetry is absent at the west end of the dike(plate 7).

The author believes that Jones Camp dike is a composite dike of at least six comagmatic intrusive phases. Differentiation of these phases occurred in the magma chamber, not in situ. The most convincing evidence is provided by a dike of Tjh flanking the south side of the dike in section 11 T5S R6E(plate 7). This dike is very coarse-grained, bearing hornblende crystals greater than one centimeter in length. This narrow, tabulate sheet is bounded by gypsum and sandstone on its hanging wall. Such a circumstance would prevent any appreciable crystallization in situ.

SOUTH SIDE ANTICLINE

Several authors(Kelley, 1949; Bickford, 1980; Jenkins, 1985) have noted small anticlinal folds of Torres member sediments against the dike. On the north side of the

dike, these folds are sporadic and of limited extent, mainly in the east pit, the west pit and western section 17 T5S R7E. On the south side, an anticline is more or less continuous for over eight miles, from the central part of section 13 T5S R6E eastward to the section 19 prospect in T5S R8E. Jenkins(1985; plate 1) has documented this structure with abundant strike and dip determinations along its length and was the first to recognize it as a continuous structure(personal communication, 1985). The dikeward-dipping northern limb is truncated by erosion in some areas, but the anticline has sufficient continuity to merit status as a single structure. The author will refer to this structure as the south side anticline. It is wider in the western part of the dike than in the eastern part(compare plates 5 and 6).

INTRUSIVE IGNEOUS FACIES

As stated above, the author believes that the Jones Camp dike is a composite dike formed by consecutive igneous pulses which ascended a single conduit. Each pulse ascended along the margin of a previous pulse, along the contact between two previous pulses or along joint planes in a previous pulse or in sediments. Most facies followed two or more of these pathways. Six distinct facies are recognized in this study; Tjb, Tjc, Tjp, Tjm, Tja and Tjh. Two additional facies may exist, but are not presently proposed due to a paucity of field evidence. One is a late

fine-grained facies which postdates Tjc. The other is a medium-grained syenodiorite without mica. The latter rock, which was encountered at several locations at the west end(plate 7), has been included in Tjm. A sequence of emplacement has been established for four of the facies. The sequence, from earliest to latest, is; Tjb, Tjc, Tjp and Tjm. Tja postdates Tjc, as it sometimes bears xenoliths of the central facies. There is presently no evidence for the timing of Tjh, but the author suspects that it came late in the sequence. In the past, Tjp("diabase") has been somewhat of a "garbage pail" designation. Tja, Tjm, Tjp and heavily altered examples of Tjb and Tjc have been lumped into this designation. Throughout this thesis, the author has used Tjp to describe only the dark green porphyritic rock bearing 1mm white feldspar phenocrysts. This pulse constitutes the bulk of the material in the sills in Permian sediments. Brief descriptions of Tjm, Tja and Tjh are given below. These descriptions are based on hand samples and field observations. No petrographic study was conducted. The facies are defined on the basis of mineralogy and grain size.

Mica syenodiorite(Tjm)

Tjm is the desination for mica syenodiorite. It is leucocratic, medium to coarse-grained, albitic, holocrystalline syenodiorite. It has 2-3% medium-grained phlogopite with minor biotite and 20-30% ferromagnesian

minerals. Phenocrysts are subhedral to euhedral. It is often sausseritized. It was initially recognized at three locations in the east-central portion of the dike; at SW4 SE4 NW4 section 24, T5S R7E(descriptive outcrop A, plate 9), at SW4 SW4 NE4 section 23 T5S R7E (descriptive outcrop B, plate 9) and at two locations south of the section 19 grid(plate 5). At these outcrops, intrusive necks of Tjm pierce sills of Tjp from beneath.

Four occurrences of leucocratic to light green, albitic, medium-grained syenodiorite are mapped on the west end geologic map(plate 7). These occurrences carry little or no mica. They contain up to 40% ferromagnesian minerals. The outcrop in section 18 carries xenoliths of Tjb, Tjc and magnetite ore as well as scant coarse-grained phenocrysts of quartz. Although the west end occurrences don't have the mica characteristic of Tjm, they are tenatively included in that facies because of similar grain size and mineralogical proportions.

Albitite(Tja)

Tja is the designation for albitite. This facies includes all rocks which are composed predominantly of albite and scapolite and which are not recognizable as belonging to any other facies. Grain size is variable, but usually Tja is fine or medium-grained. Most rocks mapped as albitite contain no more than 20% ferromagnesian minerals. It often carries secondary minerals such as actinolite,

tremolite, epidote, hematite or sphene. Tja is often an alteration product of other igneous rocks, but many outcrops are fresh and unaltered. These are interpreted as a primary igneous phase. Paleomagnetic site PM-10 sampled albitite. Several occurrences of Tja bearing xenoliths of previous pulses were mapped. Figure 26 shows large clasts of Tjc carried by Tja which intruded the central facies south of the east pit(western portion of plate 5). The apophysitic dike of Tja at the eastern edge of the section 16/17 map area(plate 6) also carries xenoliths of Tjc. At the west end(plate 7) Tja bears clasts of Tjb and Tjc in section 18 and in the central part of the map(4500W-7000W). A fine to medium-grained albitite(90+% albite) in the central portion of the map has ~1% phlogopite. In the section 16/17 and section 19/30 map areas, albititic rocks were initially mapped as alteration products. Subsequent field checks confirmed some outcrops as Tja, But it is probably more widespread in those areas than indicated on plates 5 and 6. It is likely that pulses of Tja ascended with large liquid fractions and that sodium-rich fluids migrated into surrounding rocks and albitized them as the pulses were emplaced. Albite bands one to two millimeters wide are occasionally seen in both sediments and igneous rocks.

Figure 26. Tjc xenoliths in Tja. This outcrop is to the south of the east pit, on the western edge of plate 5. Bar is one foot long.

Hornblende diorite(Tjh)

Tjh is the designation for hornblende diorite. It is a very coarse-grained rock containing up to 50% very coarse(1cm) hornblende crystals. The remainder of the rock contains feldspar and small amounts of pyroxene. Miarolitic cavities are filled with buff very fine-grained material. It has local occurrences of phlogopite and quartz crystals and secondary epidote smears. A dike of Tjh crops out between 5000W and 6400W at the west end, where it forms a prominent ledge(plate 7). It faces Tja and altered Tjb on the footwall, while Torres member gypsum and sandstone form the hanging wall. It is associated with a high-level magnetic anomaly at 6000W, but no iron ore crops out. Tjh probably correlates to Nogueira's(1970) outer-intermediate hornblende facies. This rock also occurs at the intrusive east of the Bingham Post Office.

Late stage very fine-grained facies(?)

There is limited evidence to support a very fine-grained facies which was emplaced late in the intrusive sequence. A light green very fine-grained igneous rock was observed intruding Tjc on the crest of the dike in the center of section 17 T5S R7E(descriptive outcrop C, plate 9). This rock carries a 5cm xenolith of Tja(?Tjc?), mottled texture and ~1% fine-grained specular hematite. On the westend map(plate 7) near 6000W, the altered ?Tjb? appears

to carry xenoliths of Tja. Presently there is little evidence to propose a late-stage very fine-grained intrusive facies.

SECTION 19/30 GEOLOGIC MAP

The area adjacent to the dike in southern section 19 and northern section 30 T5S R8E was mapped at the scale of 1"=500'(plate 6). The section 19 magnetic grid(plates 1 and 3) is located in the central part of the map area. That grid was the site of small scale mining, including the excavation of a 77 foot shaft. The map area is immediately to the east of the east pit and numerous prospect pits and trenches are found in the vicinity.

The dike has arched upper Yeso, Glorieta and San Andres sediments into a broad anticline. The south side anticline is expressed as expressed as a discontinuous, tightly folded warp of Torres member sediments approximately 3000 feet long. To the east and west of the anticline the sediments form a monocline dipping away from the dike. Magnetite deposits occur in Torres sediments on the south side. Those sediments show an assortment of normal, strike-slip and hinge faults adjacent to the dike. These faults are perpendicular to the strike of the dike and less than 200 feet long.

The bulk of the dike in the map area is composed of Tjb and Tjc. Lesser amounts of Tjp, Tja and Tjm occur in a variety of intrusive modes. On the main dike, apophysitic dikes and necks of Tjc intruded Tjb as the main body of Tjc was emplaced. A neck of Tjp subsequently ascended the contact between the two earlier facies. Finally, pulses of Tja pierced the contact, the southern belt of Tjb and the sediments adjacent to the Torres-Tjb contact. These pulses brecciated the previously emplaced rocks. Large xenoliths of Tjc may be seen floating in Tja at the western edge of the map, south of the east pit(figure 26).

Later apophysitic intrusions probably affected the attitude of Torres sediments in the south side anticline. Dikes of Tjb and Tjc have been documented under the crest of the anticline on the section 19 grid(plate 3). In the west-central part of the map, to the north of Teds Tanks, float indicates an intrusion of Tja. This intrusion faulted and lifted up a slice of Torres sandstone and gypsum. The intrusion carries xenoliths of albitized Tjb(?) with reaction rims.

Necks and sills of Tjp, Tjm and Tjc have intruded the sediments to the south of the dike. Sills of Tjp intruded the Glorieta sandstone, its upper and lower contacts and the base of the San Andres limestone. A large exposure of Tjp caps two hills in the southeastern part of the map. This body is interpreted as a sill due to the southerly dip of a

limestone bed in Pyc adjacent to one of these hills. However, this exposure may lie over a neck of Tjp. This outcrop and the Tjp to the northwest of the grid are the only exposures which might be interpreted as necks ascending from the magma chamber. Yet there are widespread sills in the map area whose source is problematic.

In the south-central portion of the map these sills have been intruded by Tjm. The isolated, equant outcrops are interpreted as necks which ascended from below and pierced Tjp sills. Breccia clasts of Tjp within the Tjm clearly demonstrate the relationship between the two igneous phases. As Tjm is not seen anywhere closer to the dike, it is assumed to have ascended vertically along joint planes in the sediments. It is conjectural whether the magnetic anomaly along the Pyc-Pyj contact represents a sill of either facies.

Alteration of igneous rocks is somewhat common, particularly in Tjb. Alteration includes addition of or replacement by one or mare of the following minerals: albite, scapolite, actinolite, tremolite, calcite, sphene, hematite and magnetite. The necks of Tjm show saussuritization at their margins.

The sedimentary rocks exposed in the map area include the upper Torres, Canas and Joyita members, the Glorieta formation and the San Andres formation. Only one sandstone roof pendant, tenatively identified as Pyts, was seen.

Figure 27. Iron ore outcrops on the section 19 prospect grid. Upper photo shows paleomagnetic site PM-1, seen from the west. This spot is ten feet from line 450W(figure 12). The ore pod is four feet thick at the surface. The lower photo shows the trench at 50N 620W. The magnetite mineralization which outcrops is only two or three feet deep. The trench is floored by gypsum and sandstone. The magnetometer shows only a slight low-level anomaly. Bar is one foot.

Magnetite ore was introduced in the Torres limestone and sandstone to the south of the dike. Two exposures of sandstone hosted ore on the section 19 prospect grid are shown in figure 27. To the north, small, isolated ore pods occur in Canas limestone beds. Actinolite contact rock is found on the northern limb of the south side anticline as a replacement of Torres sandstone beds. A small exposure of this alteration occurs at the Tjb/Tjc contact 1700 feet northwest of the section 19 shaft. Its precursor is unknown.

SECTION 16/17 GEOLOGIC MAP

The geology of western section 16 and eastern section 17 T5S R7E was mapped at the scale of 1"=300'(plate 6). The composite Jones Camp dike has arched upper Yeso, Glorieta and San Andres sediments into a broad anticline overhead. On the southern shoulder of the dike, Torres member sediments have been folded into the tighter south side anticline. The dike averages 600 feet in width here. Several apophysitic dikes and necks pierce earlier emplaced igneous rocks. No sills were found in the sedimentary rocks dipping away from the dike. Tjb and Tjc are widely altered by the introduction of and replacement by albite, scapolite, ferrosilicates and iron oxides.

Tjc exposures in the area average only about 200 feet and it is only 60 feet at its narrowest point. This is less than seen at other places along the dike. It is heavily

altered and albitized. Some of the albite rich rocks mapped as altered Tjc may be later intrusions of primary Tja. It is noteworthy that only one small neck of Tjp is seen at the eastern edge of the map. This is likely the western limit of that facies, as none was found in the west end study area.

The wide belt of Tjc on the north shoulder of the dike has been pierced by apophysitic dikes and necks of Tjc, Tja and Tjp. The dike of Tja at the eastern edge of the map carries xenoliths of coarse-grained diorite. This is evidence that it contacted and brecciated Tjc at depth before ascending a fracture in Tjb. On the northern, dikeward dipping limb of the south side anticline an apophysitic sill of Tjb intruded the uppermost Pytg bed. Smaller fingers of this apophysis intruded the uppermost Pytl and Pyts beds(plate 4). This sill is fine to medium-grained and heavily altered. It exhibits some mottled texture. It is not known whether this sill intruded the Torres bedding before, during or after it was folded into its present position.

The Permian sedimentary section exposed in the study area ranges from the second highest gypsum bed in the Torres member through upper Yeso, Glorieta and lower San Andres formations. Roof pendants of Pytl, Pyts and Pyj were noted at several locations, indicating that only the top of the Jones Camp dike has been exposed by erosion. These rest

atop Tjc and Tjb. Two large sandstone pendants were encountered: one on a hill a couple hundred feet east of the section 17 east grid and another on the western edge of the map. Both appear to be stratigraphically higher than the uppermost Pytl bed. As Bickford's(1980) stratigraphic sections MS-2 and MS-3 show no Canas sandstone beds in this area, the pendants are interpreted as Pyj. The intrusion of the dike squeezed the Canas gypsum completely out of the overlying section. Float of Pytl was found at the southern edge of the western pendant. These pendants indicate that Pyj was the highest stratigraphic level of penetration by the dike. This is the same ceiling as that seen at the easternmost exposure of the dike six miles to the east.

Iron ore occurrences in Pytl, Pytg and Pyts beds to the north of the dike have been mined on a small scale. The area is pockmarked by prospect pits and trenches. At the western edge of the map, the uppermost Pytl bed has been folded accordian-style. This tight buckling may have made the ground favorable for iron mineralization.

To the south, the north limb of the south side anticline is mineralized along much of its length. Less than a ton of ore is exposed in poor outcrop at the southwest corner of the section 17 east grid(paleomagnetic site PM-7). However, magnetic anomalies and ore float indicate widespread mineralization in the Torres limestone beds on the northern limb. This matter is discussed in some

detail in the section covering detail magnetic work and on plates 2A, 2B and 2C.

The iron ore seen in the map area is much like ore all along Jones Camp dike: it is predominantly very fine and fine-grained magnetite with very minor hematite and limonite. Actinolite contact rock was found in Torres sandstone a couple hundred feet west of the section 17 east grid and at the edges of the Joyita roof pendant east of that grid.

WEST END GEOLOGIC MAP

Portions of sections 10-15 T5S R6E and section 18 T5S R7E were mapped at the scale 1"=600'(plate 7). Five intrusive phases form a composite dike. Complex structure in Pytl beds west of the last igneous outcrops indicate an extension of the dike in the subsurface. A ranch road runs along the crest of the dike through most of the map area, as it provides a much firmer surface in wet weather than the Torres gypsum and sandstone to either side.

The intrusive activity at the west end is marginal to that of the main dike. The dike is narrower and was emplaced at a lower level within the intruded sediments. Roof pendants of Torres sediments indicate that the west end, like the rest of the dike has been barely uncovered. The top of the dike intruded to a level approximately 500 feet lower than the top of the main dike on Chupadera Mesa.

The dike forms discontinuous outcrops separated by in situ Torres sediments, though magnetic data indicate that the dike is continuous at depth. Marginal anticlines are smaller and less abundant than those seen by the main dike. These lines of evidence suggest that the igneous rocks here were not emplaced as forcefully as those of the main dike.

At the offset trend to the west, the igneous facies cease to form a single sheeted dike outcrop. Small parallel dikes of several facies offset a probable extension of the dike in the subsurface. Presumably these coalesce into a single sheeted body at depth. Pytl beds west of that point are contorted, accordian-style, into domes and folds. These structures indicate that igneous dikes and necks have intruded beneath the limestone beds. Float of magnetite and igneous rocks is found in this area. The small dikes of the offset trend probably ascended parallel imbricate faults created by the emplacement of earlier facies below or to the east.

In the eastern part of the map Pytl beds north of the dike dip between 15 and 25 degrees to the northwest(plate 7) This attitude was determined by several strike and dip measurements in sections 11 and 12 and was confirmed by a similar attitude at the north end of the transverse magnetic line in S2 SE4 section 1. An unreliable strike and dip taken on a butte southwest of Hale Well indicates a southwesterly dip. The structure here on the flats to the

west of the mesa appears to be more complex than mapped by Wilpolt and Wanek(1951). The dip reversal west of the mesa scarp suggests that the limestone beds are the same upper Torres beds exposed on the mesa scarp. As this mapping exercise focused on the Jones Camp igneous rocks, the stratigraphic level of the limestone beds within the Torres member was not ascertained. A Pytl bed 1000 feet south of the dike in section 13 strikes parallel to the dike and dips to the south. Outcrops 300 feet north of the dike (section 12) conform to the regional northwesterly dip. The sediments to the south, forming a western extension of the south side anticline, were more profoundly affected by the intrusion of the dike.

On the main dike atop Chupadera Mesa, Tjc bisects Tjb with only subordinate amounts of other igneous facies. At the west end, this familiar scenario occurs only in the vicinity of the range boundary between 6E and 7E.

Tjb is the dominant rock type in the eastern portion of the map. It is altered where other intrusions occur nearby. Where it is the sole exposed facies, it is fresher and retains more of its primary magnetic mineralogy, though alteration and albitization are still fairly common. Presumably it is not cut by other facies at depth in these areas, though magnetic data at the transverse line might suggest another interpretation(see figure 21). To the east, it is cut by Tjc, Tjm and Tja.

In the central portion of the map, Tja forms the bulk of the dike. It is generally a primary intrusive phase, though the outcrop at 2600W(figure 22) on the axial line is an alteration of Tjb. Tja generally forms a sheeted dike with Tjb or Tjh, with small necks of Tjc or Tjm at the edges of or between the more dominant phases. The igneous pulses form small, solitary dikes to the west on the offset trend.

At the west end, the dike intrudes limestone, gypsum and sandstone beds in the top or middle of the Torres member. The sandstone and gypsum only rarely form competent outcrops. The limestone beds occur mainly as rubble-crops or as caps on small buttes, though good outcrops are found at the western edge of the map. Pytl beds are tan-brown and have undergone aggrading neomorphism and local dolomitization. A ten centimeter oolitic horizon is seen in several limestone beds. The limestone is often fossiliferous, bearing crinoids, bryozoans and bivalved organisms. Pytl overlaps the edges of dike outcrops at several locations in the central portion of the map. These overlaps are often altered, with the introduction of one or more of the following minerals; dolomite, actinolite, tremolite, siderite, epidote, sphene or hematite. The dark grey to black color of Pytl beds adjacent to the dike on Chupadera Mesa is not seen at the west end.

Magnetite ore in sandstone beds at 6000W(figure 24) has been exposed by prospect trenches. A broad, high-level magnetic anomaly farther south on that line suggests that iron concentrations may occur in that apophysitic dike of Tjh. Such orebodies may be continuous along the 1300 foot length of that dike. The morphology of the dike next to soft Yeso sandstone and gypsum could facilitate pit design if ore is confirmed there. Magnetite mineralization is found in sandstone and limestone beds dipping away from the northern edge of the dike near the 6E/7E range line. A 36 foot exploration shaft was sunk to sample the mineralization. Jenkins(1985) conducted a petrographic study of ore and gangue at this site. Actinolite contact rock was found in Tja 250 feet southeast of the shaft. Another orebody occurs 600 feet west of the shaft. It is interesting to note that a piece of magnetite float was found near Hale Well, 2500 feet south of the dike in section 13. To the south of the zero station of the transverse line, alluvium in Hale Wash contains a few percent of fine-grained magnetite. This occurrence may be a viable placer deposit. Magnetic data and the above geological observations indicate that the west end may hold economic concentrations of iron ore and that it should be considered an attractive exploration target.

BINGHAM POST OFFICE

The author visited an unnamed intrusive immediately to the west of the post office at Bingham, New Mexico on U. S. 380. It is six miles west of the western scarp of Chupadera Mesa, on strike with Jones Camp dike. The intrusive is 4000 feet long and 800 feet wide. It plunges under bolson deposits to the west and the eastern end abuts against the upthrown side of a normal fault. Two igneous rock types were observed. The first is a green very fine-grained rock with secondary calcite, tremolite and epidote. It displays no attraction to a hand magnet. The second rock type is a very coarse-grained, hornblende rich, micaceous diorite or monzonite which shows moderate attraction to a hand magnet. In hand specimen, these rocks are quite similar to Tjb and Tjh, respectively, of the Jones Camp dike. There is pervasive hydrothermal alteration. The dike intruded the Yeso formation, including a massive light grey limestone bed similar to those in the Torres member. Several prospect pits and shallow shafts are found over the length of the dike. One such pit exposes a two foot magnetite layer replacing limestone in contact with the intrusive. The rock types, alteration, outcrop patterns and styles of intrusion and mineralization are very similar to those of Jones Camp dike. This intrusion appears to be a western extension of Jones Camp dike or closely related to it. The deposit would be an appealing prospect for exploration. There are two factors to be considered in any decision to develop this deposit: it lies adjacent to U. S. 380 and it is privately owned land.

UNNAMED INTRUSIVES, T4S R6E

The author visited unnamed intrusives in sections 1, 2, 12, 24 and 25 T4S R6E and sections 7 and 30 T4S R7E. The intrusive is dark green to grey and porphyritic with 5-8% fine-grained white plagioclase phenocrysts and looks very similar to Tjp. It occurs as dikes, necks and sills which intrude Yeso formation sedimentary rocks. Two limestone beds crop out in the area: a dense, dark grey, fossiliferous, sparry bed and a light grey oolitic bed. The intrusive tilted the sediments, with dips varying between 10 degrees and vertical. No magnetite ore was encountered, though widespread iron mobilization is evident as hematite concretions and stains of hematite and limonite.

IRON HORSE DEPOSIT

The author visited the Iron Horse deposit a few miles south of Jones Camp in section 9 T6S R7E. At Iron Horse, a dike of medium-grained diorite or monzonite intruded the Yeso formation. The uppermost limestone, sandstone and gypsum beds of the Torres member have been mineralized with magnetite. An anticline in the top Pytl bed carries an ore deposit which was mined on a small scale during World War II. The dike is identical to Jones Camp with respect to structure, mineralization and rock type. The intrusive rock at Iron Horse appears to have come from the same magma chamber as the Jones Camp dike. The deposit is described by Kelley(1949).

Johnson(1953) conducted a magnetic study at Iron Horse. The present author remeasured three of Johnson's profile lines with a G-816 proton precession magnetometer. The resulting data(Appendix II) were only 15-20% of the level of those reported by Johnson. The discrepancy is due to different instrument heights. The shapes of anomalies were similar in both studies. The data obtained by the G-816 was plagued by the same scatter effect encountered at Jones Camp dike.

Iron Horse should be considered in any regional iron exploration program undertaken near Chupadera Mesa. Although surface exposures indicate low tonnage of ore, The deposit's location adjacent to U. S. 380 would greatly facilitate transportation of ore. Additionally, it is possible that more such deposits lie undiscovered between Iron Horse and Jones Camp.

CONCLUSIONS

A paleomagnetic study of igneous rocks, iron ore and alteration was conducted at Jones Camp dike(figures 5 and 8). Samples were collected from magnetite ore pods, actinolite contact rock and four of the syenodioritic facies(mottled border facies, central facies, albitite and pyroxene syenodiorite). Precisely imprinted field directions of the remanent magnetization was observed only in two samples of heavily altered mottled border facies. These rocks were hydrothermally altered during a period of reversed polarity of the earth's magnetic field. Two outcrops of pyroxene syenodiorite and an outcrop of Tjb intruded by Tjp were sampled. The declinations imprinted on these rocks are fairly well defined, though not as precisely as the two reversed Tjb samples. The inclinations, however, do not approximate the Oligocene average and appear to show rotation of these outcrops. All other sites sampled at Jones Camp, including an exposure of fairly fresh Tjb, show a wide range in remanent field directions.

The low precision in remanent field directions is due to grain-to-grain interactions between magnetite crystals and to chemical alteration which occurred as the rocks were cooling past the Curie and Neel temperatures. The acquisition of chemical remanent magnetization by the rocks was complicated by hydrothermal activity accompanying the emplacement of the rocks. Some evidence supports a

hypothesis that the dike was emplaced during a reversal of the earth's magnetic field. That hypothesis is not favored by the author. Other studies(Strangeway, 1961; Ueno, 1967) suggest that thin, tabulate bodies with high magnetite contents may have inherent problems acquiring accurate or well defined remanent field directions.

Two detailed studies and one reconnaissance study with a Geometrics G-816 proton precession magnetometer establish that instrument as a good qualitative exploration tool at Jones Camp. Quantitatively, however, it fails to predict the size or dip length of magnetite ore pods accurately. Measured susceptibilities of paleomagnetic samples of iron ore are only one third to one quarter the magnitude estimated using empirical formulae for ore with identical amounts of magnetite(figure 10). Similarly, most igneous rocks carried only one half to one tenth as much susceptibility as calculated, with extreme samples showing only 1/1000 as much. Theoretical anomaly profiles generated by any of several formulae in the literature do not accurately predict the shapes of anomalies over orebodies or igneous rocks at Jones Camp dike.

Anomaly patterns are often discontinuous, even over continuous outcrops of ore, indicating discontinuity within ore bodies. Large-scale anomalies are also seen in areas with no surface exposure of iron ore, indicating orebodies at depth. Several such anomalies are found along the south

side of the dike in sections 16 and 17 T5S R7E(plates 2B and 2C). A large-scale anomaly over hornblende diorite at the west end(plates 7 and 8; figures 24 and 25) is believed to represent a buried ore pod. Such an orebody may be associated with the Tjh ledge over its entire strike length of 1400 feet. Bickford(1980) estimates 1,117,940 tons of probable ore reserves and 1,575,630 tons of possible reserves based on an average thickness of six feet and a 75 foot depth of outcropping orebodies. The discovery of buried ore pods with the magnetometer persuades the author that Bickford's estimates are conservative.

Gibbons(1981) states that his geochemical study supports a model of the Jones Camp dike as a composite dike formed by multiple intrusions. The present author's field mapping(plates 3, 4, 5, 6 and 7) also support that model. Three major igneous rock types have long been recognized at Jones Camp dike; the fine-grained border facies, the coarse-grained central facies and the porphyritic pyroxene syenodiorite(field name: "diabase"). The mapping in the present study has identified at least three additional facies; a medium-grained mica syenodiorite, an albitite and a very coarse-grained hornblende diorite. These may correspond to facies proposed by Noguiera(1970). There is abundant field evidence that these facies are intrusive, including xenoliths, visible cross-cutting relationships and sharp contacts. As later facies ascended from the magma chamber, they branched, sending apophyses up fractures in

previously emplaced facies. Large scale differentiation in situ is rejected as a cause for textural and mineralogical variations in the Jones Camp rocks.

A more-or-less continuous anticline on the southern shoulder of the dike extends for eight miles between section 13 T5S R6E and section 19 T5S R8E. It is referred to as the "south side anticline" in this study. There are numerous ore outcrops and magnetic anomalies along its length and it should be considered a very good target for future exploration.

Only one location along the dike was identified in this study as having potential as a placer magnetite deposit. That location is in Hale Wash, south of the zero station (paleomagetic station PM-13) at the west end(plate 7). Careful exploration in the future could identify other placer deposits near the dike.

The west end of the dike was mapped and a reconnaissance scale magnetic study was conducted(plates 7 and 8). Two ore pods along the north edge of the dike show evidence of having been evaluated in the past. A magnetic anomaly over a ledge of hornblende diorite indicates magnetite mineralization associated with that body. The west end should be included in any exploration program trying to increase ore reserves at Jones Camp.

Dioritic dikes and magnetite pods at Iron Horse and Bingham Post Office are strikingly similar to Jones Camp dike. These also hold promise as viable iron deposits.

BIBLIOGRAPHY

Anderson, E. C., 1958, Report of investigation of the Jones Camp iron deposits, Socorro County, New Mexico: unpubl. rpt. for Dotson Mineral Corp. Copy on file at New Mexico Bur. of Mines and Min. Res.

Balsley, J. R. and Buddington, A. F., 1958, Iron-titanium oxide minerals, rocks and aeromagnetic anomalies of of the Adirondack area, New York: Econ. Geol., vol.53, no. 7, p. 777-805.

Bates, R. L., Wilpolt, R. H., MacAlpin, A. J. and Vorbes, G., 1947, Geology of the Gran Quivera quadrangle, New Mexico: New Mexico Inst. Min. and Tech., State Bur. Mines and Mineral Res., Bull. 26, 57 p.

Bath, G. D., 1962, Magnetic anomalies and magnetizations of the Biwabik iron formation, Mesabi area, Minnesota: Geophysics, vol. 27, p. 627-650.

Bickford, D. A., 1980, Economic geology of the Jones Camp iron deposit, Socorro County, New Mexico: Unpub. Master of Science thesis, New Mexico Inst. Min. and Tech., 226 p.

Breiner, S., 1973, Applications manual for portable magnetometers: Geometrics, Sunnyvale, Ca., 58 p.

Chapin, C. E., Chamberlin, R. M., Osburn, G. R., White, D. W. and Sanford, A. R., 1978, Exploration framework of the Socorro geothermal area, New Mexico: New Mexico Geol. Soc. Spec. Publ. 7, p. 114-129.

Cordell, L., 1985, Geothermal resources map of New Mexico: New Mexico Energy Research and Development Institute.

Cook, K. L., 1950, Quantitative interpretation of vertical magnetic anomalies over veins: Geophysics, vol. 15, no. 4, p. 667-686.

Dane, C. H. and Bachman, G. O., 1965, Geologic map of New Mexico: U. S. Geol. Survey, Washington, D. C.

Darton, N. H., 1922, Geologic structure of parts of New Mexico: U. S. Geol. Survey Bull. 726, p. 173-275.

Department of Energy, 1977, Tularosa Quadrangle; Residual intensity magnetic anomaly contour map: DOE open-file map no. GJM-403.

Diehl, J. F., Beck, M. E. and Lipman, P. W., 1974, Paleomagnetism and magnetic-polarity zonation in some Oligocene volcanic rocks of the San Juan mountains, southwest Colorado: Geophysical Journal of the Royal Astronomical Society, vol. 37, p.323-332.

Dobrin, M. B., 1976, Introduction to geophysical prospecting: McGraw-Hill, New York, 630 p.

Dodson, R, Dunn, J. R., Fuller, M., Williams, I., Ito, H., Schmidt, V. A., Wu, Y. M., 1978, Paleomagnetic record of a late Tertiary field reversal: Geophysical Journal of the Royal Astronomical Society, Vol. 53, p. 373-412.

Ehrlich, M., Sun, S., Scharon, L. H. and Soffel, H. C., 1969, Magnetic and paleomagnetic investigations of the Precambrian Iron Mountain deposits, southeast Missouri: Inst. Mining and Met. Trans., vol. 78, bull. 753, B114-122.

Emmons, N. W., 1906, The Jones iron fields of New Mexico: Mining Magazine, vol. 13, p. 109-116.

Epstein, A. G., Epstein, J. B., and Harris, L. D., 1977, Conodont color alteration-an index to organic metamorphism: U. S. Geological Survey Professional Paper 995.

Fabiano, E. B., Peddie, N. W. and Jones, W. J., 1976, Magnetic total intensity in the United States, epoch 1975.0: U. S. Geol. Survey Map I-915, U.S.G.S., Reston, Va.

Fischer, R. A., 1953, Dispersion on a sphere: Proc. Royal Soc., A217, pp. 29-305.

Gibbons, T. L., 1981, Geochemical and petrographic investigation of the Jones Camp magnetite ores and associated intrusives, Socorro County, New Mexico: Unpub. Master of Science thesis, New Mexico Inst. Min. and Tech.

Hager, D. and Robitaille, A. E., 1919, Geologic report on oil possibilities in eastern New Mexico: Unpub. report. cited by Wilmarth(1938), Lexicon of geologic names in the United States, U. S. Geol. Survey Bull. 896, p. 831.

Jahren, C. E., 1963, Magnetic susceptibility of banded iron formation: Geophysics, vol. 28, no. 5, pp. 756-766.

Jenkins, J., 1985, Geology and geochemistry of the Jones Camp magnetite deposits, Socorro County, New Mexico: unpublished Master of Science thesis, New Mexico Institute of Mining and Technolgy.

Johnson, D., 1953, A magnetometric survey of the Iron Horse magnetite deposit, Socorro County, New Mexico: unpublished Master of Science thesis, New Mexico Institute of Mining and Technology, 43 p.

Jones, F. A., 1902, Plats of claims at the Jones Camp District: copy on file at New Mexico Bur. of Mines and Min. Res.

Jones, F. A., 1904, New Mexico Mines and Minerals (1904 World's Fair edition): the New Mexico Printing Co., Santa Fe, N. M., p. 102-103.

Kedzie, L. L., Sutter, J. F. and Chapin, C. E., 1985, High-precision 40Ar/39Ar ages of widespread Oligocene ash-flow tuff sheets near Socorro, New Mexico: abstracts with programs, 98th annual meeting, Geological Society of America, Orlando, Florida, October 28-31, 1985.

Kelley, V. C., 1949, Geology and economics of New Mexico iron ore deposits: Univ. New Mexico Publ. in Geol. no. 2, The Univ. of New Mexico Press, Albuquerque, N. M. 246 p.

Kelley, V. C. and Thompson, T. B., 1964, Tectonics and general geology of the Ruidoso-Carrizozo region, central New Mexico: New Mexico Geol. Soc. Guidebook, 15th Field Conference, Ruidoso Country, p. 110-121.

Koulomzine, T., LaMontagne, Y. and Nadeau, A., 1970, Methods for the direct interpretation of magnetic anomalies caused by inclined dikes of infinite length: Geophysics, vol.35, no. 5, p. 812-830.

Keyes, C. R., 1915, Conspectus of the geologic formation of New Mexico: Iowa Acad. Sci., Pr., vol. 22, p. 249-267.

Lee, W. T. and Girty, G. H., 1909, The Manzano Group of the Rio Grande Valley, New Mexico: U. S. Geol. Survey Bull. 389, 141 p.

Lochman-Balk, C., 1964, Lexicon of stratigraphic names used in Lincoln County, New Mexico: New Mexico Geol. Soc. Guidebook, 15th Field Conference, Ruidoso Country, p. 57-61.

McIntosh, W. C., 1983, Preliminary results from a paleo- and rock-magnetic study of Oligocene ash flow tuffs in Socorro County, New Mexico: Socorro II, New Mexico Geological Society guidebook, 34th field conference, p. 205-210.

Merrill, R. T. and McIlhinny, M. W., 1983, The earth's magnetic field: vol. 32, International Geophysics Series, Academic Press.

Muehlberger, W. R. and Denison, R. E., 1964, Precambrian geology of south-central New Mexico: Ruidoso Country, New Mexico Geological Society guidebook, 15th field conference, p. 62-69.

Needham, C. E. and Bates, R. L., 1943, Permian type sections in central New Mexico: Geol. Soc. America Bull., vol. 54, p. 1653-67.

Nogueira, A. C., 1971, Mineralogy and geochemistry of contact metasomatic iron deposits at Jones Camp, Socorro County, New Mexico: Unpub. Master of Science thesis, New Mexico Inst. Min. and Tech.

Parasnis, D. S., 1972, Principles of applied geophysics: Chapman and Hall, London, 214p.

Parasnis, D. S., 1975, Mining geophysics: 2nd edition, Elsevier Publishing Co., Amsterdam, 308 p.

Read, C. B. and Andrews, D. A., 1944, United States Geological Survey oil and gas investigations, preliminary map 8; U. S. Geol. Survey.

Spahr, C. L., 1983, Economic Geology of the Midnight, Black Knight and associated magnetite claims, Lone Mountain, Lincoln County, New Mexico: Unpublished Master of Science thesis, New Mexico Institute of Mining and Technology, 196 p.

Strangeway, D. W., 1961, Magnetic properties of diabase dikes: Journal of Geophysical Research, vol. 66, no. 9.

Streckeisen, A., 1967, Classification and nomenclature of igneous rocks: Neues Jahrb. Mineral. Abhandl., 107, p. 144-240.

Tarling, D. H., 1983, Paleomagnetism: Chapman and Hall, New York, N. Y., 379 p.

Telford, W. M., Geldart, L. P., Sheriff, R. E., and Keys, D. A., 1976, Applied Geophysics: Cambridge University Press, Cambridge, U. K., 860 p.

Travis, R. B., 1955, Classification of rocks: Quarterly of the Colorado Sch. Mines, vol. 50, no. 1.

Ueno, H., 1967, Studies on the magnetic properties of the Kamaishi iron and copper ore deposits, northeastern Japan: Science Reports of Tohoku University, Sendai, Japan, Series III, vol. X, no. 1.

Ward, W. S., 1902, Limestone report no. 27: unpubl. rpt. for CFI. Copy on file at New Mexico Bur. of Mines and Min. Res.

Weber, R. H. and Kottlowski, F. E., 1959, Gypsum Resources of New Mexico: New Mexico Bur. Mines and Mineral Res., Bull. 68, 68 p.

Weed, L. B., 1920, Report to CFI: Copy on file at New Mexico Bur. of Mines and Min. Res.

Wilpolt, R. H. and Wanek, A. A., 1951, Geology of the region from Socorro and San Antonio east to Chupadera Mesa, Socorro County, New Mexico: U. S. Geol. Survey Oil and Gas Investigations, map OM-121.

APPENDIX I

MAGNETIC BASE STATION DESCRIPTIONS

Section 19 T5S R8E

The base station for the section 19 prospect grid is located to the south of a tree in the drainage ca. 900 feet west of the shaft on the grid. It is 650 feet SSW(perpendicular) of the crest of the dike. It stands over Pyj near its contact with Pyc. See plates 5 and 9.

Sections 17/16 T5S R7E

This base station serves the section 17 east and west grids and the east and west magnetic lines. It is located by a tree on the south edge of the road ca. 1000 feet north of ON 200W, section 19 prospect grid (Paleomagnetic site PM-9). It is 850 feet north of the crest of the dike and stands over the Pyj/Pyc contact. See plates 6 and 9.

West End

The base station for the long transverse and axial lines is 1050 feet NNW of the zero station for both lines(Paleomagnetic site PM-13). It is located on a 50 foot high butte capped by Pytl(stratigraphic level undetermined). See plates 7 and 9.

Iron Horse deposit(section 9 T6S R7E)

The base station for proton precession magnetometer readings taken at the Iron Horse deposit is located 700 feet north of BL 5+72E. See Johnson(1953) for location of magnetic lines. The base station is located on Pg.

APPENDIX II

Appendix II is a list of total field magnetic measurements taken during the course of this study. This appendix is subdivided into sections for each magnetic survey conducted:

SECTION 19 PROSPECT GRID
SECTION 17 WEST MAGNETIC LINE
SECTION 16 EAST MAGNETIC LINE
SECTION 17 EAST GRID
SECTION 17 WEST GRID
WEST END - LONG TRANSVERSE LINE
WEST END - AXIAL LINE
(includes short transverse lines)
IRON HORSE DEPOSIT

Only those measurements taken on the long transverse line have been corrected for diurnal variation.

Points on grids may be thought of as points on a graph. Stations are surveyed from a zero point located off the grid. The baseline is measured west from the zero point. All stations on the baseline are marked ON ___W (zero-north, _ft west). Stations are designated by the distance (in feet) north or south of the baseline and distance west of the zero station(for example, 100N 650W). During the surveys, 100' to 200' stretches were measured along east-west or north-south lines on the grid. Each station is listed by its location along that line.

Magnetic lines were run due north, south, east or west of designated zero stations.

and * will be used to indicate range in scatter of readings:
= 10γ to 100γ range(average of five readings)
* = >100γ range(average of nine readings)
The long transverse line is an exception. # and * on that survey are lower:
= 3γ to 5γ range(average of five readings)
* = >5γ range(average of nine readings)

Entries will follow the following format:
750W 54944 * 2:45
750W - station designator; 54944 - reading; * or # - scatter effect indicator; 2:45 - time(AM or PM).

The following abbreviations will be used:
BL - Baseline BS - Base station

APPENDIX II

Surveying problems on the section 17 east grid produced errant lines which were oblique to east-west. They are referred to as oblique lines A, B, C or D. Their location on the grid is noted after the data.

Magnetic lines measured at the Iron Horse deposit are the same as those measured by Johnson(1953).

SECTION 19 PROSPECT GRID
July 17, 1984

Base Station 52119 4:20
cloudy to overcast, showers at noon

	ON		
0E	52186		
50W	52264		
100W	52399		4:44
150W	52238		
200W	52380		
250W	52870		
300W	52353		4:50
350W	51957		
400W	51686		
450W	51187	#	4:56
500W	53480	*	
550W	53000	*	5:00
600W	54313	*	
650W	52355		
700W	52478		
750W	52467		
800W	52486		5:13
BS	52125		5:17

	ON		
450W	51442	#	5:55
460W	50649	*	
470W	51895	*	
480W	50465	*	
490W	51382	*	
500W	53852	*	
510W	54892	*	
520W	53487	*	6:15
530W	53767	*	
540W	52855	*	
550W	52816	*	
560W	53673	*	6:23
570W	53476	*	6:27
580W	56179	*	
590W	54794	*	
600W	54400	*	
610W	55884	*	
620W	52815		
630W	52896		
640W	52856		6:39
BS	52128		6:47

SECTION 19 PROSPECT GRID
July 19, 1984

Base Station 52108 12:00
sunny/clear

450W			
100S	52026		
90S	52311		
85S	52331		
80S	53448	*	
75S	54074	*	
65S	52292	*	
60S	52555	*	
55S	52327	*	
50S	52353	*	12:26
45S	52569	*	12:35
40S	54492	*	
35S	55577	*	
30S	54545	*	12:42
25S	55269	#	
20S	55630	*	
15S	54686	*	
10S	54352	*	
5S	53502	*	
0N	51441	*	
5N	50834	*	
10N	50998	*	
15N	51450	#	
20N	52362	#	
25N	52081	#	
30N	50577	*	
35N	50517	#	
40N	50369	*	

450W			
45N	50189	#	
50N	50334	#	1:27
55N	50894		
60N	51599		
70N	51638	#	
75N	51222		1:32
80N	50819		
85N	50857		
90N	50983		
95N	51114		
100N	51346		
105N	51569	#	1:40
110N	51814	#	
115N	51840	*	
120N	52606	*	
125N	54447	*	
130N	54158	*	
135N	53049	#	
140N	52559		
145N	52241		
150N	51970		
155N	51809		1:58
160N	51716		
170N	51777		
180N	51925		
190N	52015		
200N	52097		

SECTION 19 PROSPECT GRID
July 19, 1984

500N			300W			
200N	51839		30N	50253	#	
190N	51736	2:10	25N	50327	*	
180N	51555		20N	50303	*	
170N	51137		15N	50318	*	
160N	51024		10N	50638	*	
155N	51211	#	5N	52334	#	
150N	51379		0N	53158	*	
145N	51525	2:19	5S	53988	*	3:18
140N	51608		10S	53692	*	
135N	51686		15S	52527	*	
130N	51762	#	20S	53627	*	
120N	51869		25S	52779	*	
110N	51976	2:26	30S	52434	*	
100N	51198	*	35S	52498	*	
95N	52584	*	40S	52373	*	
90N	53685	* 2:37	45S	53777	*	
85N	53647	*	50S	55151	*	
80N	53784	*	55S	54986	*	
75N	54176	*	60S	54470	*	
70N	53312	*	65S	54019	#	
65N	52452	#	70S	53665		
60N	51529	#	75S	53098	#	
55N	51065		80S	52735		
50N	51167		85S	52649		
45N	51144	3:02	90S	52833		
40N	51379		100S	52545		
35N	50870	#				
			BS	52116		3:55

SECTION 19 PROSPECT GRID
July 19, 1984

550W			550W		
100S	52354	5:39	35N	51059 *	
90S	52274		40N	50957 *	
80S	52068		45N	51178	
70S	51946		50N	51454	
60S	51701		55N	51672	6:16
50S	51460		60N	51782	
40S	51027		70N	51654	
30S	50137 *		80N	51215	
25S	50560 *		90N	51054	
20S	52175 *		100N	51668	
15S	52336 *		110N	52374 #	6:23
10S	52595 *		120N	52642	
5S	52478 *		130N	52510	
0N	52478 *		140N	52097	
5N	52592 *		150N	52161	
10N	52830 *	6:04	160N	52371	
15N	52704 *		170N	52611	
20N	54196 *		180N	52579	
25N	52791 *		190N	52060	
30N	51258 #		200N	51959	

SECTION 19 PROSPECT GRID
July 19, 1984

600W			
200N	51867		6:35
190N	51800		
180N	51678		
170N	51684		
160N	51978		
150N	52433		
140N	52404		6:42
130N	52113		
120N	51983		
110N	51861		
100N	51917		
95N	52287		
90N	52988	*	6:47
85N	53442		
80N	53615		
75N	53570		
70N	53401		
65N	53194		
60N	52697		
55N	52579		
50N	52083		
45N	51794		7:00

600W			
40N	52066	*	
35N	52370	#	
30N	53238	*	
25N	55047	*	
20N	55716	*	
15N	56114	*	
10N	55479	*	
5N	54774	*	
0N	54291	*	
5S	53332	#	7:18
10S	52782	#	
15S	52483		
20S	52310		
25S	52257		
30S	52253		
40S	52220		
50S	52307		
60S	52388		7:26
70S	52396		
80S	52543		
90S	52468		
100S	52442		
BS	52127		7:37

SECTION 19 PROSPECT GRID
July 22, 1984

Base Station 52130 4:15
 showers with moderate thunder/lightning from 5:00-5:30

10N				20N			
450W	51536	*	4:55	650W	52269		5:24
460W	51287	*		640W	51618		
470W	51817	*		630W	52149		
480W	52155	*		620W	53928	*	
490W	51728	*		610W	55455	*	
500W	51716	*		600W	55399	*	
510W	51587	*	4:53	590W	54160	*	5:43
520W	51814	*		580W	55170	*	
530W	54124	*		570W	53091	*	
540W	52919	*		560W	52256	#	
550W	52706	*		550W	54765	*	
560W	54651	*		540W	53719	*	5:52
570W	54282	*	5:06	530W	51817	#	
580W	54104	*		520W	50285	*	
590W	52861	*		510W	50077	*	
600W	56068	*		500W	50559	*	
610W	55027	*		490W	50241	*	
620W	53437	*	5:17	480W	51144	*	6:03
630W	53052			470W	51976	*	
640W	51988			460W	51364	*	
650W	52517		5:19	450W	52712	*	6:08

SECTION 19 PROSPECT GRID
July 22, 1984

30N			
480W	50902	*	6:13
460W	52157	*	
470W	54342	*	
480W	53614	*	
490W	51819	*	
500W	50342	*	
510W	50402	*	6:24
520W	50412	*	
530W	50868	*	
540W	51275	*	
550W	51651	*	
560W	52347		6:34
570W	52759	#	
580W	52921	*	
590W	52876	*	
600W	52906	*	
610W	55190	#	6:42
620W	54458	*	
630W	52076	*	
640W	50775	#	
650W	52010		

40N			
650W	51656	*	7:30
640W	51720	*	
630W	52377	*	
620W	52740	#	
610W	53109	#	
600W	51978	*	
590W	52378	*	7:42
580W	52886	#	
570W	53664		
560W	52311		
550W	51039	*	
540W	51133	*	7:49
530W	50951	*	
520W	50535	#	
510W	50632	#	
500W	51358		
BS	52128		8:00

windy & cloudy

SECTION 19 PROSPECT GRID
July 23, 1984

Base Station 52118 8:52
ON CE 52171 9:08

40N

490W	51951	#	9:15
480W	52823	#	
470W	53071	#	
460W	51548	*	
450W	50409	*	

50N

450W	50245	#	9:26
460W	51170	#	
470W	52349		
480W	51605		
490W	51318		
500W	51257		
510W	50670	#	
520W	50766	#	
530W	52107	#	
540W	52167	#	
550W	51440		
560W	51982		9:44
570W	53503		
580W	53199		
590W	52540		
600W	52065		
610W	52949		
620W	53280	*	
630W	51108	*	
640W	52634	*	
650W	52706	*	9:59

SECTION 19 PROSPECT GRID
July 16, 1984

Base Station 52152 4:12
ON OE 52154 4:25

10S				20S			
600W	52883	#	4:57	450W	55559	*	5:34
590W	53197	#		460W	54696	#	
580W	55565	*		470W	54102	*	
570W	52944	*		480W	52987	*	
560W	51493	*		490W	53255	*	
550W	53023	*		500W	53079	*	
540W	53003	*	5:12	510W	52732	*	5:49
530W	52968	*		520W	52586	*	
520W	52348	*		530W	52736	*	
510W	52645	*		540W	51973	*	
500W	52947	*		550W	53074	*	
490W	52837	*	5:32	560W	51081	*	6:01
480W	51742	*		570W	51441	*	
470W	51415	*		580W	52174	#	
460W	53589	*		590W	52586		
450W	54562	*		600W	53324		

SECTION 19 PROSPECT GRID
July 23, 1984

30S				40S			
600W	52233		6:14	400W	53802		6:55
590W	52050			410W	53876		
580W	51704	#		420W	53479		
570W	50977	#		430W	53758		
560W	50186	#		440W	55149	*	
550W	50456	*		450W	54046	*	
540W	50279	*	6:28	460W	53495	*	
530W	51849	*		470W	53921	*	7:04
520W	53550	*		480W	52574	*	
510W	53461	*		490W	52586	*	
500W	53593	*		500W	52743	*	
490W	53649	*	6:38	510W	56106	*	7:13
480W	55191	*		520W	54319	*	
470W	55120	*		530W	52393	*	
460W	54509	*		540W	51109	*	
450W	54950	*		550W	50887	#	

SECTION 19 PROSPECT GRID
July 25, 1984

	50S		
550W	51475		7:30
540W	51700		
530W	52225	#	
520W	53377	#	
510W	54624	*	
500W	55208	*	
490W	54843	*	7:41
480W	52065	*	
470W	53216	*	
460W	52838	*	
450W	53046	*	
440W	55560	*	7:50
430W	51895	*	
420W	53454	#	
410W	54455		
400W	54321		7:55
BS	52125		8:16
ON OE	52187		8:22

SECTION 19 PROSPECT GRID
October 11, 1984

Base Station 52101 6:27
overcast, rain from
2:30-6:30

60N

450W	51499	#	6:40
460W	52174	#	
470W	52291		
480W	51193	#	
490W	51239		
500W	51547	#	
510W	51503	*	6:50
520W	51302		
530W	53500	*	
540W	53519	*	
550W	51758	#	
560W	51736		6:57
570W	52634	#	
580W	53327		
590W	53328	#	
600W	52818		7:01

BS 52116 7:08

October 12, 1984

Base Station 52085 9:51

70N

450W	51744		
460W	52443		10:12
470W	51952		
480W	52760	#	
490W	52500		
500W	53067	*	
510W	52635	#	10:19
520W	52205		
530W	53751		
540W	53054		
550W	51638		
560W	51531		
570W	52012		
580W	52983		
590W	53364		
600W	53548		10:29

80N

450W	50773	#	10:36
460W	50755	*	
470W	51116	#	
480W	51921	#	
490W	53281	*	
500W	54057	*	
510W	52169	#	
520W	52142	*	
530W	52594	#	
540W	51481		
550W	51223	#	
560W	51464		10:51
570W	51767		
580W	52341		
590W	53379		
600W	53590		10:55

SECTION 19 PROSPECT GRID
October 19, 1984

90N

450W	50846		11:19
460W	51278	#	
470W	51924	#	
480W	51810		
490W	53311	*	
500W	54498	*	
510W	50818	*	11:30
520W	50695	*	
530W	50203	*	
540W	50585	*	
550W	51031	#	
560W	51651		11:35
570W	51840		
580W	52023		
590W	52358		
600W	52965	#	11:38

100N

450W	51209		11:43
460W	51019		
470W	51075	#	
480W	51212	#	
490W	51895	#	
500W	51959	*	
510W	50306	*	11:50
520W	50256	*	
530W	50287	*	
540W	51072	#	
550W	51747		
560W	52126		
570W	52101		
580W	51985		
590W	51941		
600W	51872		12:02

BS	52085		12:09

60N

650W	52422		2:12
640W	52335		
630W	51705		
620W	51525		
610W	52194		
600W	52812		

70N

600W	53444		2:17
610W	52816		
620W	52001	#	
630W	51287	*	
640W	53081	*	
650W	52453	*	

80N

650W	55303	*	2:22
640W	54094	*	
630W	53207		
620W	53122		
610W	53413		
600W	53615	*	

90N

600W	52969		2:31
610W	53365	*	
620W	53826	#	
630W	53751		
640W	53335	#	
650W	53447	*	

100N

650W	52994		
640W	53213		
630W	53368	#	
620W	52404	#	
610W	51925		
600W	51888		2:46

BS	52106		2:51

SECTION 19 PROSPECT GRID
October 12, 1984

Base Station 52101 4:57
cloudy to overcast

	110W			120N		
450W	51973	*	5:04	52892	#	5:38
460W	50777			52030	#	
470W	50577	*		51012	*	
480W	51089	*		52128		
490W	51551			52334	#	
500W	51894			52004	#	5:45
510W	51357	#	5:17	52084		5:54
520W	52176	#		52665		
530W	51941	#		52794		
540W	52200			52713		
550W	52330			52605		
560W	52510		5:23	52660		5:58
570W	52380			52661		
580W	52135			52439		
590W	51942			52117		
600W	51842			51954		6:00
610W	51685		5:28			
620W	51774	#		BS 52103		6:07
630W	52048	#				
640W	52637					
650W	53032		5:32			

SECTION 19 PROSPECT GRID
October 13, 1984

Base Station 52098 10:09

	120N		
610W	51917		10:24
620W	51942		
630W	51964		
640W	52078		
650W	52404		10:32
	130N		
450W	54386	*	10:39
460W	52810	#	
470W	51737	*	
480W	52758	#	
490W	52784		
500W	52095	#	
510W	51852		10:58
520W	52106		
530W	52350		
540W	52472		
550W	52480		
570W	52761		10:25
590W	52595		
600W	52101		
620W	51984		
640W	52142		
650W	52159		11:07

	140N		
450W	52554	#	11:15
460W	52962	#	
470W	53467		
480W	52648	#	
490W	51954	#	
500W	51749		
510W	51584		11:22
520W	51722		
530W	52086		
540W	52131		
550W	52079		
570W	52391		11:28
590W	52858		
600W	52384		
620W	52106		11:32
630W	52239		
640W	52186		
650W	52220		11:34
	150N		
450W	51976	#	
460W	52268	#	
470W	51926		
480W	51042	#	
490W	51192		
500W	51394		
510W	51385		11:47
520W	51843	#	
530W	51779		
540W	51973		
550W	52131		
570W	51851		11:52
590W	52233		
600W	52371		
620W	51984		
640W	52129		
650W	52182		11:58
BS	52085		12:03

SECTION 19 PROSPECT GRID
October 13, 1984

Base Station 52087 1:41

	150N			120N	
450W	51974		450W	52830 *	2:58
440W	51881	1:48	440W	53422 #	
430W	51846		430W	52417	
420W	51842		420W	52507	
410W	51882		410W	52209	
400W	51938		400W	51958	
	140N			110N	
450W	52528	1:55	450W	52083 #	2:58
440W	52128		440W	52746	
430W	51894		430W	52324	
420W	51783		420W	52245	
410W	51816		410W	52106	
400W	51888		400W	52015	
	130N			100N	
450W	53956 *	2:30	450W	51310	3:09
440W	53055 #		440W	51694	
430W	52341		430W	51896	
420W	52051 #		420W	51945	
410W	51813		410W	51992	
400W	51885		400W	52012	3:13
			BS	52106	3:25

SECTION 19 PROSPECT GRID
January 17, 1985

Base Station 52090 3:29
clear and sunny

	90N			60N	
450W	51007	3:58	350W	52162	4:28
440W	51425	3:45	360W	52104	
430W	51694		370W	52052	
420W	51819		380W	52003	
410W	51906		390W	51948	
400W	51972		400W	51811	4:31
390W	52003		410W	51673	4:35
380W	52055	3:51	420W	51476	
370W	52119		430W	51254	
360W	52170		440W	51019	
350W	52223		450W	51250	4:38
	80N			50N	
350W	52225	3:57	450W	50536 #	4:43
360W	52160		440W	50632	
370W	52095		430W	50987	
380W	52017		420W	51290	
390W	51959		410W	51469	
400W	51891		400W	51692	4:47
410W	51797	4:02	390W	51835	4:49
420W	51700		380W	51944	
430W	51515		370W	52018	
440W	51241		360W	52067	
450W	50826 #	4:06	350W	52115	4:52
	70N		BS	52093	5:02
450W	51638	4:10			
440W	51256				
430W	51414				
420W	51598				
410W	51759	4:16			
400W	51873				
390W	51957	4:21			
380W	52004				
370W	52057				
360W	52131				
350W	52202	4:25			

SECTION 19 PROSPECT GRID
February 12, 1985

Base Station 52080 1:54
sunny, 40's

	700W			700W	
0N	52428	2:00	10N	52516	
10S	52571		20N	52504	2:48
20S	52494		30N	52528	
30S	52378		40N	52614	
40S	52360		50N	52677	
50S	52353		60N	52696	2:53
60S	52366	2:07	70N	52636	
70S	52348		80N	52505	
80S	52332		90N	52335	
90S	52249		100N	52154	
100S	52141		110N	52480	3:05
110S	52195	2:13	120N	53126	
120S	52244		130N	53526	
130S	52340		140N	53421 #	
140S	52450		150N	51784 #	
150S	52591		160N	51310 #	
160S	52675	2:20	170N	51836 #	
170S	52649		180N	52054	
180S	52594		190N	52005	
190S	52584		200N	51744	
200S	52546		210N	51485	3:21
210S	52481	2:31	220N	51649	
220S	52395		230N	51758	
230S	52343		240N	51868	
240S	52301		250N	51926	
250S	52279		260N	51974	
260S	52263	2:38	270N	52001	3:31
270S	52244		280N	52016	
280S	52228		290N	51993	
290S	52210		300N	51957	3:33
300S	52192	2:41			
			BS	52093	4:31

SECTION 19 PROSPECT GRID
February 13, 1985

Base Station 52092 8:53
clear, 40's

	0N	
650W	52273	8:59
660W	52452	
670W	52483	
680W	52480	
690W	52448	
	10N	
690W	52618	9:06
680W	52526	
670W	52475	
660W	52402	
650W	52261	
	20N	
650W	no reading	
660W	52471	9:15
670W	52640	
680W	52571	
690W	52581	
	30N	
650W	51996 #	9:34
660W	52598	
670W	52783	
680W	52815	
690W	52647	
	40N	
690W	52867	9:43
680W	53196 #	
670W	53399	
660W	53308	
650W	52248	
	50N	
650W	53988 *	9:56
660W	54582 *	
670W	54095	
680W	53531	
690W	53043	
BS	52086	10:47

	60N	
650W	53173 *	10:55
660W	57549 *	
670W	55797 *	
680W	54282	
690W	53283	
	70N	
690W	53306 #	11:19
680W	54431	
670W	56350 *	
660W	55746 *	
650W	53070 *	
	80N	
690W	53150	11:33
680W	53895 #	
670W	54909 *	
660W	54944 *	
650W	56280 *	
	90N	
650W	53643 #	11:52
660W	53686 #	
670W	53497	
680W	53152	
690W	52775	
	100N	
690W	52397	12:01
680W	52699	
670W	52840	
660W	52911	
650W	52956	
BS	52075	1:07
	110N	
650W	52979	1:15
660W	52822	
670W	52635	
680W	52548	
690W	52371	

SECTION 19 PROSPECT GRID
February 13, 1985

	120N	
690W	52434	1:39
680W	52367	
670W	52409	
660W	52517	
650W	52224	
	130N	
650W	52102	1:46
660W	52153	
670W	52149	
680W	52200	
690W	52394	
	140N	
690W	52281	1:52
680W	52216	
670W	52228	
660W	52244	
650W	52178	1:55
	150N	
650W	52152	2:05
660W	52371	
670W	52383	
680W	52151	
690W	51993	
	160N	
690W	51973	2:23
680W	52284	
670W	52651	
660W	52803	
650W	52226	
	170N	
650W	52329	2:29
660W	52925	
670W	53270	
680W	52771	
690W	52522	
	180N	
690W	52457	2:36
680W	52736	
670W	53042	
660W	52769	
650W	52217	
BS	52086	2:44
	190N	
650W	52391 #	3:41
660W	53034	
670W	53012 #	
680W	52576	
690W	52178	
	200N	
650W	51597	3:56
660W	51556	
670W	51550	
680W	51658	
690W	51713	4:02
	60S	
500W	54424	4:40
490W	54842	
480W	55370 #	
470W	56431 *	
460W	54407 *	
450W	53037 *	
440W	52939 *	
430W	52996 *	
420W	52863 *	
410W	54189 *	
400W	54990 *	

SECTION 19 PROSPECT GRID
February 13, 1985

70S

400W	53040	*	5:03
410W	53090	*	
420W	53255	*	
430W	53309	*	
440W	53011	*	
450W	57123	*	
460W	55407	*	5:15
470W	55067	*	
480W	54253		
490W	53763	#	
500W	53682		

80S

500W	52646		5:27
490W	52883		
480W	53037		
470W	53156		
460W	53688	#	
450W	53840	*	
440W	51150	#	5:35
430W	52372	*	
420W	52942	*	
410W	53227	*	
400W	53870	*	

90S

400W	57080	*	5:48
410W	55547	*	
420W	53039	*	
430W	51116	#	
440W	51661		
450W	52338		
460W	52601		5:57
470W	52659		
480W	52598		
490W	52659		
500W	52610		5:59

BS	52093	6:07

February 14, 1985

Base Station 52102 8:46
clear, 30's

100S

500W	52464		8:52
490W	52410		
480W	52414		
470W	52361		
460W	52185		
450W	51992		
440W	51926		9:00
430W	52260		
420W	52726		
410W	54063	*	
400W	54971	*	
390W	54669	#	9:16
380W	54364		
370W	53870	#	
360W	53558		
350W	53423		
340W	52471	#	9:23
330W	52536		
320W	53002		
310W	53536		
300W	53322	#	

90S

300W	53532		9:29
310W	54139		
320W	53535		
330W	53825		
340W	54671	*	
350W	55379	*	
360W	55158	#	9:37
370W	55145		
380W	56038	*	
390W	56268	*	
400W	56647	*	

SECTION 19 PROSPECT GRID
February 14, 1985

	80S				50S		
400W	54076	*		300W	52355		11:36
390W	58507	*	9:52	310W	52339		
380W	57213	*		320W	52266		
370W	55906	*		330W	52161		
360W	54996			340W	52012		
350W	54555	#		350W	52176		
340W	54024			360W	53239	#	11:42
330W	53465			370W	54073	#	
320W	53215			380W	54080		
310W	53574			390W	54032		
300W	53180	#		400W	54251	#	

	70S				40S		
300W	52642		10:08	400W	53789		11:53
310W	53004			390W	53630	#	
320W	53545			380W	53526	#	
330W	53690			370W	53149	#	
340W	53311			360W	52358	#	
350W	53389			350W	51854		
360W	54040	#	10:14	340W	51949		
370W	55101			330W	52062		
380W	56432			320W	52178		
390W	55197	*		310W	52266		
400W	53352	*		300W	52326		

	60S				30S		
400W	55285	*	10:35	300W	52274		12:06
390W	54427			310W	52238		
380W	54722	#		329W	52169		
370W	54550			330W	52084		
360W	53799			340W	51959		
355W	53325			350W	51820		
350W	52904			360W	51730		
340W	52725		10:44	370W	51831	#	
330W	52743			380W	52323	#	
320W	52680			390W	53127		
310W	52571			400W	53795	#	
300W	52417		10:47				

SECTION 19 PROSPECT GRID
February 14, 1985

20S

400W	53880 #	12:16
390W	52698	
380W	51794	
370W	51605	
360W	51676	
350W	51848	12:21
340W	51981	12:30
330W	52058	
320W	52137	
310W	52198	
300W	52246	

10S

300W	52255	12:34
310W	52196	
320W	52127	
330W	52052	
340W	52000	
350W	51892	
360W	51746	
370W	51567	12:39
380W	51541	
390W	51856	
400W	52732	

BASELINE

400W	51672	
390W	51400	
380W	51478	
370W	51652	
360W	51794	
350W	51910	12:45
340W	52000	
330W	52071	
320W	52148	
310W	52214	
300W	52279	12:50

BS 52085 12:55
sunny, clear, 50's

June 23, 1985

BS 52061 5:22
sunny, 80's

BASELINE

450W	51487 *	5:29
440W	50862 *	
430W	50683 *	
420W	50761 *	
410W	51288 #	
400W	51660	

10S

400W	52584	5:41
410W	52385 #	
420W	51345 *	
430W	50977 *	
440W	52352 *	
450W	54013 *	5:48

20S

450W	55226 *	5:22
440W	53565 *	
430W	52148	
420W	52258 #	
410W	53262	
400W	53756 #	5:58

30S

400W	53838	6:01
410W	53694 #	
420W	53105	
430W	53061	
440W	54159 #	
450W	55038 *	

SECTION 19 PROSPECT GRID
June 23, 1985

	10N			30N		
450W	51156 *	6:51	450W	51244 *	7:28
440W	52741 *		440W	51106	
430W	51431 *		430W	50528	
420W	50660 #		420W	50747	
410W	51094		410W	51073	
400W	51219	6:58	400W	51347	7:35
390W	51382	7:00	390W	51569	7:37
380W	51529		380W	51732	
370W	51697		370W	51850	
360W	51829		360W	51940	
350W	51933	7:03	350W	52013	7:40
340W	52005	7:05	340W	52075	7:43
330W	52078		330W	52108	
320W	52150		320W	52140	
310W	52204		310W	51286	
300W	52244	7:07	300W	52203	
	20N			40N		
300W	52170	7:11	300W	52372	7:49
310W	52173		310W	52290	
320W	52156		320W	52198	
330W	52112		330W	52129	
340W	52048		340W	52094	
350W	51974	7:15	350W	52048	7:52
360W	51862	7:17	360W	51993	7:54
370W	51763		370W	51919	
380W	51597		380W	51810	
390W	51440		390W	51697	
400W	51251	7:20	400W	51505	7:56
410W	51011	7:22	410W	51300	7:58
420W	50820		420W	51016	
430W	50778		430W	50600	
440W	51901		440W	50519 *	
450W	52597	7:26	450W	50715 *	8:03

BS 52059 8:09

SECTION 19 PROSPECT GRID
June 24, 1985

Base Station 52067 8:59
sunny & clear

	10S	
700W	52539	9:04
690W	52497	
680W	52481	
670W	52464	
660W	52483	
650W	52399	
640W	52260	9:12
630W	52248	
620W	52343	
610W	52534	
600W	52749	9:16
	20S	
600W	52256	9:21
610W	52304	
620W	52166	
630W	52245	
640W	52496	
650W	52501	
660W	52423	9:29
670W	52462	
680W	52522	
690W	52456	
700W	52463	9:34
	30S	
700W	52357	9:37
690W	52391	
680W	52428	
670W	52438	
660W	52458	
650W	52455	
640W	52494	10:12
630W	52451	
620W	52366	
610W	52369	
600W	52178	10:16
	40S	
550W	50901 #	10:21
560W	51019	
570W	51291 #	
580W	51546	
590W	51850	
600W	52046	
610W	52436	10:32
620W	52642	
630W	52553	
640W	52569	
650W	52468	
660W	52444	10:38
670W	52404	
680W	52396	
690W	52381	
700W	52341	10:41
	50S	
700W	52329	10:47
690W	52346	
680W	52344	
670W	52355	
660W	52409	
650W	52510	
640W	52503	10:54
630W	52385	
620W	52655	
610W	52715	
600W	52252	
590W	52003	11:00
580W	51936	
570W	51737	
560W	51455	
550W	51400	11:04

BS 52065 11:10
sunny & clear

SECTION 19 PROSPECT GRID
June 24, 1985

70S

500W	53588	12:47
510W	53191	
520W	52671	
530W	52196	
540W	51971	
550W	51920	12:51
560W	51947	
570W	52091	
580W	52272	
590W	52331	
600W	52292	12:56

BS 52055 1:05
partly cloudy

60S

600W	52256	2:14
590W	52217	
580W	52205	
570W	52053	
560W	51681	
550W	51666	
540W	52011	2:22
530W	52328	
520W	52877	
510W	53739	
500W	54528 #	2:25

80S

500W	52649 #	2:31
510W	52429	
520W	52213	
530W	52256	
540W	52077	
550W	51962	
560W	52116 #	2:37
570W	52272	
580W	52339	
590W	52358	
600W	52419	2:40

600W

90S	52407	2:44
100S	52374	
110S	52373	
120S	52343	
130S	no reading - tree	
140S	52296	
150S	52258	
160S	52223	
170S	52206	
180S	52272	
190S	52311	
200S	52315	
210S	52441	2:57
220S	52580	
230S	52587	
240S	52475	
250S	52395	
260S	52367	3:03
270S	52335	
280S	52298	
290S	52279	
300S	52257	
310S	52242	3:08
320S	52225	
330S	52209	
340S	52196	
350S	52177	3:12

BS 52065 3:18
distant thunder, overcast, windy

SECTION 19 PROSPECT GRID
June 24, 1985

Base Station 52060 6:06
rain from 4:00 to 6:00 PM

500W			110S			
90S	52591	6:20	490W	52315		6:50
100S	52449		480W	52286		
110S	52399		470W	52264		
120S	52403		460W	52198		
130S	52402		450W	52188		6:53
140S	52329		440W	52244	#	6:58
150S	52316		430W	52283		
160S	52296	6:25	420W	52555		
170S	52282		410W	53122		
180S	52348		400W	53404	#	7:02
190S	52355		390W	53176		7:07
200S	52327		380W	53056		
210S	52348	6:30	370W	53017	#	
220S	52366		360W	52898	#	
230S	52424		350W	52649		7:13
240S	52508		340W	52250		7:17
250S	52545		330W	52261		
260S	52493	6:34	320W	52647		
270S	52450		310W	53058		
280S	52418		300W	53030		7:19
290S	52395					
300S	52370					
310S	52340	6:38				
320S	52308					
330S	52280					
340S	52263					
350S	52250					
360S	52232	6:42				
370S	52215					
380S	52204					
390S	52192					
400S	52171	6:46				

SECTION 19 PROSPECT GRID
June 24, 1985

120S		
300W	53192	7:21
310W	52845	
320W	52257	
330W	52195	
340W	52311	
350W	52419	7:25
360W	52508	7:27
370W	52572	
380W	52619	
390W	52754	
400W	52902	
410W	52868	7:33
420W	52572	
430W	52460	
440W	52407	
450W	52369	7:36
460W	52257	7:40
470W	52297	
480W	no reading-tree	
490W	52332	7:41

130S		
490W	52313	7:45
480W	52281	
470W	52272	
460W	no reading - tree	
450W	52374	7:49
440W	52481	7:53
430W	52540	
420W	52607	
410W	52823	
400W	52925	7:55
390W	52740	7:58
380W	52594	
370W	52567	
360W	52541	
350W	52483	8:00
340W	52321	8:03
330W	52261	
320W	52245	
310W	52646 #	
300W	52954	8:06

BS 52063 8:12
overcast, distant thunder

SECTION 17 - WEST MAGNETIC LINE
July 8, 1985

Base Station 51227 2:53
Sunny & clear

Line was run on or near contact between dike and sediments.
Station 0W is station 0N 750W of Section 17 east grid.

0W	51748	# 3:13		360W	52207		4:07
10W	52430	*		370W	52108		
20W	53373	*		380W	52074		
30W	51600	*		390W	52086		
40W	51432	#		400W	52163		4:11
50W	52500		3:21	410W	52269		4:14
60W	52762		3:23	420W	52358		
70W	52651			430W	52314		
80W	52643			440W	52457		
90W	52839	#		450W	52571		4:17
100W	52914		3:26	460W	52755	#	4:21
110W	54254	#		470W	52921		
120W	55210	*		480W	53138		
130W	55201			490W	53418		
140W	54980			500W	53613		4:26
150W	55113	# 3:33		510W	53613		4:28
160W	54982	# 3:38		520W	53344		
170W	55136	#		530W	53008		
180W	55416	#		540W	52830		
190W	55620	#		550W	52788		4:31
200W	55602	* 3:43		560W	52816		4:35
210W	54781	# 3:46		570W	52763		
220W	53455			580W	52726		
230W	52982			590W	52695		
240W	52723	#		600W	52630		4:38
250W	52550		3:50	610W	52489		4:41
260W	52435		3:52	620W	52430		
270W	52478			630W	52352		
280W	52635			640W	52277		
290W	52774	#		650W	52183		4:44
300W	52714		3:56	660W	52089		4:47
310W	52556	# 3:59		670W	52014		
320W	52732	#		680W	51953		
330W	52726			690W	51898		
340W	52572	#		700W	51877		4:50
350W	52364		4:03				

SECTION 17 - WEST MAGNETIC LINE
July 8, 1985

710W	51865		4:54
720W	51828		
730W	51779		
740W	51768		
750W	51793		4:57
760W	51834		
770W	51881		
780W	51939		
790W	52004		
800W	52072		5:04
810W	52159		
820W	52208		
830W	52212		
840W	52103		
850W	52420	#	5:10
860W	52957		
870W	53753	#	
880W	54808	*	
890W	55673	*	
900W	56402	#	5:17
910W	56886	#	
920W	57111	*	
930W	56954	*	
938W	57014	#	5:24

938W is station 100N
50E of Section 17-
west grid

B[illegible]	51222	5:46

SECTION 16 - EAST MAGNETIC LINE
July 9, 1985

Base Station 51214 9:56
Sunny & clear

Line was run on or near contact between dike and sedimants.
Station 0E is station 100S 200W of section 17 east grid.

0E	51651	10:12	360E	52810	11:02
10E	51616		370E	52727	
20E	51568		380E	52660	
30E	51573		390E	52710	
40E	51653		400E	52882	11:07
50E	51712	10:16	410E	53205	
60E	51760		420E	53520	
70E	51789		430E	53752	
80E	51817		440E	53871	
90E	51854		450E	54076	11:12
100E	51873	10:21	460E	54457	
110E	51902		470E	55073 #	
120E	51911		480E	55383 *	
130E	51918		490E	55493 *	
140E	51920		500E	54933 #	11:20
150E	51914	10:25	510E	54250 *	
160E	51900		520E	53510 #	
170E	51882		530E	52499 *	
180E	51853		540E	54726 *	
190E	51827		550E	56364 *	11:30
200E	51824	10:31	560E	56509 *	12:10
210E	51952		570E	55407 *	
220E	52252		580E	54050 *	
230E	52794		590E	52495 #	
240E	52789 #		600E	51446 *	12:17
250E	52149	10:38	610E	51431 *	
260E	52409 #		620E	51638 *	
270E	52993 #		630E	51275 *	
280E	53575 #		640E	52426 *	
290E	53865 #		650E	54591 *	12:29
300E	53392 #	10:48	660E	56993 *	
310E	52822 #		670E	56412 *	
320E	53232		680E	56245 *	
330E	53249		690E	54736 *	
340E	53109		700E	53281	12:37
350E	52869	10:57			

SECTION 16 - EAST MAGNETIC LINE
July 9, 1985

710E	53297	# 12:43		1060E	51916	1:51
720E	53223	#		1070E	51915	
730E	52675	#		1080E	51904	
740E	52115	#		1090E	51894	
750E	51851	12:49		1100E	51893	1:55
760E	51887			1110E	51901	
770E	51781			1120E	51905	
780E	51821			1130E	51908	
790E	51862			1140E	51909	
800E	51903	12:56		1150E	51919	2:01
				1160E	51931	
BS	51227	1:07		1170E	51932	
				1180E	51934	
810E	51829	1:19		1190E	51908	
820E	51926			1200E	51922	2:07
830E	51919			1210E	51935	
840E	51904			1220E	51963	
850E	51889	1:22		1230E	52033	
860E	51883			1240E	52103	
870E	51868			1250E	52225	2:11
880E	51855			1260E	52324	
890E	51851			1270E	52394	
900E	51855	1:27		1280E	52376	
910E	no reading			1290E	52296	
920E	51895			1300E	52307	2:16
930E	51947			1310E	52890	#
940E	52026			1320E	54228	#
950E	52070	1:33		1330E	55086	*
960E	52175			1340E	55171	*
970E	52434			1350E	54353	#
980E	52282			1360E	53876	#
990E	52145			1370E	53796	#
1000E	52099	1:42		1380E	53620	#
1010E	52041			1390E	52943	*
1020E	51986			1400E	52166	*
1030E	51952			1410E	51604	* 2:31
1040E	51928					
1050E	51916	1:49		BS	51227	2:46

SECTION 17 EAST GRID
December 16, 1983

Base Station 51364 9:07
profiles are from early reconnaissance survey. line located by pace and compass method.

	500W			600W	
260S	51957	10:33	130N	51655	
235S	51645	10:37	105N	51635	12:02
210S	51866		80N	51472	
185S	51914		55N	51225	
160S	51901		45N	51069	12:04
135S	51890		35N	50851	
110S	51930	10:43	25N	50567	
85S	52109	10:44	15N	50520	
75S	52233	10:46	5N	51514 *	12:08
65S	52331		0N	51962 *	12:10
55S	52358	10:48	5S	53126 *	12:39
50S	52446	10:55	10S	54584 *	
45S	52673	10:57	15S	51498 *	
40S	53231		20S	50642 *	
35S	53969 *	10:59	25S	54273 *	12:52
30S	54484 *	11:01	30S	53308 *	
25S	53228 *	11:04	35S	53404 *	1:04
20S	53132 *	11:07	40S	52786	
15S	52680 *	11:11	45S	52386	1:07
10S	51739 *	11:15	50S	52160	1:10
0N	50925	11:17	55S	52053	
15N	51032	11:20	60S	51933	1:12
25N	51186		70S	51776	
35N	51327	11:23	80S	51779	
45N	51420		95S	51752	
55N	51527	11:24	120S	51841	1:17
65N	51623				
90N	51709	11:25	line bears S8°W		
115N	51696	11:27			

line bears S1°W

SECTION 17 EAST GRID
December 16, 1983

715W

160S	51925		1:38
135S	52139		1:39
125S	52296		1:55
120S	52378		
115S	52528		1:57
110S	52697		
105S	53069		
100S	53527		
95S	54297	*	2:00
90S	54070	*	
85S	54297	*	
80S	53862	*	2:07
75S	53481	*	
70S	no reading		
65S	52430		
60S	51771		2:15
50S	50961		
40S	50610		
30S	51180		2:18
25S	53303	*	
20S	53935	*	
15S	53246	*	2:26
10S	52853	*	
5S	52070		
0N	51521		2:30
5N	51127		
10N	50906		
15N	50793		2:33
20N	50788		
25N	50807		
30N	50890		2:37
35N	50996		
40N	51093		
50N	51219		
60N	51307		2:41
70N	51400		
80N	51498		2:44
90N	51589		
115N	51600		

line bears S8 W

BS	51353	5:25

SECTION 17 EAST GRID
January 12, 1984

Base Station 51352 9:57

	200W			250W	
0N	51716	10:44	0N	51656	11:32
10N	51782		10N	51718	
20N	51822		20N	51770	
30N	51829		30N	51804	
40N	51838		40N	51815	
50N	51834		50N	51817	
60N	51821	10:52	60N	51812	11:37
70N	51825		70N	51822	
80N	51785		80N	51808	
90N	51791		90N	51808	
100N	51846		100N	51795	
10S	51644	11:01	10S	51613	11:49
20S	51603		20S	51602	
30S	51567		30S	51607	
40S	51597		40S	51595	
50S	51562		50S	51609	
60S	51320	11:08	60S	51778	
70S	50711 *		70S	51388	
80S	50481 *		80S	52128 *	
90S	51525		85S	53551 *	
100S	51790		90S	53546 *	12:07
110S	51961		95S	52919	
120S	51992		100S	52557	
130S	51922		110S	52370	
140S	51925		120S	52269	
150S	51899		130S	52129	
			140S	52021	
			150S	51974	

SECTION 17 EAST GRID
January 12, 1984

	300W		
0N	51604		
10N	5.636		12:34
20N	51675		
30N	51710		
40N	5.751		
50N	51783		
60N	51785		12:40
70N	51780		
80N	51787		
90N	5.776		
100N	51757		
10S	5.560		12:56
20S	51505		
30S	5.419		
40S	5.285		
50S	5.170		
60S	50053	*	1:02
70S	50064	*	
80S	5.543		
90S	52031		
100S	5211.8		
110S	52095		
120S	52028		
130S	51979		
140S	5.946		
150S	51936		1:13

	350W		
0N	5139.		2:23
10N	51462		
20N	5.514		
30N	5.588		
40N	51640		
50N	5.701		
10S	51251		2:37
20S	51133		
30S	51177		
40S	52211		
45S	52454		
50S	52223		
60S	51753		
70S	51670		
80S	51843		
90S	51961		
100S	5.912		

	400W		
0N	5.166		2:59
10N	51276		
20N	5.38.		
30N	51422		
40N	5.505		
50N	51589		
10S	51161		3:16
20S	5.919	*	
25S	52151	*	
30S	53478	*	
35S	50711	*	
40S	54457	*	
45S	53997	*	
50S	53774		
55S	53190		
60S	52729		
70S	52153		
80S	52111		
90S	52042		
100S	52001		3:40

	450W		
0N	50836		3:48
10N	51004		
20N	5.155		
30N	51292		
40N	51418		
50N	5.482		
10S	50795		3:59
20S	51500		
30S	52871	*	
35S	53901	*	
40S	53852	*	
45S	53935	*	
50S	53018		
55S	52276		4:12
60S	52119		
70S	52070		
80S	52088		
90S	52029		
100S	5199.		

SECTION 17 EAST GRID
January 12,1984

	550W	
50N	51292	
40N	51171	4:32
30N	51067	
20N	50988	
10N	50938	
0N	51141	
10S	51934	4:42
20S	52613	
30S	52095	
40S	51859	
50S	52000	
60S	52087	
70S	51996	
80S	51922	
90S	51908	
100S	51902	4:52
BS	51358	5:22

SECTION 17 EAST GRID
January 13,1984

Base Station 51361 9:14

650W			750W		
0N	49793	* 9:47	0N	51616	10:42
10N	49322		10N	50568	
20N	49888		20N	50488	
30N	50386		30N	50658	
40N	50750		40N	50877	
50N	51027		50N	51061	
			60N	51191	
10S	51603	* 10:08	70N	51270	
15S	52767	*			
20S	53835	*	5S	51807	*
25S	53874	*	10S	53672	*
30S	52966	*	15S	52176	*
35S	52351	*	20S	52214	* 11:02
40S	52126	*	25S	50759	*
45S	52061		30S	50512	
50S	52141		35S	50365	
55S	52388		40S	50685	
60S	52604		50S	51887	
65S	52836	10:27	55S	52387	
70S	53116		60S	52827	
75S	53239		65S	53134	*
80S	53060		70S	53433	*
85S	52710		75S	53623	*
90S	52537		80S	53726	
95S	52225		85S	53407	
100S	52088		90S	53072	
			95S	52766	
			100S	52563	
			BS	51335	12:02

SECTION 17 EAST GRID
February 10, 1984

Base Station 51298 11:02
Sunny and clear, 50's

100S

750W	52948		11:45
745W	53396	*	
740W	53729	#	
735W	53921	*	
730W	54387	*	
725W	54233	*	
720W	53506	*	
715W	53868	*	
710W	53785	*	
705W	53750	*	
700W	53578	*	12:00
690W	53456	*	1:29
680W	53400		
670W	53007		
660W	52513		
650W	52151		

90S

650W	52663	#	
660W	53536	*	
670W	54950	*	
680W	55021	*	
690W	55370	*	
700W	55216	#	
710W	54941	*	
720W	55373	*	
730W	54471	*	
740W	53950	#	
750W	53195		
760W	52803		1:58
770W	52411		
780W	52185		

80S

780W	52242		
770W	52565		
760W	53026		
750W	53833	#	
740W	54939	*	2:47
730W	54741	*	
720W	55194	*	
710W	55169	*	
700W	53335	*	
690W	53400	*	
680W	53829	*	
670W	54245	*	
660W	54376	*	
650W	53337	*	
640W	52081		

70S

650W	53130	#	
660W	53989	*	
670W	53332	*	
680W	52844	*	
690W	52726	*	
700W	52724	*	
710W	53734	*	
720W	54869	*	
730W	54358	*	
740W	54590	*	
750W	54181		
760W	53228		
770W	52714		
780W	52261		3:33

60S

780W	52154		
770W	52450		
760W	52850		
750W	52976	#	
740W	52639	#	
730W	52089	#	
720W	51823		
710W	51815		
700W	51964		3:46

SECTION 17 EAST GRID
February 10, 1984

5S

550W	51417 #	
560W	51506	
570W	51610	4:14
580W	52148 #	
590W	53233 *	
600W	53593 *	

OBLIQUE LINE D

610W	52527 *	
620W	50860 *	
630W	51755 #	
640W	51341 #	
650W	50806 *	
660W	51912 *	
670W	54643 *	
680W	53842 *	
690W	54806 *	
700W	53722 *	
710W	53531 *	
720W	54152 *	
730W	53449 *	
740W	53611	
750W	52586 *	

Oblique line D runs from 5S 600W to 10S 750W.

10S

550W	51925	5:09
560W	52204	
570W	52342	
580W	53672 #	
590W	54382 *	
600W	55136 *	5:20

OBLIQUE LINE A

610W	55005 *	
620W	50247 *	
630W	51540 *	
640W	53000 *	
650W	54020 *	
660W	50456 *	5:30
670W	50088 *	
680W	50139 *	
690W	50143 *	
700W	55132 *	
710W	53735 *	
720W	52102 *	
730W	52015 *	
740W	51121 *	
750W	50723 *	5:53

Oblique line A runs from 10S 600W to 26S. 610W to 650W not included on plate 2A.

BS 51315 6:15

SECTION 17 EAST GRID
February 11, 1984

Base Station 10:05 51301
clear & sunny; 40's

20S

550W	52538	10:42
560W	52569	
570W	52796	
580W	53663 *	
590W	54960 *	10:50

20S(good bearing)

650W	54841 *	11:54
640W	52969 #	
630W	51977 *	
620W	55306 *	
610W	55900 *	

OBLIQUE LINE B

600W	56270 *	
610W	56170 *	
620W	54702 *	
630W	52298 *	
640W	52021	
650W	52560 *	
660W	54542 *	11:08
670W	54644 *	
680W	54943 *	
690W	53337 *	
700W	52630	

Oblique line B runs from 20S 600W to 50S 700W.

OBLIQUE LINE C

650W	53360 *	12:22
640W	52775 #	
630W	51823 *	
620W	50326 *	
610W	53318 *	
600W	55088 *	
590W	55892 *	
580W	53644 *	
570W	52785	
560W	52497	
550W	52522	12:33

Oblique line C runs from 15S 650W to 18S 550W.

30S

550W	52059	11:34
560W	51985	
570W	52020	
580W	52529	
590W	53780 #	
600W	54657	
610W	53649 *	
620W	53359 *	
630W	52406 #	
640W	51805	11:48
650W	52351 #	

15S

550W	52261	2:10
540W	52675	
530W	53944 #	
520W	53901	
510W	53288 *	
500W	52510 *	
490W	52231 *	
480W	52024 *	
470W	51756 #	
460W	51472	
450W	51041	2:25

SECTION 17 EAST GRID
February 11, 1984

20S

540W	52927		2:30
530W	54308		
520W	55360	*	
510W	55035	*	
500W	54599	#	
490W	54198	*	
480W	53420	*	
470W	52587	*	
460W	52137	*	
450W	51656	#	2:45

30S

540W	52540		2:50
530W	53843	#	
520W	54436	#	
510W	54857	*	
500W	54909	#	
490W	55345	#	
480W	54738	*	
470W	54773	*	
460W	54817		
450W	54001	*	
440W	53687	#	
430W	51803	*	
420W	51534	*	
410W	53056	*	
400W	54130	*	
390W	53179	*	
380W	51675	#	
370W	51297		3:20

40S

500W	53022		3:30
490W	53267	#	
480W	53492	#	
470W	53812		
460W	54134	#	
450W	54375	*	
440W	54685	*	
430W	54463		
420W	54583	*	
410W	55081	*	
400W	55413	*	
(50873 @ 35S 400W)			
390W	54656	*	
380W	52517		
370W	51857	#	3:48

50S

500W	52343		
490W	52544		3:59
480W	52685		
470W	52785		
460W	52849		
450W	52764	*	
440W	52445	*	
430W	53248	#	
420W	53654	*	
410W	54305	#	
400W	no reading		
390W	53175	*	
380W	52309	#	
370W	51866		4:12

SECTION 17 EAST GRID
February 11, 1984

80S			100S		
300W	51633	5:37	300W	52072	5:29
290W	53414 *		290W	52246	
280W	53716 *		280W	52351	
270W	53412		270W	52325	
260W	54259 *		260W	52438	
250W	53053 *		250W	52579	
240W	54376 *		240W	52703	
230W	55639 *		230W	53003	
220W	55340 *		220W	52791	
210W	52834 *		210W	52129	
200W	50471		200W	51748	5:39
90S			BS	51298	6:16
200W	51549	5:12			
210W	52610				
220W	53671 *				
230W	53706 *				
240W	53462 *				
250W	53232				
260W	53043 #				
270W	52618				
280W	52665				
290W	52466				
300W	52023	5:22			

SECTION 17 WEST GRID
February 12, 1984

Base Station 51310 8:23
clear & sunny, 40's

	50E			50W	
0N	52163	12:02	0N	52078	1:16
10N	52226		10N	52133	
20N	52298		20N	52197	
30N	52411		30N	52274	
40N	52572		40N	52362	
50N	52802		50N	52495	
60N	53145		60N	52746	
70N	53701		70N	53110	
80N	54537		80N	53726	
90N	55878		90N	54573	
100N	57096		100N	55312	
110N	56372 *	12:25	110N	55705	
120N	55477 #		120N	55687	
130N	52822		130N	55096	
140N	51537		140N	53935	
150N	51031		150N	52658	1:33

	0E	
0N	52113	12:44
10N	52173	
20N	52224	
30N	52283	
40N	52385	
50N	52545	
60N	52876	
70N	53460	
80N	54483	
90N	55989	
100N	57463	
110N	56510 #	
120N	55322	
130N	53107 #	
140N	51697	
150N	51019	

SECTION 17 WEST GRID
February 12, 1984

	90N		
0E	56057	*	
10E	56155	*	
20E	55978	#	
30E	55693	*	
40E	55714	*	
50E	56126		1:44
	100N		
50E	57133		
40E	56868	#	
30E	56799		
20E	57113	*	
10E	57346	*	
0E	57511	#	
10W	56996	#	
20W	56615		
30W	56342		
40W	55736		
50W	55268		2:08

	110N		
50W	55781		
40W	55607		
30W	55817		
20W	56247		
10W	56746		
0E	56858	*	
10E	57322	*	
20E	56965		
30E	56514		
40E	57036	*	
50E	56771	*	2:30
	120N		
0E	55617	#	
10W	55071	#	
20W	54882		
30W	55085		
40W	55260		
50W	55679		2:40

BS 51311 3:08

WEST END - LONG TRANSVERSE LINE

Measurements taken on this profile have been corrected for drift as determined by base station readings. The scatter effect is determined differently on this profile than on the axial line and other magnetic work in this thesis:

* = greater than 5γ range(9 readings)
\# = " " 3 " (5 ")

April 23, 1985

BS	51281	12:19
sunny & clear, 50's		
BS	51277	1:41
BS	51288	3:09
BS	51295	4:47
BS	51293	6:31
sunny & clear		

April 24, 1985

BS	51304		6:33
clear & sunny			
BS	51290		8:47
Ø	51494	*	9:02
10S	51568		
20S	51539		
30S	51539		9:06
40S	51614		
50S	51612		
60S	51608		9:09
70S	51567		
80S	51557		
90S	51583		9:14
100S	51661		
110S	51724		9:17
120S	51700		
130S	51671		
140S	51662		9:23
150S	51644		
160S	51625		9:26
170S	51613		
180S	51607		
190S	51593		
200S	51577		9:30
210S	51572		9:40
220S	51586		9:41
230S	51573		
240S	51576		
250S	51598		
260S	51606	#	9:46
270S	51611	#	
280S	51612	#	
290S	51624		
300S	51631		9:49
BS	51627		10:02
300S	51627		10:12
320S	61620		10:13
340S	51625		
360S	51628		

WEST END - LONG TRANSVERSE LINE
April 24, 1985

380S	51628		10:17	60N	51376		3:07
400S	51598			70N	51377		
420S	51590			80N	51404		3:09
440S	51597		10:21	90N	51435		3:10
460S	51591		10:23	100N	51465		3:12
480S	51578			110N	51306		
500S	51562		10:25	120N	51116		3:13
550S	51562		10:30	130N	51044		
600S	51557		10:31	140N	51087		3:14
650S	51541		10:33	150N	51134		
700S	51521		10:34	160N	51154		3:17
750S	51507		10:35	170N	51161		
800S	51471		10:36	180N	51167		3:18
850S	51454		10:37	190N	51170		
900S	51441		10:39	200N	51181		
950S	51431		10:40	210N	51180		3:21
1000S	51418		10:41	220N	51184		
1250S	51394		10:55	230N	51187		
1500S	51374		11:12	240N	51184		3:23
1750S	51364		11:14	250N	51186		
2000S	51361		11:16	260N	51185		3:26
2250S	51362		11:22	270N	51185		
				280N	51184		3:27
BS	51285		11:49	290N	51185		
				300N	5117		3:28
2250S	51360		12:25	320N	51171	#	3:34
2500S	51353		12:29	340N	51170	*	
2750S	no reading; wire fence			360N	51167		3:38
				380N	51168		3:39
2850S	51352	#	12:36	400N	51173		3:41
3000S	51349		12:40	420N	51184		
3250S	51350	#	12:48	440N	51186		3:43
3500S	51328		12:54	460N	51189		3:44
3750S	51353	#	1:01	480N	51187		
4000S	51351		1:06	500N	51191		3:46
4250S	51352		1:13	550N	51200	#	3:51
4500S	51348		1:20	600N	51208		3:53
4750S	51344		1:25	650N	51221		3:54
5000S	51345	#	1:28	700N	51238		3:56
5250S	51349	#	1:35	750N	51245		3:58
				800N	51258	#	3:59
BS	51289		2:31	850N	51262		4:01
				900N	51271		4:02
Ø	51547	*	2:59	950N	51276		4:03
10N	51500	*	3:01	1000N	51285		4:05
20N	51426		3:03				
30N	51348			BS	51292		4:08
40N	51365	#	3:04				
50N	51391			1250N	51308	#	4:21

WEST END - LONG TRANSVERSE AND AXIAL LINES
April 24, 1985 January 14, 1986

LONG TRANSVERSE LINE

1500N	51341		4:17
1750N	51343	#	4:21
2000N	51355	#	4:23
2250N	51348		4:29
2500N	51355		4:31
2750N	51355		4:34
3000N	51357	#	4:36
3250N	51365		4:51
3500N	51361		4:54
3750N	51359	#	4:56
4000N	51365		5:01
4250N	51365	#	5:07
4500N	51364		5:10
4750N	51363		5:16
5000N	51364		5:19
5250N	51366	#	5:24
BS	51294		5:55

clear, sunny, warm and very windy all day.

AXIAL LINE

* = >100% (9 readings)
\# = 10-100% (5 readings)
scatter ranges

BS	51245		12:40
Ø	51427	#	12:48
100W	51395		12:51
200W	51411		
300W	51295		
400W	51301		
462W	road		
500W	51368		12:56
600W	51299		
700W	51343		
800W	51396		
900W	51234		1:02
1000W	50943		
1100W	51192		
1200W	51157		
1300W	51189		
1400W	51224		1:08
1500W	51179		
1600W	50964		
1700W	50947		
1800W	50946		
1900W	50954		1:15
2000W	50961		
2100W	50963		
2200W	50924		
2300W	50852		
2400W	50557	#	1:22
2500W	51248	#	
2600W	52718	*	
2700W	51267		
2800W	51256		1:32
2900W	51571		1:33
3000W	51731		1:42
3100W	51226		1:49
3200W	51352		1:50
3300W	51413		
3400W	51347		
3500W	51436		2:00
3600W	51418		2:03
3700W	51240		
3800W	51189		
3900W	51146		
4000W	51296		2:09
4100W	51413		

WEST END - AXIAL LINE
January 14, 1986

4200W	51285	
4300W	51236	
4400W	51207	
4500W	51242	
4600W	51249	2:17
4700W	51188	
4800W	51085	
4900W	51047	
5000W	51016	2:22
5100W	51023	
5200W	50968	
5300W	50996	
5400W	50841	
5500W	50841	2:32

5490W TRANSVERSE LINE

10S	51379	2:37
20S	53031 #	
30S	53863 #	
40S	53219	
50S	54067 *	
60S	53107 #	
70S	53008	
80S	53474 #	
90S	52964	
100S	52431	
110S	53064	
120S	54035	
130S	52176 *	
140S	51696 #	
150S	52084	
160S	52426	
170S	52518	
180S	52501	
190S	52440	
200S	52384	2:54

5600W	50777	3:19
5700W	50590	
5800W	50640	
5900W	50787	
6000W	50788	
6100W	50658	3:25
6200W	50841	
6300W	50843	
6400W	50885	3:30
6500W	50455	
6600W	50770	
6700W	50599	
6800W	50756	
6900W	50632 #	
7000W	50527	3:38
7100W	50921	
7200W	50996	
7300W	51026	
7400W	51027	3:46
7500W	51029	
7600W	50906	
7700W	50897	
7800W	50888	3:58
7900W	51032	
8000W	51100	
8100W	51104	
8200W	51112	3:57
8300W	51155	
8400W	51194	
8500W	51230	
8600W	no reading 10 ft from 10/11 section line fence	
8700W	51254	4:00
8800W	51258	4:10

OFFSET TREND

Ø on 10/11 section line

50W	51917	4:23
150W	52810	
250W	51529	
250W	52008	
	2nd 250W station is 40 ft NNW of first.	
350W	51512	4:28
50E	51913	4:33
150E	52810	
250E	51799	
350E	51790	
450E	51090 #	
550E	51596	
650E	51811	
750E	51288	4:46
BS	51261	5:22

WEST END - AXIAL LINE
January 15, 1986

Base Station 51264 8:25

Ø	51352	8:30
100E	51420	
200E	51604	
300E	51457	
400E	51566	8:46
500E	51389	8:54
600E	51461	
700E	51363	
800E	51569	8:58
900E	51471	
1000E	51431	
1100E	51378	
1200E	51601	9:04
1300E	51559	
1400E	51792	
1500E	51774	
1600E	51912	9:11
1700E	51498	
1800E	51701	
1900E	51362	
2000E	51341	9:17
BS	51251	9:39
BS	51252	12:30

2400W TRANSVERSE LINE

2400W	50559	2:14
10S	50708	
20S	50877	
30S	51057	
40S	51260	
50S	51563	
60S	51940	2:20
70S	52215	
80S	52209	
90S	51931	
100S	51692	
110S	51564	2:23
120S	51527	
130S	51526	
140S	51538	
150S	51550	
160S	51570	2:27
170S	51584	
180S	51613	
190S	51652	
200S	51684	
210S	51733	2:31
220S	51782	
230S	51834	
240S	51878	
250S	51919	
260S	51949	2:35
270S	51980	
280S	52003	
290S	52024	
300S	52034	2:37
10N	50517	2:44
20N	50553	
30N	50621	
40N	50681	
50N	50721	
60N	50759	2:47
70N	50791	
80N	50822	
90N	50847	
100N	50870	2:51

2600W TRANSVERSE LINE

2600W	53227 *	2:57
10N	53607 *	
20N	52284 *	
30N	51081 #	
40N	51391	
50N	51484	
60N	51061 #	3:06
70N	50640	
80N	50423	
90N	50425	
100N	50518	
110N	50604	3:11
120N	50680	
130N	50738	
140N	50778	
150N	50813	3:14
10S	52178 *	3:21
20S	50761 #	
30S	51196	
40S	51429	
50S	51413	
60S	51435	3:27
70S	51453	
80S	51464	

WEST END - AXIAL LINE
January 15, 1986

2600W TRANSVERSE LINE

90S	51480		
100S	51497		
110S	51533		3:31
120S	51575		
130S	51629		
140S	51693		
150S	51768		
160S	51847		3:34
170S	51929		
180S	52009		
190S	52072		
200S	52123		
210S	52156		3:39
220S	52181		
230S	52198		
240S	52201		
250S	52189		3:41

6000W TRANSVERSE LINE

6000W	50815		4:33
10N	50932		
20N	51182		
30N	51798		
40N	53322	#	
50N	55818	*	
60N	56080	*	4:33
70N	52568	*	
80N	51657	*	
90N	51049	*	
100N	50531		
110N	50668		4:53
120N	50755		
130N	50818		
140N	50853		
150N	50893		
160N	50920		4:58
170N	50938		
180N	50961		
190N	50978		
200N	50998		5:01
10S	50755		5:03
20S	50740		
30S	51010		
40S	51548		
50S	52155	#	

6000W TRANSVERSE LINE

60S	53032	#	5:08
70S	54056	#	
80S	52055	*	
90S	53807	*	
100S	54721	*	
110S	55963	*	5:15
120S	55799	*	
130S	55218	*	
140S	55192	#	
150S	54933	#	
160S	53737		5:22
170S	53351		
180S	52733		
190S	52233		
200S	52004		
210S	51842		5:27
220S	51657		
230S	51591		
240S	51552		
250S	51538		
260S	51568		5:30
270S	51649		
280S	51648		
290S	51609		
300S	51637		
BS	51259		5:54

IRON HORSE DEPOSIT
July 7, 1985

Base Station 51327 3:00
sunny, 80's, distant
thunder. set on 53

0+19E

BL	58691	*	3:15
10N	57006	*	
20N	56527	*	
30N	52923	*	3:22
40N	52411	*	
50N	52461	*	3:25
10S	55754	*	3:30
20S	54550	#	
30S	52907		
distant thunder			
40S	52341	#	
50S	52313		3:35

1+40E

BL	57590	*	3:39
distant thunder			
10N	55120	*	
20N	57454	*	
30N	55263	#	
40N	53622	#	
50N	52125	#	3:47
60N	51850	#	3:50
70N	50867	*	
80N	51347	*	
90N	51151	*	
100N	51018	*	3:56
10S	57036	*	4:02
20S	54597	#	
30S	52010	#	
40S	51285	*	
50S	51281		4:06
60S	51094	#	4:09
70S	51259		
80S	51326		
90S	51502		
100S	51498		4:14
fence 50' south			
of station			

5+72E

BL	51257	*	4:35
10N	52042	*	
20N	51857	*	
30N	51562	*	
40N	50362		
50N	50545		4:43
60N	50716		
70N	50844		
80N	50938		
90N	51005		
distant thunder			
100N	51059		4:51
distant thunder			
10S	52155	#	4:59
sprinkling			
20S	52978	#	
thunder			
30S	54162	#	
40S	55520	*	
50S	55519	*	4:59
stone cairn @ station			
60S	53215	*	5:02
70S	52235		
80S	52211		
90S	51819		
100S	51629		5:05
BS	51325		5:10

APPENDIX III

PALEOMAGNETIC DATA

This appendix lists locations of paleomagnetic sites, directions and intensities of remanent magnetization and statistical estimates. Data are shown for each demagnetzation level. data are for average remanent field of all cores measured for that site.

mT - milliTesla

incl - Inclination of average field direction in degrees. Negative(-) inclinations point above horizontal, positive( ) inclinations point below level.

decl - Declination of average field direction in degrees. 0 = north.

int - remanent field intensity in Oersteds.

k - precision estimate. k > 10 indicates close approximation. Not to be confused with susceptibility, which is also designated k.

a95 - alpha-95 confidence estimate. a95 < 10 indicates good confidence.

PM-1

PM-1 is located at 60S 440W section 19 prospect grid. Magnetite ore is sampled. Six cores measured.

	incl	decl	int	k	a95
0mT	3.9	313.2	978.0	1.6	83.38
5mT	6.7	283.8	1090.0	9.1	84.02
10mT	3.1	315.6	664.0	1.6	82.66
20mT	-1.5	321.6	523.0	2.2	60.06
30mT	-4.2	320.5	410.0	3.0	47.35
42mT	-5.6	319.2	203.0	3.4	43.18

PM-2

PM-2 is located on walls of a prospect pit in actinolized Pyts. Pit is at 130N 410W of section 19 prospect grid. Seven cores measured.

	incl	decl	int	k	a95
0mT	50.8	114.3	47.4	3.9	35.06
5mT	35.3	155.3	0.0896	14.7	70.80
10mT	52.6	157.1	4.94	3.1	41.64
20mT	25.0	195.2	1.46	2.3	52.32
30mT	29.9	211.4	0.716	1.7	69.46
42mT	26.1	239.5	0.452	1.6	76.38

PM-3

PM-3 is located at 200N 350W on the section 19 prospect grid. It samples Tjc. Eight cores measured.

	incl	decl	int	k	a95
0mT	-39.6	158.8	17.6	1.5	77.38
5mT	-22.5	174.4	15.7	1.2	53.51
10mT	-13.6	194.0	7.82	1.2	69.21
20mT	-10.7	198.6	2.39	1.4	80.24
30mT	-9.9	197.3	1.25	1.7	66.07
40mT	-6.1	186.9	0.68	1.9	70.43
42mT	-29.5	196.1	0.305	1.6	70.85

PM-4

PM-4 is located 460 feet ESE of shaft on section 19 prospect grid. It samples intensely altered Tjb. Ten cores measured.

	incl	decl	int	k	a95
0mT	-61.4	173.9	0.353	5.7	22.07
5mT	-60.1	184.8	0.373	13.5	14.53
10mT	-63.0	194.2	0.354	42.3	7.51
20mT	-62.5	199.8	0.355	96.2	4.95
30mT	-62.6	201.1	0.36	123.4	4.37
40mT	-62.7	201.3	0.376	159.6	5.32
42mT	-63.0	201.8	0.357	151.4	3.94

PM-5

PM-5 and PM-6 were collected from the north face of a hill 600 feet ESE of the west pit in Jones Camp district. The hillside has been excavated. PM-5 is from stringers of Tjp which intruded Tjb(PM-6). Six cores were measured

	incl	decl	int	k	a95
0mT	3.8	303.4	2.39	3.1	46.18
5mT	-8.8	298.5	1.87	3.5	48.35
10mT	-19.0	307.9	1.31	4.8	39.23
20mT	-27.7	319.5	1.04	7.9	29.05
30mT	-24.9	323.3	0.804	11.5	23.55
40mT	-12.3	331.2	0.587	10.5	21.65
42mT	-20.2	328.6	0.351	3.1	45.41

PM-6

PM-6 was collected at the same site as PM-5. PM-6 is altered Tjb. Location of site is NE4 NE4 NE4 section 23 T5S R7E. Eight cores measured.

	incl	decl	int	k	a95
0mT	27.1	266.0	2.57	1.7	63.95
5mT	6.9	297.0	1.24	1.7	66.37
10mT	-10.0	311.2	0.497	2.0	55.24
20mT	-23.6	330.7	0.228	2.6	43.85
30mT	-27.6	342.2	0.133	3.6	33.86
40mT	-26.0	350.3	0.112	5.5	25.90
42mT	-31.4	1.7	0.0966	11.0	17.44

PM-7

PM-7 is located at 100S 700W on the southwest corner of section 17 east grid. Magnetite ore was sampled. Ten cores were measured.

	incl	decl	int	k	a95
0mT	-17.7	8.8	81.4	1.4	69.99
5mT	-17.9	350.2	48.5	1.6	60.99
10mT	-2.3	348.1	35.3	1.6	64.97
20mT	1.5	354.9	21.5	1.6	64.67
30mT	-7.2	358.1	13.2	1.7	57.15
40mT	-5.7	355.5	8.51	1.6	58.58
42mT	-4.5	17.7	5.74	1.5	89.07

PM-9

PM-9 is located at 0N 200W at the eastern edge of section 17 east grid. Intensely altered Tjb was sampled. Eight cores were measured.

	incl	decl	int	k	a95
0mT	-46.8	210.0	0.314	27.6	10.73
5mT	-40.0	195.4	0.265	9.2	19.28
10mT	-48.7	206.6	0.226	11.1	17.36
20mT	-53.9	206.4	0.218	37.7	9.14
30mT	-55.4	202.8	0.216	82.9	6.12
40mT	-55.4	199.6	0.206	80.9	7.49
42mT	-55.3	201.6	0.217	127.1	4.93

PM-10

PM-10 is located 200 feet NW of PM-9. It samples Tja. Eight cores measured

	incl	decl	int	k	a95
0mT	23.5	325.3	0.00492	2.0	51.24
5mT	16.2	311.9	0.00440	1.9	58.43
10mT	-13.2	307.6	0.00414	1.7	63.40
20mT	-11.1	304.6	0.00419	1.8	59.63
30mT	-24.8	317.0	0.00415	2.6	42.65
40mT	-20.7	305.1	0.00484	2.7	50.26
42mT	-19.1	317.2	0.00383	2.0	59.11

PM-11

PM-11 is located on an arroyo bank in NW4 NE4 SW4 section 15 T5S R7E. It samples Stringers of Tjp. Six cores measured.

	incl	decl	int	k	a95
0mT	30.1	9.8	2.95	2.8	49.65
5mT	19.5	12.5	1.94	1.9	80.57
10mT	3.2	12.6	0.627	3.5	41.91
20mT	-6.3	9.0	0.277	4.7	34.38
30mT	-3.8	5.7	0.176	6.5	28.53
40mT	16.0	359.7	0.102	53.1	34.97
42mT	4.2	359.2	0.129	8.6	24.25

PM-12

PM-12 is located on top of a hill of Tjp 1200 feet SE of the shaft on section 19prospect grid. Only two unoriented cores collected. Susceptibility only.

PM-13

PM-13 is located the crest of the dike 2000 feet west of the 6E/7E range line. It is the zero point for the transverse and axial lines at the west end. Moderately altered Tjb was sampled. Seven cores measured

	incl	decl	int	k	a95
0mT	-5.9	89.6	71.7	1.6	74.97
5mT	-6.6	83.2	57.8	1.6	180.00
10mT	-7.4	86.5	33.9	1.6	76.78
20mT	-3.3	84.2	10.1	1.5	79.89
30mT	-1.1	84.1	3.59	1.5	82.04
42mT	-0.9	85.1	1.57	1.5	82.00

APPENDIX IV
SUSCEPTIBILITIES

Paleomagnetic cores were measured for susceptibility using a susceptibility meter. Values for each core are given in cgs units(dimensionless).

PM-1-1-01	0.0963	PM-2-1-01	0.000114
PM1-2-01	0.156	PM-2-2-01	0.000102
PM-1-3-01	0.131	PM-2-3-01	0.0829
PM-1-4-01	0.110	PM-2-4-01	0.000123
PM-1-5-01	0.127	PM-2-5-01	0.0000557
PM-1-6-02	0.105	PM-2-6-01	0.0000437
PM-1-7-01	0.114		
PM-1-8-01	0.118		
PM-1-9-01	0.0993		
PM-1-10-01	0.148		
PM-3-1-01	0.00277	PM-4-1-01	0.000191
PM-3-2-01	0.00281	PM-4-2-01	0.0000968
PM-3-3-01	0.00284	PM-4-3-01	0.0000534
PM-3-4-01	0.00283	PM-4-4-01	0.000119
PM-3-5-01	0.00296	PM-4-5-01	0.000131
PM-3-6-01	0.00301	PM-4-6-01	0.0000539
PM-5-1-01	0.00128	PM-6-1-01	0.00404
PM-5-2-01	0.00125	PM-6-2-01	0.00411
PM-5-3-01	0.00144	PM-6-3-01	0.00390
PM 5-4-01	0.00244	PM-6-4-01	0.00352
PM-5-5-01	0.00204	PM-6-5-01	0.00379
PM-5-6-01	0.00317	PM-6-6-01	0.00457
PM-7-1-01	0.129	PM-9-1-01	0.000892
PM-7-2-01	0.122	PM-9-2-01	0.00432
PM-7-3-01	0.114	PM9-3-01	0.0012
PM-7-4-01	0.15	PM-9-4-01	0.00015
PM-7-5-01	0.139	PM-9-5-01	0.0000409
PM-7-6-01	0.142	PM-9-6-01	0.0000689
PM-10-1-01	0.0000173	PM-11-1-01	0.00345
PM-10-2-01	0.0000159	PM-11-2-01	0.00319
PM-10-3-01	0.0000168	PM-11-3-01	0.00436
PM-10-4-01	0.0000160	PM-11-4-01	0.00249
PM-10-5-01	0.0000116	PM-11-5-01	0.00345
PM-10-6-01	0.0000154	PM-11-6-01	0.00329
PM-12-1-02	0.00399	PM-13-1-01	0.0027
PM-12-1-03	0.00377	PM-13-2-01	0.00259
PM-12-2-01	0.00176	PM-13-3-01	0.00197
PM-12-1-01	0.00305	PM-13-4-01	0.00253
		PM-13-5-01	0.00292
		PM-13-6-01	0.00309
		PM-13-7-01	0.00298

TERM(SYMBOL)	SI	CGS(MKSA)	CONVERSION FACTOR
Magnetic field strength(H)	A/m	Oersted(Oe)	1 A/m = 4π X 10^{-3}
Magnetic induction(B)	Tesla(T) = KgA/s	Gauss(G)	1 T = 10^{4}G
Magnetization(M)	A/m	emu/cm^{3}(=Gauss)	1 A/m = 10^{-3} emu/cm^{3}
Susceptibility(X or k)	4 (dimensionless)	Gauss/Oersted	

Volume magnetic susceptibility is dimensionless.

Susceptibility in SI units is 4π greater than in CGS units.

1 milliTesla(mT) = 10 Gauss $\cong$ 10 Oersteds

1 gamma(γ) = 10^{-5} Oersted

The earth's field in New Mexico ranges between 51000γ and 52000γ.

APPENDIX V - COMMON MAGNETIC TERMS

APPENDIX VI

Petrographic description of selected paleomagnetic cores. Point counts were conducted on polished sections. 100 to 200 points per section were counted.

PM-1-8-01 Section 19 prospect grid; magnetite ore
84% magnetite and maghemite
8% goethite
<1% gangue
7% porosity
Predominant magnetite with interstitial maghemite. Late magnetite, maghemite and goethite line vugs.

PM-1-3-01
53% magnetite
29% maghemite
1% hematite
13% goethite
4% porosity
Magnetite occurs as subhedral grains; maghemite as interstitial fill and as an alteration product of magnetite. Goethite coats the surfaces of maghemite.

PM-1-7-01
46% magnetite
21% maghemite
1% hematite
18% goethite
13% porosity
<1% gangue
Maghemite occurs as an alteration product of early magnetite and as interstitial fill. Goethite lines and fills vugs. Hematite is a late vug filling.

PM-7-3-01 Section 17 prospect grid; magnetite ore
47% magnetite
26% maghemite
8% hematite
18% gangue
1% goethite
Euhedral to subhedral magnetite crystals are quite corroded and altering to maghemite. Secondary calcite and hematite fill interstices. Titanium-rich magnetite replaces fossils.

PM-7-4-11
46% magnetite
18% maghemite
6% hematite
3% porosity
26% gangue
1% goethite
Abundant fossils(mostly oncolites) are replaced by high-titanium magnetite. Euhedral to subhedral magnetite crystals are corroded, broken and altered to maghemite. Abundant gangue(calcite) in vugs and interstices.

APPENDIX VI.

PM-7-5-01
54% magnetite
15% maghemite
4% hematite
26% gangue
1% goethite
Corroded and broken euhedral to subhedral crystals of magnetite are altering to maghemite. Abundant fossils are replaced by titanium-rich magnetite. Calcite fills interstices, cracks and vugs.